Dissertation

submitted to the

Combined Faculties for the Natural Sciences and for Mathematics

of the Ruperto-Carola University of Heidelberg, Germany

for the degree of

Doctor of Natural Science

presented by

Eva Katharina Möller, M.Sc.

born in Jülich, Germany

Oral examination: 5th May 2017

Modulation of the Wnt pathway at single-cell level uncovers diverging functional domains in the ciliary marginal zone of medaka

Referees:

Prof. Dr. Joachim Wittbrodt

Prof. Dr. Nicholas S. Foulkes

Abstract

The continuous life-long growth of the fish retina is fuelled by neural stem cells located within the ciliary marginal zone (CMZ). These stem cells are characterised by their multipotency and ability to self-renew. Through asymmetric divisions, the neural stem cells give rise to progenitor cells with restricted proliferation potential that ultimately commit to terminally differentiated neurons of the mature retina.

In this process, pharmacological manipulation suggests that Wnt signalling acts on both cell proliferation and differentiation, but a refined analysis is missing. Therefore, I present here a detailed analysis of Wnt signalling localisation and function within different cell types and their lineages in the post-embryonic CMZ of medaka.

In this thesis, I show that Wnt ligands are expressed by cells of the retinal pigment epithelium, which is located directly adjacent to the CMZ. Wnt/β-catenin signalling activity is restricted to stem cells, whereas β-catenin independent Wnt/LRP6 signalling extends to dividing progenitor cells.

To address the role of Wnt signalling in proliferation and differentiation of specific stem and progenitor cells, I created transgenic lines that allow inducible clonal labelling combined with upregulation of Wnt signalling in individual cells. My lineage tracing experiments suggest that Wnt upregulation has diverging effects on stem and progenitor cells. First, stem cells lose stemness characteristics presumably through induction of apoptosis or symmetric division. Second, progenitor cells reacquire the capacity to self-renew, but their pre-existing fate restrictions are irreversible. Finally, committed progenitors shift their fate and/or change their division mode and proliferation characteristics upon Wnt upregulation.

Taken together, my results indicate that Wnt signalling functionally divides the CMZ into stem cells, non-committed and committed progenitors, which has far reaching implications for Wnt functions in other stem cell niches.

Zusammenfassung

Das kontinuierliche, lebenslange Wachstum der Fischretina wird durch neurale Stammzellen angetrieben, die sich in der ciliären marginalen Zone (CMZ) befinden. Diese Stammzellen zeichnen sich durch Multipotenz und ihre Fähigkeit zur Selbsterneuerung aus. Durch asymmetrische Zellteilung bilden neurale Stammzellen sogenannte Vorläuferzellen mit eingeschränktem Potenzial zur Zellteilung, welche sich schließlich zu differenzierten Neuronen der vollentwickelten Retina entwickeln.

Pharmakologische Manipulationen deuten darauf hin, dass der Wnt Signalweg in diesem Prozess sowohl in Proliferation als auch Differenzierung eingreift, jedoch fehlt hier eine zellgenaue Analyse. Darum lege ich hier eine detaillierte Analyse der Lokalisation und Funktion des Wnt Signalweges in den verschiedenen Zelltypen und deren Nachkommen der Postembryonalen CMZ von Medaka dar.

In dieser Arbeit zeige ich, dass Wnt Liganden von Zellen des retinalen Pigmentepithels exprimiert werden, welches sich in direkter Nachbarschaft zur CMZ befindet. Wnt/β-Catenin Signalaktivität ist auf Stammzellen beschränkt, wohingegen β-Catenin unabhängige Wnt/LRP6 Signalaktivität sich auf sich teilende Vorläuferzellen ausdehnt.

Um die Funktion des Wnt Signalweges in Proliferation und Differenzierung spezifischer Stamm- und Vorläuferzellen zu adressieren, habe ich transgene Linien hergestellt, die induzierbare klonale Markierung in Kombination mit Hochregulation des Wnt Signalweges in individuellen Zellen erlauben. Meine Experimente zur Verfolgung der Nachkommen von Zellen legen nahe, dass Hochregulation von Wnt divergierende Auswirkungen auf Stamm- und Vorläuferzellen hat. Erstens verlieren Stammzellen ihre charakteristischen Stammzelleigenschaften vermutlich durch Apoptose oder symmetrische Zellteilung. Zweitens erwerben Vorläuferzellen die Fähigkeit der Selbsterneuerung zurück, wobei ihre bereits vorhandenen Zelltypbeschränkungen irreversibel sind. Zuletzt verlagern determinierte Vorläuferzellen ihre Zelltypbeschränkungen und/oder ändern ihren Zellteilungsmodus und Proliferationseigenschaften bei Hochregulation von Wnt.

Zusammenfassend deuten meine Ergebnisse an, dass der Wnt Signalweg die CMZ funktionell in Stammzellen, nicht determinierte und determinierte Vorläuferzellen aufteilt, was entscheidende Implikationen für Wnt Funktionen in anderen Stammzellnischen mit sich bringt.

Table of contents

1 Introduction

Already in 1957, Conrad Waddington described development with a famous metaphor that is now used to explain the differentiation process of a stem cell: A ball rolling down a hill with predefined slopes and at each branching point is a cell fate decision ultimately leading to differentiation (Figure 1) (Waddington, 1957). Today, we know much more about the factors that govern stem cell behaviour. Understanding the decision-making processes of stem cells is essential to comprehend development, homeostasis and a plethora of diseases. With this thesis I aim to expand this knowledge about stem cells.

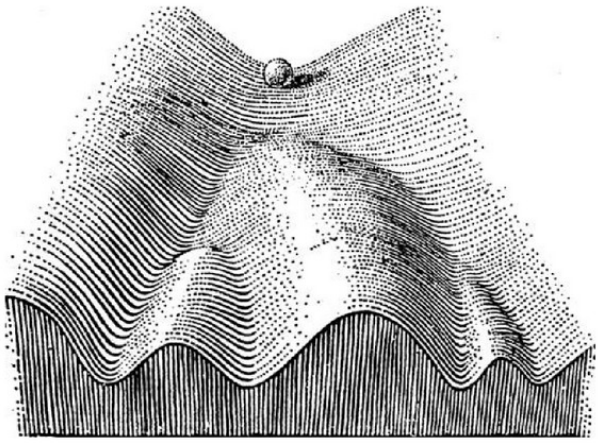

Figure 1. Waddington's Landscape. Metaphor for stem cell decision-making process: Ball rolling down a hill with predefined slopes. Originally published in (Waddington, 1957), figure taken from (Ghaffarizadeh et al., 2014).

1.1 Adult stem cells

Stem cells are characterised by the ability to self-renew and to give rise to multiple differentiated cell types, termed multipotency. In postembryonic tissues those features are exclusive to stem cells. In addition, stem cell characteristics frequently include quiescence, which does not hold true for all tissues though (Orford and Scadden, 2008; Rumman et al., 2015). Stem cells give rise to non-self replicating progenitor cells (or transit amplifying cells), which in turn give rise to cells with more and more restricted differentiation potential ultimately resulting in differentiated functional cells (Weissman, 2000). The balance between stem cell proliferation and differentiation is essential for

tissue homeostasis and thus tightly regulated. How this regulation is achieved is of fundamental importance in stem cell biology.

1.1.1 Stem cell self-renewal

Self-renewal of stem cells in homeostasis can be achieved at two different levels: self-renewal at single-cell level and by population asymmetry (Watt and Hogan, 2000) (Figure 2).

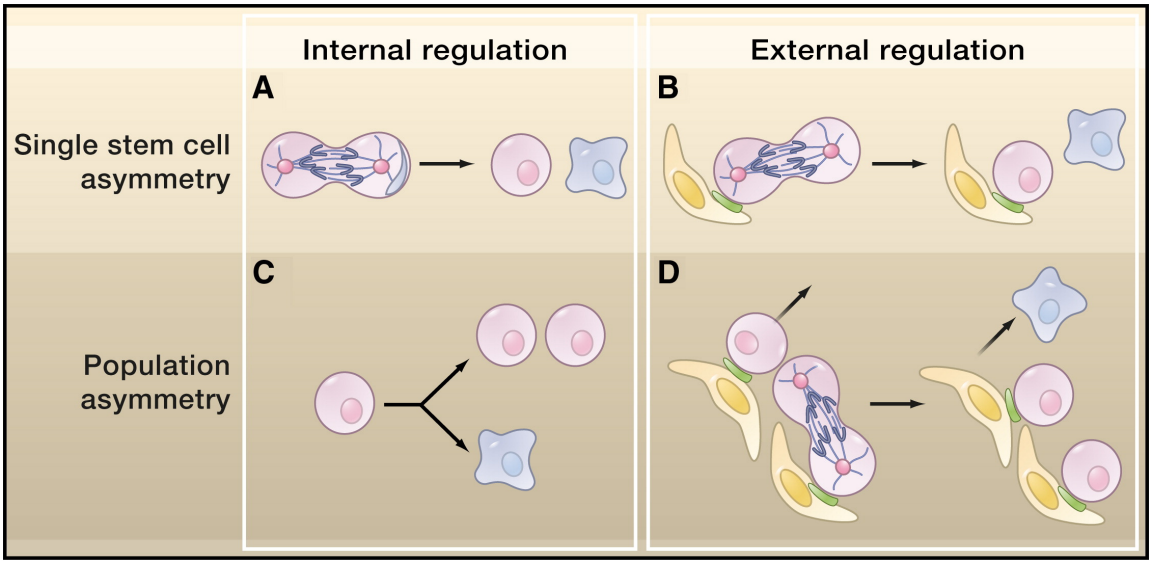

Figure 2. Stem cell self-renewal and regulation. Long-term homeostasis can be achieved through different mechanisms, depending on whether fate asymmetry is obtained at single cell or population level and whether it is regulated via cell autonomous mechanisms or by niche factors. (A) Stem cells divide asymmetrically governed by cell intrinsic factors resulting in one stem cell and one differentiating cell. (B) In each Stem cell division one cell gets displaced from the niche and loses stem cell features whereas the niche proximal cell retains stem cell capacity. (C) Symmetric stem cell divisions and differentiation are balanced out and regulated by cell autonomous factors. (D) For each symmetric stem cell division in the niche one cell is displaced from niche factors and differentiates. From (Simons and Clevers, 2011) with permission.

At single-cell level, each stem cell divides strictly asymmetrically always giving rise to one stem cell that remains in the niche and one progenitor cell that exits the stem cell compartment on its way to differentiation (Figure 2 A and B). This single-cell asymmetry (or invariant asymmetry) had been the classical view of how self-renewal is accomplished. Examples for single-cell asymmetry can be found in the *Drosophila* central nervous system (CNS) development (Egger et al., 2008) and in the germline (Fuller and Spradling, 2007). Recently, evidence accumulated for a second strategy of

self-renewal: population asymmetry (Simons and Clevers, 2011) (Figure 2 C and D). In this strategy self-renewal is accomplished on population level. This means that some stem cells can be lost due to differentiation or cell death, which is compensated by other stem cells dividing symmetrically. To keep homeostasis, the events resulting in loss of or gain of stem cells must be balanced. Hence, the fate outcome for individual stem cells is stochastic, but the population remains predictable. Examples for population asymmetry are present in several mammalian organs: the intestinal crypt (Lopez-Garcia et al., 2010; Snippert et al., 2010), interfollicular epidermis (Clayton et al., 2007; Doupé et al., 2010), hair follicle (Zhang et al., 2009) and the germline (Klein et al., 2010).

1.1.2 Stem cell regulation

Independently of the scenario, single-cell asymmetry or population asymmetry, both proliferation and differentiation need to be regulated to ensure generation of appropriate cell numbers and types. This regulation can be achieved via two mechanisms: intrinsic and extrinsic (Morrison and Kimble, 2006). Intrinsic regulation comprises the asymmetric segregation of cell components that determine cell fate during division (Figure 2 A and C). A well-known example for intrinsic regulation of asymmetric cell division is the *C. elegans* zygote, where asymmetrically localised PAR proteins control spindle orientation as well as the asymmetric distribution of cytoplasmic cell fate determinants (Mello et al., 1992; Mello et al., 1996; Reese et al., 2000; Strome and Wood, 1983). A closely related mechanism was observed in the *Drosophila* neuroblast (Doe and Bowerman, 2001). In contrast, extrinsic regulation of stem cell behaviour is accomplished by specialised microenvironments, called stem cell niches (Figure 2 B and D). This concept was first described in 1978 by R. Schofield (Schofield, 1978) and recently considerable efforts were invested into revealing factors that govern the instructions stem cells receive from their niches. In *Drosophila* for instance, JAK-STAT, BMP and Wg were identified as niche cell factors in several organs including the gonads and the gut. In mammalian organs Wnt, Notch, BMP, Hedgehog and FGF are reoccurring pathways involved in niche regulation (Voog and Jones, 2010).

1.1.3 Neural stem cells

The adult mammalian brain comprises two stem cell niches: the subgranular zone (SGZ) in the dentate gyrus of the hippocampus and the subventricular zone (SVZ) of the lateral ventricles (Gage, 2012). The neuronal stem cells (NSC) of the SGZ feature four different modes to produce progeny. They can divide symmetrically to expand the stem cell pool, asymmetrically to either produce a stem cell and an astrocyte or a stem cell and a neural progenitor and they can directly transform into astrocytes. Neural progenitors are able to divide symmetrically, but also produce neuroblasts, which subsequently mature into differentiated neurons (Bonaguidi et al., 2011). The neurogenic niche comprises endothelial cells, astrocytes, microglia, mature neurons and progeny of adult neural precursors. In cell culture, vascular cells (Palmer et al., 2000) as well as astrocytes (Ma et al., 2005) are known to promote NSC proliferation; the latter additionally promotes neuronal fate commitment through secreted and membrane-associated factors (Barkho et al., 2006). Microglia, on the other hand, rapidly phagocytose apoptotic neurons and eliminate them from the niche (Sierra et al., 2010). Also, several extrinsic niche cell factors were shown to impact on the SGZ. Notch and Hedgehog are essential for maintenance of the pool of quiescent NSCs (Han et al., 2008; Pierfelice et al., 2011). Wnt3a may be secreted by niche astrocytes (Song et al., 2002) and induces proliferation in neural progenitors in addition to promoting neuronal fates (Lie et al., 2005). On the other hand, BMP inhibits neurogenesis in the SGZ, which can be antagonised by Neurogenesin-1 (Lim et al., 2000; Ueki et al., 2003). Apart from the extrinsic factors that govern the SGZ also various intrinsic factors were shown to be involved (Ming and Song, 2011). Two examples are the orphan nuclear receptor TLX, which is essential for NSC self-renewal and maintenance possibly via canonical Wnt signalling (Qu et al., 2010), and FoxOs, which are important for long-term maintenance of adult NSCs (Renault et al., 2009).

1.2 Medaka retina and ciliary marginal zone

To study stem cells *in vivo*, fish constitute ideal model organisms as they grow constantly throughout their adult life, which is a unique feature among vertebrates. This growth is

fuelled by adult stem cells, which continually add all cell types to every organ. Moreover, the fish retina is an excellent model to study NSCs for its stereotypic cell type composition and spatiotemporal organization that is well conserved across vertebrates (Fischer et al., 2013; Livesey and Cepko, 2001; Perron and Harris, 2000).

1.2.1 Architecture of the fish retina

The neural retina (NR) of fish resembles the shape of a hemisphere formed in a radial symmetric way around the lens (Figure 3 A and B). It is composed of six neuronal and one glial cell type distributed over three nuclear layers (Figure 3 D) (Livesey and Cepko, 2001). The space in-between the nuclear layers is occupied by neuronal processes of those cells. Rod and cone photoreceptors are located in the outermost (apical) layer, the outer nuclear layer (ONL). They convert photons entering the eye through the lens into chemical signals. Bipolar, horizontal and amacrine cells as well as Müller glia cells form the inner nuclear layer (INL) directly adjacent to the ONL. Bipolar cells have processes towards the ONL and the ganglion cell layer (GCL), the third and innermost layer. They transmit the information from the photoreceptors towards the ganglion cells. Horizontal and amacrine cells both integrate and refine the visual information via lateral connections. The processes of horizontal cells connect to photoreceptors and enhance visual contrast, whereas amacrine cells interact with ganglion cells (and bipolar cells) to pre-compute visual information (e.g. object motion detection). Müller glia cells, the only non-neuronal cell type, span all the retinal layers, provide structural and metabolic support during homeostasis and are important for regeneration of injuries. Retinal ganglion cells, which constitute the GCL, transmit the visual information to the brain. Axons of the GCL exit the eye through the optic nerve and project to the optic tectum where visual information is processed. The diversity of cells within the retina goes beyond those 7 cell types, as each cell type can be further classified into subtypes. The apical side of the NR is covered with the retinal pigment epithelium (RPE). The RPE is functionally important for the eye, because it ensures that light only enters the eye through the lens.

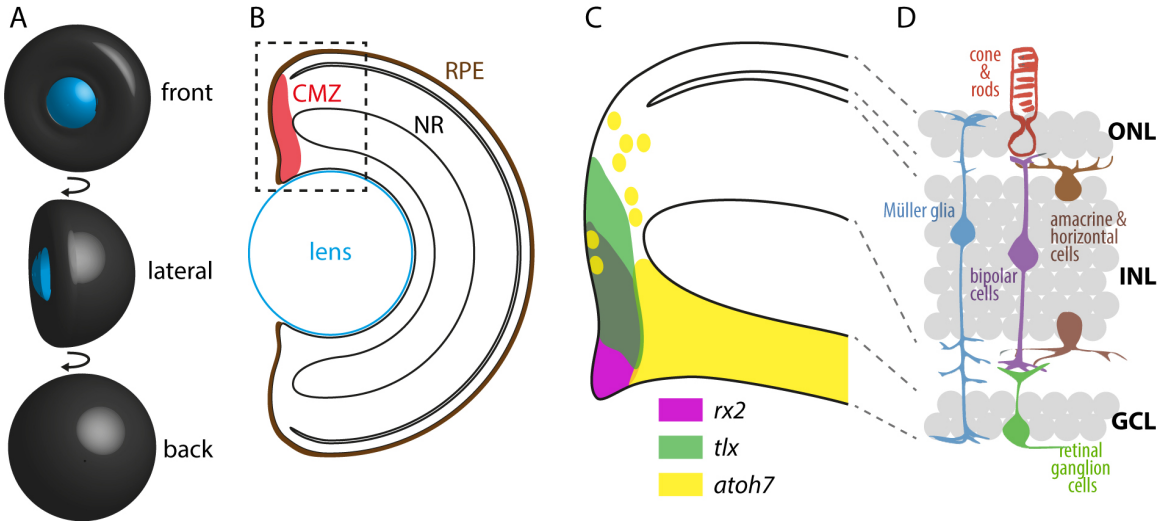

Figure 3. Shape and composition of the fish eye and CMZ. (A) 3D views of the fish eye. The retina (black) has the shape of a hemisphere surrounding the lens (blue). There are three common ways to image the retina: front view, lateral view and back view. (B) Lateral section through the eye. The neural retina (NR, black) is surrounded by the retinal pigment epithelium (RPE, brown) on its apical side. The RPE ensures that light can only enter the eye through the lens (blue). The ciliary marginal zone (CMZ, red) is located at the extreme periphery of the NR. Here, new cells are added continuously to the NR to fuel growth. (C) Periphery of the NR. Genetic markers of the CMZ are shown: *rx2* marks stem cells, *tlx* marks stem and progenitor cells and *atoh7* marks differentiated retinal ganglion cells as well as proliferating progenitors. (D) The differentiated retina is composed of six neuronal (rod and cone photoreceptors, bipolar, amacrine and horizontal cells as well as retinal ganglion cells) an one glial (Müller glia) cell types distributed over three nuclear layers (outer nuclear layer – ONL, inner nuclear layer – INL and ganglion cell layer - GCL) Scheme in D adapted from (Centanin et al., 2014).

1.2.2 The ciliary marginal zone (CMZ)

The fish retina grows continuously from the ciliary marginal zone (CMZ, Figure 3 B), a circumferential ring of cells localised at the periphery of the NR. The CMZ is composed of stem and progenitor cells in a stereotypic central to peripheral arrangement. It functions to add concentric rings of new cells to the periphery of the retina (Amato et al., 2004; Centanin and Wittbrodt, 2014; Johns, 1977; Reh and Levine, 1998; Straznicky and Gaze, 1971). The life-long control of proliferation and differentiation requires a precise spatiotemporal coordination. Retinal stem cells give rise to progenitor cells that pass through stages of subsequently more and more restricted competences to eventually give rise to the full complement of differentiated retinal cell types (Centanin et al., 2011; Livesey and Cepko, 2001; Perron and Harris, 2000; Wan et al., 2016). It is thought that the competence states of cells correlate with their localisation within the CMZ (Figure 4) (Perron and Harris, 2000; Perron et al., 1998). The slowly cycling, multipotent stem cells reside at the most peripheral tip of the CMZ. They are followed by fast cycling transit amplifying cells with restricted proliferation capacity. Committed progenitors on their way to differentiation are situated at the central edge of the CMZ. Moreover, several

genetic markers have been identified in the CMZ (Figure 3 C). The *retina-specific homeobox gene-2* (*rx2*, magenta) is expressed in the most peripheral part of the CMZ and was identified as bona fide marker for adult multipotent retinal stem cells (Reinhardt et al., 2015). *tlx* (green) overlaps with *rx2*, but extends more towards the apical side (towards the progenitors). It was shown to be a stem cell marker in the mammalian brain (Liu et al., 2008) and induces stem cell characteristics in the fish retina (Reinhardt et al., 2015). The *atonal bHLH transcription factor 7* (*atoh7*, yellow) marks differentiated retinal ganglion cells, but also localises to proliferating progenitors closer to the *rx2* domain (Lust et al., 2016). In addition to molecular markers, also a number of prominent niche factors are active in the CMZ: Wnt, Notch, FGF, IGF and Hedgehog (Borday et al., 2012; Das et al., 2006; Inoue et al., 2006; Kubo et al., 2005; Moshiri and Reh, 2004; Moshiri et al., 2005; Ohnuma et al., 2002; Van Raay et al., 2005; Zygar et al., 2005). Although those pathways are involved in regulation of cell proliferation, it is not understood how they function in the transition from stem cell over transit amplifying cell to terminally differentiated cell.

1.2.3 Competence states and division modes within the developing retina show similarities to the postembryonic CMZ

It has been proposed that the spatially encoded sequence of events in the CMZ from stem cell to differentiated neuron recapitulates the temporal progression of embryonic retinogenesis (Perron and Harris, 2000). This is supported by the expression patterns of proneural and neurogenic genes: their special distribution within the CMZ, from peripheral to central, is very similar to their temporal distribution in the developing retina (Perron et al., 1998). The competence model for retinal development proposes, that progenitors go through waves of competences where they can only produce a certain subset of retinal cells at a given time point in development (Figure 4). Hence, the competence of progenitors gets more restricted with time (Centanin and Wittbrodt, 2014; Livesey and Cepko, 2001). However, whether retinal progenitor cells in the adult retina go through the same competence states distributed in space within the CMZ is not unambiguously shown yet.

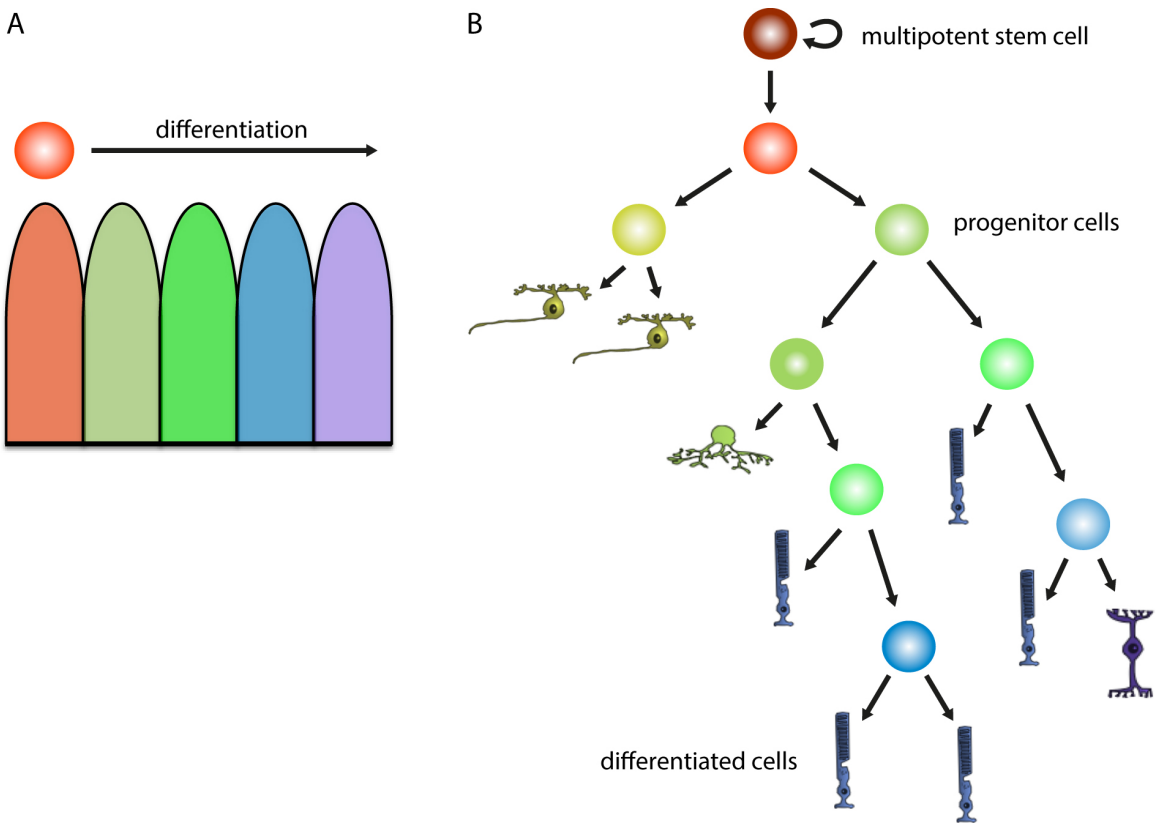

Figure 4. Competence model for the developing retina and the CMZ. (A) The competence model proposes that progenitor cells in the retina go through waves of competence states with successive restriction of their differentiation potential. (B) Example of a possible lineage tree resulting in two ganglion cells (lime green), one amacrine cell (green), one bipolar cell (lilac) and five rod photoreceptors (blue). Redrawn from (Livesey and Cepko, 2001) with permission.

More recently it has been suggested that embryonic and adult retinal progenitor cells (RPCs) share common division modes (Wan et al., 2016). Embryonic RPCs divide symmetrically at first, producing two progenitor cells. Then, they go through a stochastic phase of divisions with all possible outcomes: two progenitors, one progenitor and one differentiated cell or two differentiated cells. Towards the end of retinogenesis the probability for symmetric divisions resulting in two differentiated cells increases (He et al., 2012). Adult stem cells in the CMZ preferentially divide asymmetrically giving rise to one retinal stem cell (RSC) and one RPC (Centanin et al., 2014). The division behaviour of the resulting RPCs fits the same model describing divisions in embryonic RPCs (Wan et al., 2016). However, the view that the spatial distribution within the CMZ equals the temporal distribution in the embryonic retina is challenged by a forward-genetic screen claiming that the genetic programmes used by embryonic and adult RSCs are fundamentally different (Wehman et al., 2005). Wehman *et al.* base this claim on their

observation that a substantial portion of fish mutants shows CMZ-specific phenotypes but no developmental defects of the retina.

1.3 Identification and characterisation of stem cells

To understand how organs grow or maintain homeostasis, in other words how a given stem cell niche functions, it is vital to identify and characterise its stem cells.

As mentioned, quiescence is a frequent feature of stem cells. Traditionally, this has been used to identify stem cells. Usually, labels incorporated into the DNA or chromatin (e.g. BrdU or H2B-GFP) get diluted in every division. Hence, those labels can be used to assess whether a cell cycles fast or slowly and therefore retention of those labels was used to pinpoint quiescent stem cells (Cotsarelis et al., 1989; Cotsarelis et al., 1990). However this method has one major drawback: quiescent cells are not necessarily stem cells and stem cells are not necessarily quiescent (Barker et al., 2007; Kiel et al., 2007; Margolis and Spradling, 1995).

Embryonic Stem cells (ESCs) and induced pluripotent stem cells are characterised by the expression of *Oct4*, *Sox2* and *Nanog* (Jaenisch and Young, 2008). Yet, no such universal molecular signature has been found in adult stem cells (Snippert and Clevers, 2011). Therefore it is safest to functionally characterise stem cells through the hallmarks of stemness: self-renewal and multipotency. To demonstrate those features *in vivo* one would have to follow single cells for extended time spans in their tissues. As this is technically challenging, one alternative is to study their behaviour *in vitro*. Growing individual clones in primary cell culture has been used in a variety of tissues to elucidate their identity and characteristics (Lawson et al., 2007; Reynolds and Weiss, 1992; Rock et al., 2009; Shackleton et al., 2006; Shinin et al., 2006). Moreover, this method enables the manipulation of stem cells in a controlled setting and in high-throughput. Even three dimensional ”mini-organ” cultures, called organoids, grown from stem cells and consisting of organ specific cell types have been developed for organs like gut, liver, brain, retina, kidney and pancreas (Clevers, 2016; Lancaster and Knoblich, 2014). However, cell culture has the major drawback that the cells are no longer in their

physiological niche and their behaviour might be altered by culture conditions. To overcome this limitation selected and labelled putative stem cells were transplanted back into host organisms and stemness was demonstrated by the formation of sustained clones and the contribution to multiple differentiated cell types. For example, it was shown in mouse that the entire hematopoietic system could be repopulated by the progeny of a single transplanted cell (Masatake Osawa, 1996). Also in the fish retina stem cells could be confirmed and characterised via transplantations (Centanin et al., 2011). Centanin *et al.* showed that RSCs generate two tissues, the NR and the RPE, via dedicated stem cells that contribute exclusively to only one of the two tissues. Moreover, stem cells forming the NR are multipotent and produce all seven cell types of the NR. However, both the isolation of cells as well as their transplantation into hosts might alter their behaviour. This was demonstrated in the hair follicle, where grafted stem cells contributed to all of the three major structures in the skin: hair follicle, sebaceous gland and interfollicular epidermis. Following those cells *in vivo* however revealed that they only contribute to the hair follicle in an unperturbed organism (Morris et al., 2004).

To circumvent perturbation of stem cell behaviour by the experimental setup, methods were developed to genetically label cells *in vivo* in an inducible, minimally invasive way. A genetic marker allows tracing the labelled cell, its progeny and their cell fates. Revealing characteristics like growth kinetics, longevity and multipotency. While inducible genetic labelling can be achieved using several different approaches (Fuchs and Horsley, 2011; Snippert and Clevers, 2011; Spradling, 2009), the most widely used one is based on a drug-inducible Cre-recombinase paired with a reporter system (Van Keymeulen and Blanpain, 2012). Typically the Cre is coupled to an oestrogen receptor (e.g. CreERT2) and expressed under the control of a gene-specific promoter. Without induction the Cre is expressed but localised to the cytoplasm and thus inactive, but is activated and enters the nucleus upon oestrogen homologue administration (e.g. tamoxifen). Here, it acts on the reporter construct and mediates the recombination of lox sites. Depending on the construct this either leads to the excision of a roadblock and expression of a reporter or a switch between two or more reporters (see section 2.3.4). Thereby, the Cre expressing cell and its progeny are irreversibly genetically marked. Titration of tamoxifen or multiple recombination possibilities (called Brainbow) allow labelling of single cells instead of populations (Blanpain and Simons, 2013).

This approach allows distinguishing between single-cell asymmetry (or invariant asymmetry) and population asymmetry. In a simplified model tissue (Figure 5 A) in which all cells are clonally labelled in different colours, clones derived from progenitors and differentiated cells become lost over time. In single-cell asymmetry, clones derived from all stem cells are sustained and their size equals the size of one clonal unit (a single stem cell and its progeny). In population asymmetry, extinction of clones that differentiate by chance is compensated by expansion of other clones. This process is called neutral drift (or neutral competition) (Blanpain and Simons, 2013).

The most prominent example in which stem cell division patterns where discovered through clonal analysis is the mouse intestinal crypt. The epithelium of the small intestine is organised into crypts and villi (Figure 5 B). Each crypt contains a stem cell niche at the base of the crypt. Paneth cells are though to be important niche cells, whereas crypt-based columnar cells (CBCs) and cells at position +4 (+4 intestinal stem cells, ISC) are the stem cells. They give rise to transit amplifying (TA) cells, which in turn produce the differentiated absorptive and secretory cells of the gut (enterocytes, Paneth, goblet and enteroendocrine cells). During those proliferation and differentiation processes the cells are conveyed along the epithelium of the crypts and villi and are eventually shed into the lumen of the gut (Barker et al., 2010). This results in a complete renewal of the epithelium within ~5 days (Marshman et al., 2002). Lineage tracing with a multicolour reporter construct resulted in multiple stem cell sustained clones in each crypt (Snippert et al., 2010) after 1 week (Figure 5 C and D). However, after longer periods of time, the number of clones decreased, whereas the size of each clone increased up until each crypt was marked entirely by one clone. This can be explained by clones being lost due to random differentiation and other clones compensating: population asymmetry and neutral drift. Hence, Snippert *et al.* (2010) showed that stem cells in the intestinal crypt divide symmetrically and undergo competition for their space-restricted stem cell niche (see Figure 2 D).

Thus, lineage tracing is a powerful method to study how stem cells and their niches function.

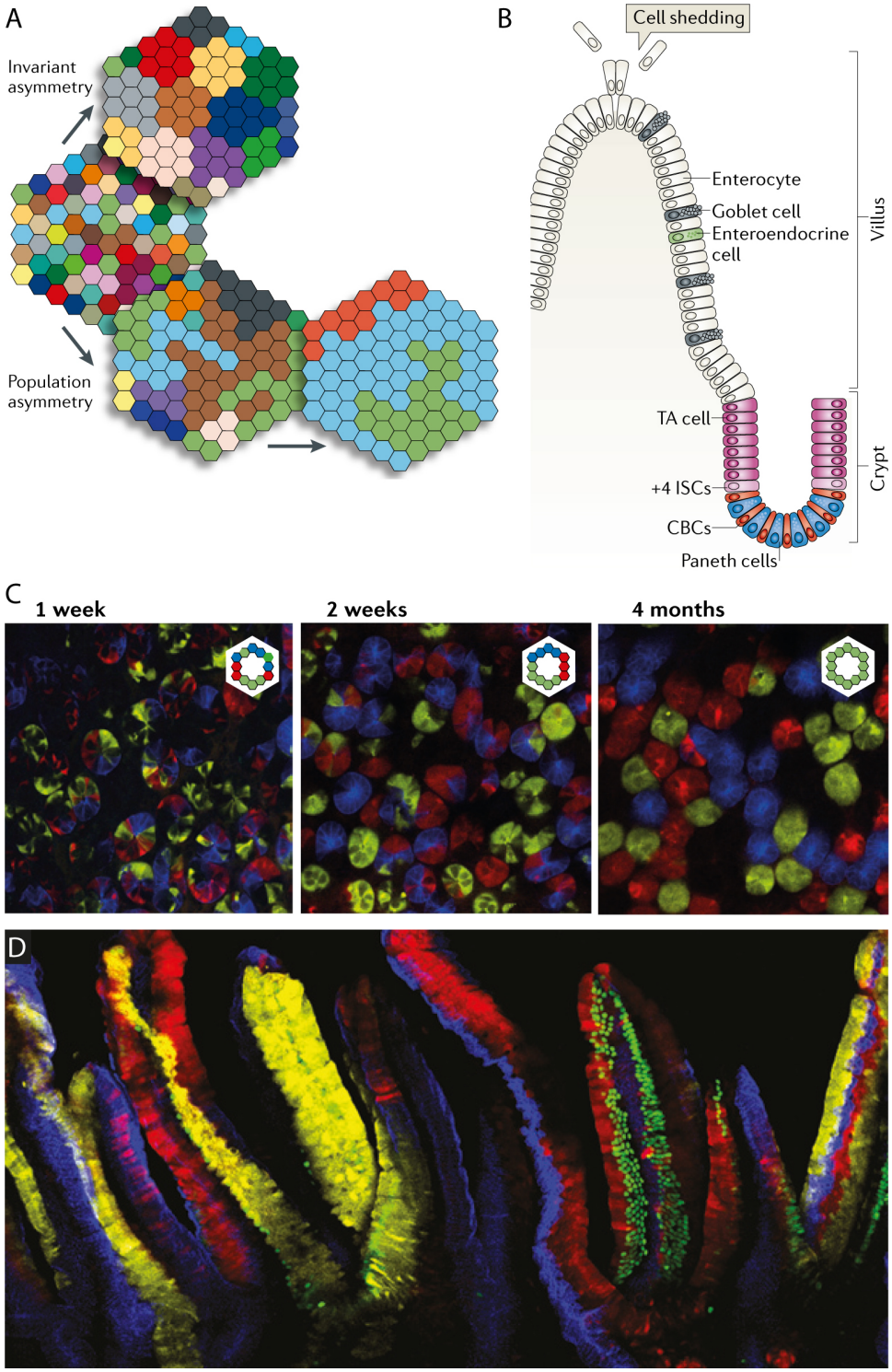

Figure 5. Intestinal stem cells achieve homeostasis through population asymmetry and neutral drift. (A) Model tissue illustrating results of lineage tracing in the division scenarios of invariant asymmetry and population asymmetry. In invariant asymmetry clones derived from each stem cell remain constant in size after an initial period in which clones derived from restricted progenitors of differentiated cells are exhausted. In population asymmetry clones from some stem cells are exhausted as the stem cell differentiated by chance. This is compensated by clones of other stem cells growing bigger. (B) Scheme of the intestinal stem cell niche. Paneth cells at the crypt base form the niche for intestinal stem cells, which divide and give rise to transit amplifying cells that go through several rounds of divisions before finally giving rise to the differentiated cell types of the intestinal epithelium (enterocytes, Paneth, goblet and enteroendocrine cells). During this process cells are conveyed along the epithelium and are finally shed into the lumen of the gut. (C) Lineage tracing in the gut reveals that clone size and number changes trough time. Initially each crypt consists of several clones, but after 4 month almost all crypts only consist of one clone showing that this stem cell system follows the pattern of population asymmetry. (D) Cross sections of the intestinal epithelium labelled by lineage tracing. Taken from (Blanpain and Simons, 2013) with permission.

1.3.1 Lineage tracing in the medaka retina: the ArCoS assay

Recently, Centanin *et al.* (2014) developed a "living" toolkit that allows clonal labelling and non-invasive fate tracking of stem and progenitor cells in the medaka retina (Figure 6). It consists of stable transgenic lines featuring temperature or hormone inducible Cre expression/activation and modified Brainbow cassettes (called Gaudi) to induce stochastic switches of fluorescent reporters (Figure 6 A). The switch is induced by Cre-mediated recombination using a ubiquitous Cre driver line (*hsp70*::Cre, heat shock inducible ubiquitous promoter) or retina specific Cre drivers (*rx2*::CreERT2 or *tlx*::CreERT2: tamoxifen-dependent nuclear localization of Cre expressed in RSCs (*rx2*, (Reinhardt et al., 2015)) or RSCs and RPCs (*tlx*, Reinhardt and Tavhelidse *et al.* unpublished)). Out of several reporter lines that were created, two are relevant for this thesis: GaudiRSG (**r**ed **s**witch **g**reen), ubiquitous promoter followed by a loxP flanked mCherry in front of a nuclear eGFP (NLSeGFP) and GaudiLxBBW (f**lox**ed red, **B**rain**b**o**w**), ubiquitous promoter followed by a loxP flanked mCherry in front of an inverted Brainbow-2.1 cassette (Livet et al., 2007). Hence, recombination causes a fluorescent colour switch from cytosolic red to nuclear green for GaudiRSG or to either membrane-bound blue, cytosolic red, cytosolic yellow or nuclear green for GaudiLxBBW. If those lines are crossed to *hsp70*::Cre fish and in their offspring stochastic recombination is induced after embryonic retinogenesis is completed, lineage tracing reveals three different types of cells (Figure 6 B - D): First, terminally differentiated cells are marked as the salt and pepper staining within the induction circle. They do not proliferate anymore and so this label does not change over time. Second, progenitor cells form footprints (open arrowheads, Figure 6 D) due to their limited proliferative potential. Third, stem cells form **ar**ched **co**ntinuous **s**tripes (ArCoSs, arrowheads, Figure 6 D). Stem cells contribute consistently to retinal growth and form continuous lines that span from the induction circle to the CMZ, even after months of growth. This is due to the unidirectional growth and highly stereotypic differentiation path of RSCs. Additionally, those experiments confirmed the transplantation studies: RSCs exclusively contribute to either RPE or NR and that the latter are multipotent, as their progeny differentiates into all seven cell types of the NR (Figure 6 E - G).

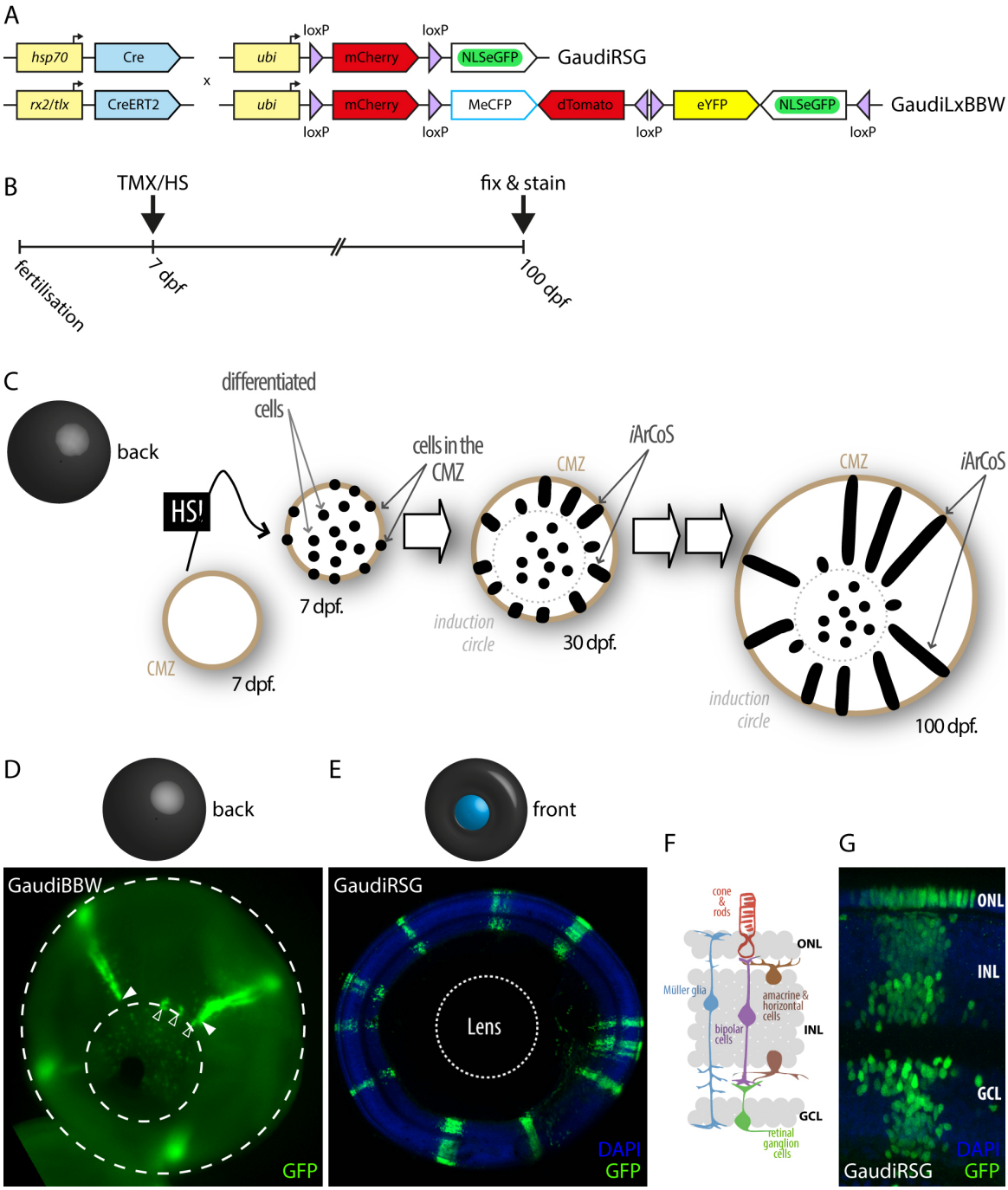

Figure 6. Lineage tracing in the medaka retina. (A) Different transgenic lines were used for lineage tracing. Cre driver lines: *hsp70*::Cre, heat shock inducible ubiquitous promoter; *rx2*::CreERT2 or *tlx*::CreERT2, tamoxifen-dependent nuclear localization of Cre expressed in RSCs (*rx2*, (Reinhardt et al., 2015)) or RSCs and RPCs (*tlx*, Reinhardt & Tavhelidse *et al.* unpublished). Fluorescent reporter lines: GaudiRSG, red switch green; GaudiLxBBW, loxP flanked red followed by a Brainbow-2.1 cassette. (B) Timeline for induction of recombination (Tamoxifen treatment, TMX or heat shock, HS) and fixation plus staining. (C & D) Lineage tracing of retinal cells results in three different outcomes: 1) Terminally differentiated cells marked as the salt and pepper staining within the induction circle. They do not proliferate and so this label does not change over time. 2) Progenitor cells form footprints (open arrowheads) due to their limited proliferative potential. Third, stem cells form **ar**ched **co**ntinuous **s**tripes (ArCoSs, arrowheads). (E - G) ArCoSs are multipotent and give rise to all seven cell types of the neural retina. dpf – days post fertilisation; CMZ – ciliary marginal zone; ONL – outer nuclear layer; INL – inner nuclear layer; GCL – ganglion cell layer. C – G adapted from (Centanin et al., 2014).

ArCoSs contribute to retinal growth very consistently while their circumferential diameter remains almost constant. In a population asymmetry scenario, some ArCoSs should terminate while others compensate with an increase in circumferential diameter. As this is not the case, RSCs follow the pattern of invariant asymmetry and only occasionally divide symmetric to compensate for an increase in retinal diameter (Centanin et al., 2014).

Recently, it was confirmed that the *rx2* promoter marks RSCs, as lineage tracing with *rx2*::CreERT2 results in ArCoSs (Reinhardt et al., 2015) and *tlx* marks RSCs and RPCs as lineage tracing with *tlx*::CreERT2 results in ArCoSs and footprints (Reinhardt and Tavhelidse *et al.* unpublished).

Consequently, this system is well suited to investigate retinal stem and progenitor cell progression *in vivo* during adult life.

1.4 Wnt signalling

1.4.1 Pathway

The Wnt signalling pathway crucially controls embryonic development. It is also implicated in maintenance and differentiation of many developmental and adult stem cells (Logan and Nusse, 2004). The canonical Wnt pathway, which stabilizes the transcriptional co-activator, β-catenin, controls key developmental gene expression programmes.

In the absence of Wnt, cytoplasmic β-catenin forms a complex with Axin and adenomatous polyposis coli (APC), whereby it is phosphorylated by casein kinase 1 alpha (CK1α) and glycogen synthase kinase 3 (GSK3). Phosphorylated β-catenin is recognized by the E3 ubiquitin ligase β-Trcp, which targets β-catenin for proteasomal degradation. In the presence of Wnt ligands, Frizzled and the low-density lipoprotein receptor-related protein 6 (LRP6) form a receptor complex. Frizzled then binds Dishevelled, which leads to LRP6 phosphorylation. LRP6 is phosphorylated by several kinases: GSK3 and a complex of CyclinY/CDK14-18 phosphorylate PPSP motifs, the former in a Wnt-

dependent manner and the latter in a cell cycle-dependent manner. In addition, S/T clusters near the PPSP motifs are phosphorylated by CK1γ upon Wnt activation (Davidson et al., 2009; Niehrs and Shen, 2010). LRP6 phosphorylation subsequently triggers Axin recruitment. This disrupts Axin-mediated phosphorylation and degradation of β-catenin, allowing β-catenin to accumulate in the nucleus where it serves as a co-activator for TCF to activate Wnt target genes (MacDonald et al., 2009). The most prominent Wnt target genes are *Axin2* (Jho et al., 2002; Lustig et al., 2002; Yan et al., 2001) and *Myc* (He et al., 1998), but numerous other target genes have been identified (Nusse, 2017) including *Lef1* (Filali et al., 2002; Hovanes et al., 2001), *Sp5* (Fujimura et al., 2007; Weidinger et al., 2005) and *Sox2* (Van Raay et al., 2005). Wnt/β-catenin target genes usually promote proliferation, survival and inhibition of differentiation (Reya and Clevers, 2005).

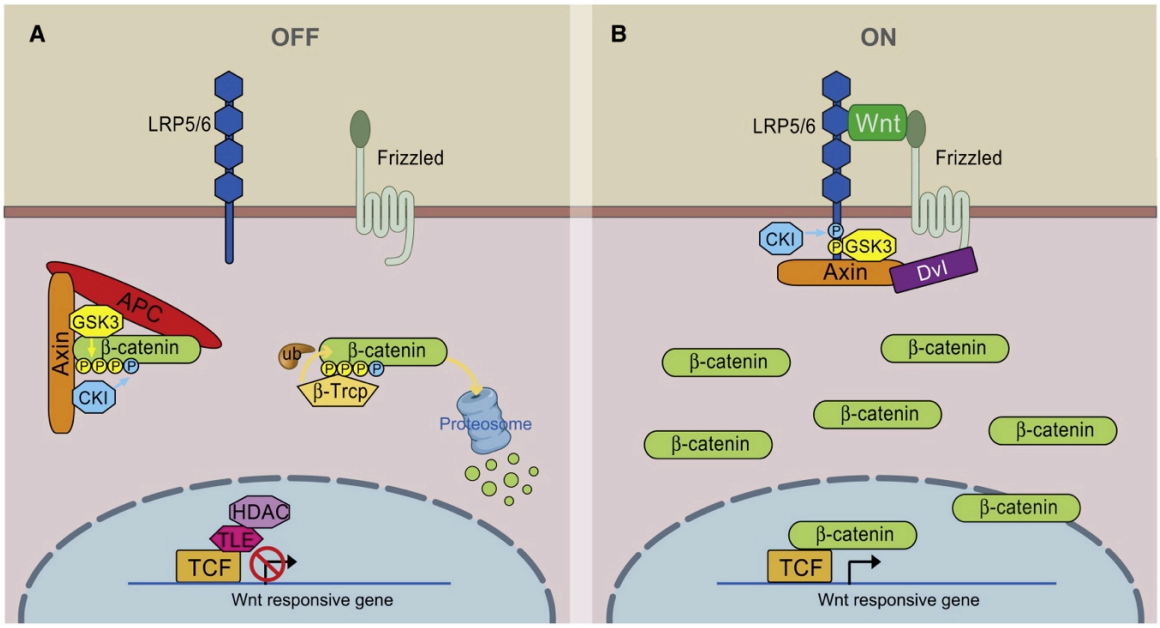

Figure 7. Wnt/β-catenin signalling. OFF: No Wnt ligand is present, so a "destruction complex" consisting of Axin, APC GSK3 and CK1 forms around β-catenin, which gets phosphorylated by GSK3 and CK1α and thereby targeted for proteasomal degradation. ON: Wnt ligand binds a complex of LRP6 and Frizzled which recruits Dvl, which in turn triggers phosphorylation of LRP6 by GSK3 and CK1γ followed by binding of Axin. Thus, no destruction complex is formed around β-catenin, it accumulates in the cytosol and enters the nucleus where it serves as a co-activator for TCF to activate Wnt target genes. From (MacDonald et al., 2009) with permission.

Wnt signalling involving the phosphorylation of LRP6 (Wnt/LRP6 signalling) has recently been shown to have β-catenin independent functions among others via the Wnt/STOP pathway (Wnt-dependent **st**abilization **o**f **p**roteins) (Acebron and Niehrs,

2016). GSK3 phosphorylates many other proteins beside β-catenin and thereby targets them for degradation. As active Wnt/LRP6 signalling sequesters a big proportion of GSK3, also other proteins are stabilised. These Wnt/STOP targets were shown to promote cell growth (Acebron et al., 2014) and cell-cycle progression (Huang et al., 2015).

1.4.2 Wnt signalling in stem cell division and fate decision

There is increasing evidence for a complex interaction between Wnt/LRP6 signalling and the cell cycle. Wnt signalling regulates cell proliferation by promoting G1 phase via β-catenin. In mitosis, components of the Wnt signalling cascade function directly in spindle formation (Niehrs and Acebron, 2012). Additionally, Wnt can promote cell cycle progression independent of β-catenin via Wnt/STOP (Huang et al., 2015). On the other hand, the cell cycle impacts Wnt signalling through phosphorylation of LRP6. The competence of LRP6 depends on phosphorylation by GSK3 or the G2/M CyclinY/CDK complex, which primes CK1 to further phosphorylate LRP6 upon Wnt stimulation. Thus, phosphorylation of the Wnt co-receptor LRP6 by CyclinY/CDK14 peaks in G2/M (Niehrs and Acebron, 2012). Studies in cultured cells show that LRP6 is more strongly phosphorylated during mitosis than during interphase (Davidson et al., 2009). Therefore, mitotic activation of Wnt signalling may play an important role in orchestrating cell division.

In vivo, cells often feature a Wnt activity gradient. Recently, localised Wnt/LRP6 signalling was shown to direct asymmetric stem cell division *in vitro* (Figure 8) (Habib et al., 2013). Wnt3a coated beads introduced into embryonic stem cell culture induced asymmetric distribution of canonical Wnt signalling components such as APC and phosphorylated active LRP6. As a result, most cells oriented the plane of mitotic division perpendicular to the Wnt gradient established by the bead. The Wnt-proximal daughter cell expressed high levels of nuclear β-catenin and pluripotency genes (e.g. *Rex1*), whereas the distal daughter cell acquired hallmarks of differentiation. Thus, a localised Wnt ligand can direct the orientation of asymmetric cell division in embryonic stem cells *in vitro*. However, whether canonical Wnt function is directing or mediating the orientation of cell division and cell type specification remains unknown.

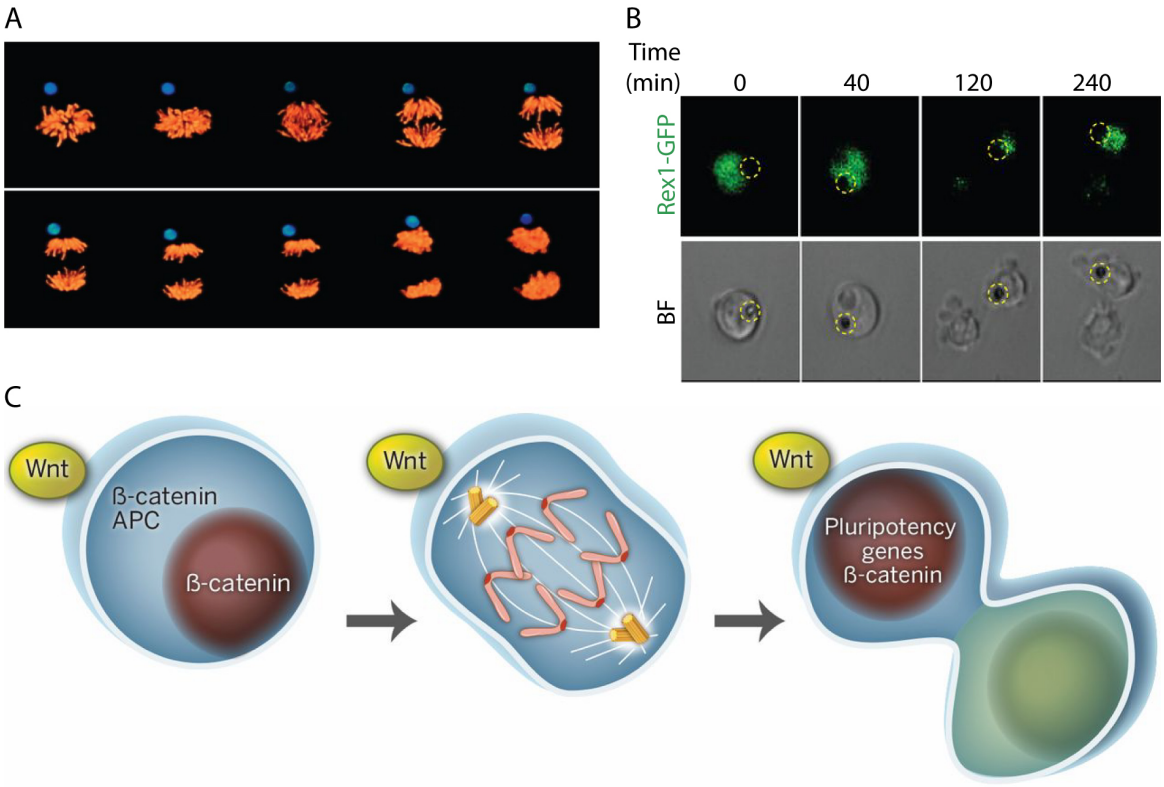

Figure 8. A localised source of Wnt directs asymmetric division in embryonic stem cells (ESCs). (A) A Wnt3a coated bead (blue) introduced into ESC culture causes nearby cells to divide in line with the bead as shown by a time series of a chromatin (orange) labelled cell. (B) During cell division the Wnt bead (here yellow dotted line) proximal cell retains pluripotency genes as rex1 (green) and the bead distal cell loses those. (C) Scheme illustrating the asymmetric division directed by a Wnt bead. Taken from (Clevers et al., 2014; Habib et al., 2013) with permission.

Wnt signalling is important for many processes during development. A Wnt signalling gradient (posterior high, anterior low Wnt) is essential for patterning of the anterior-posterior axis of vertebrates (Kiecker and Niehrs, 2001). Wnt repression is crucial for the generation of anterior neural structures and is achieved by the release of Wnt antagonists (such as Dickkopf, Dkk1) in anterior tissues (Hashimoto et al., 2000). Ectopic activation of Wnt signalling (or repression of Dkk1) leads to loss of anterior structures, whereas inhibition of Wnt signalling (or ectopic activation of Dkk1) causes enlargement or duplication of the head and/or loss of posterior structures (Darken and Wilson, 2001; Erter et al., 2001; Glinka et al., 1997; Glinka et al., 1998; Hamilton et al., 2001; Kazanskaya et al., 2000; Lekven et al., 2001; McGrew et al., 1995; McGrew et al., 1997; Mukhopadhyay et al., 2001). In two zebrafish mutant lines with anterior truncations (reduction in size or absence of eyes and forebrain), Wnt upregulation has been identified as cause for the phenotype: *masterblind* and *headless* fish carry a mutation in the Wnt signalling repressors Axin1 or Tcf3 respectively (Heisenberg et al., 2001; Kim et al., 2000; van de Water et al., 2001).

Beside its importance during development Wnt signalling has been implicated to control stem cell fate decisions in a variety of adult tissues including skin, the hematopoietic system, neural stem cells, and intestinal crypts (Clevers and Nusse, 2012; Nusse, 2008; Wend et al., 2010). In the intestinal crypt Wnt is secreted by the niche cells (Paneth cells), which are located directly adjacent to the stem cells (Sato et al., 2011). This signal is essential to maintain the stem cell pool and also to restrict the niche to the crypt base, as cells dividing and subsequently exiting the niche receive less Wnt signal and differentiate (Farin et al., 2016). In the hippocampus, Wnt signalling impacts on adult neurogenesis in two ways: Firstly, it is also secreted by niche cells, in this case astrocytes, and induces proliferation and neuronal cell fates in NSCs (Lie et al., 2005). Second, in addition to paracrine NSCs also exhibit autocrine Wnt signalling. At least in cell culture, progenitor cells derived from the adult hippocampus secrete Wnt ligands that maintain a signalling baseline cell autonomously, which is necessary for sustained proliferation and multipotency (Qu et al., 2010; Wexler et al., 2009).

Hence, Wnt signalling controls stem cell maintenance and division both *in vitro* as well as *in vivo*.

1.4.3 Wnt in the retina

Studies in the embryonic retina of chicken, *Xenopus*, and zebrafish have indicated that global alterations in canonical Wnt signalling impacts on both proliferation and differentiation of retinal precursors (Agathocleous et al., 2009; Borday et al., 2012; Denayer et al., 2008; Kubo, 2003; Kubo et al., 2005; Meyers et al., 2012; Nadauld et al., 2006; Stephens et al., 2010; Van Raay et al., 2005; Yamaguchi et al., 2005). During optic cup formation Wnt signalling acts as a fate switch between neural retina and RPE. In optic cups derived from aggregates of mouse embryonic stem cells treatment with Wnt inhibitors results in decrease of RPE cells, whereas simulation with Wnt3a has the opposite effect. Here, RPE fate is favoured at the expense of neuronal fates (Eiraku et al., 2011). *In vivo*, the RPE of β-catenin deficient mice even transdifferentiates into NR as shown by loss of RPE and gain of NR markers (Fujimura et al., 2009; Hägglund et al., 2013; Westenskow et al., 2009).

Wnt signalling also plays a crucial role in the post-embryonic CMZ. Across vertebrates it is restricted to the most peripheral part of the retina, the CMZ (Figure 9 B). More precisely, Wnt/β-catenin target genes or reporters for those are expressed within the CMZ in zebrafish, chicken and *Xenopus* (Borday et al., 2012; Denayer et al., 2008; Dorsky et al., 2002; Kubo, 2003). However, a detailed analysis of the cell identities, proliferative capacities and fate competencies of the cells featuring active Wnt/β-catenin signalling has not been performed, yet.

Interference with the pathway at post-embryonic stages had similar effects as in embryos. In zebrafish pharmacological interference with canonical Wnt signalling was used to show that it is necessary to maintain proliferation of retinal progenitors (Figure 9 C). On the other hand, hyper-stimulation of canonical Wnt signalling resulted in inhibition of normal retinal differentiation and expansion of the proliferative cell population (Figure 9 D). Neither Wnt hyper-stimulation nor inhibition had effects on terminally differentiated cells (Meyers et al., 2012). Similar effects on proliferation were observed in *Xenopus* and chicken (Denayer et al., 2008; Kubo, 2003; Kubo and Nakagawa, 2009; Kubo et al., 2005). Moreover, Denayer *et al.* (2008) reported that while Wnt hyper-stimulation also led to prolonged progenitor proliferation and CMZ enlargement, it did not block progeny of proliferating cells to differentiate and contribute correctly to the retinal layers. This indicated that misregulation does not affect all cells within the CMZ in the same manner. However, in chicken retina explants Wnt hyper-stimulation resulted in inhibition of differentiation through suppression of proneural genes including *atoh7*, which is essential for RGCs differentiation. It also caused prolonged proliferation of progenitors. Interestingly, inhibition of differentiation and stimulation of proliferation may happen independently, as blocking cell cycle progression did not rescue the differentiation phenotype (Kubo et al., 2005). Zebrafish *apc* mutants confirmed that increased Wnt signalling inhibits expression of *atoh7* (Stephens et al., 2010).

While it is clear that Wnt signalling greatly influences proliferation and differentiation in the retina, its impact on individual progenitor cells in the spatiotemporal context of the continuously growing retina is still outlined only vaguely.

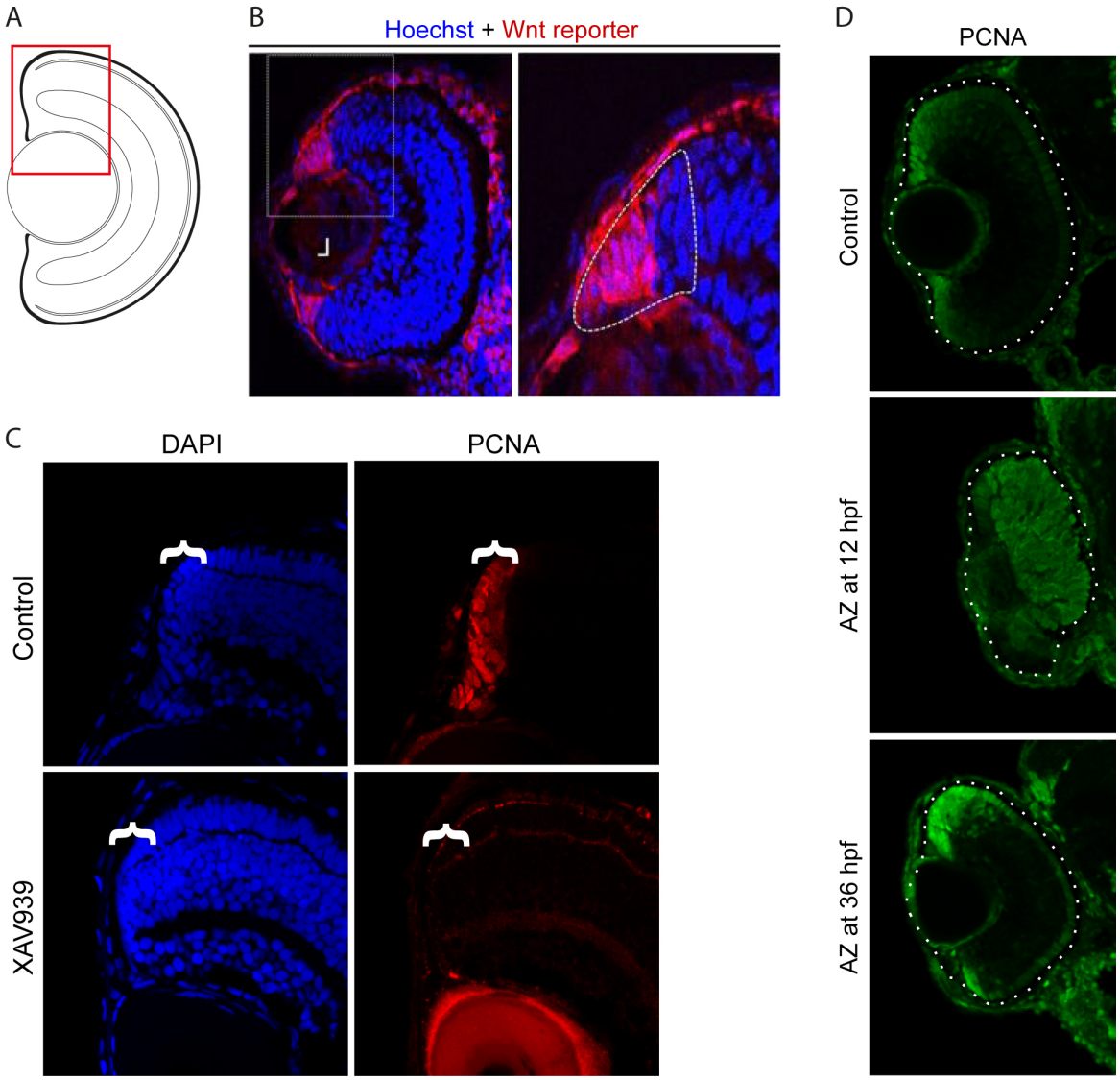

Figure 9. Wnt signalling controls proliferation in the retina. (A) Schematic cross section of the eye highlighting the close-ups shown in B and D (red rectangle). (B) The Wnt reporter (pbin8LefdGFP) is expressed in the CMZ of *Xenopus*. (C) Inhibition of Wnt signalling with XAV939 causes loss of proliferative cells (marked by PCNA) in the CMZ of zebrafish. (D) Hyper-stimulation of Wnt signalling with 1-azakenpaullone (AZ) leads to prolonged proliferation (PCNA). Already differentiated cells are not affected as shown by the treatment at 36 hours post fertilization (hpf). Adapted from (Borday et al., 2012; Meyers et al., 2012).

1.5 Objective of this thesis

The teleost retina constitutes an ideal model system to study neural stem cells *in vivo*, as retinal stem cells divide life-long to fuel growth of the retina (Amato et al., 2004; Centanin et al., 2011; Raymond et al., 2006) and their progeny follows a highly stereotypic differentiation scheme (Dowling, 2012). Moreover, available linage tracing

tools allow analysis of proliferation and fate competences of single cells and their progeny.

The Wnt signalling pathway plays a crucial role in proliferation and differentiation. However, its exact function along the lineage from stem cells via progenitor cells down to differentiated cells remains unknown for many organs including neuronal tissue and specifically the retina.

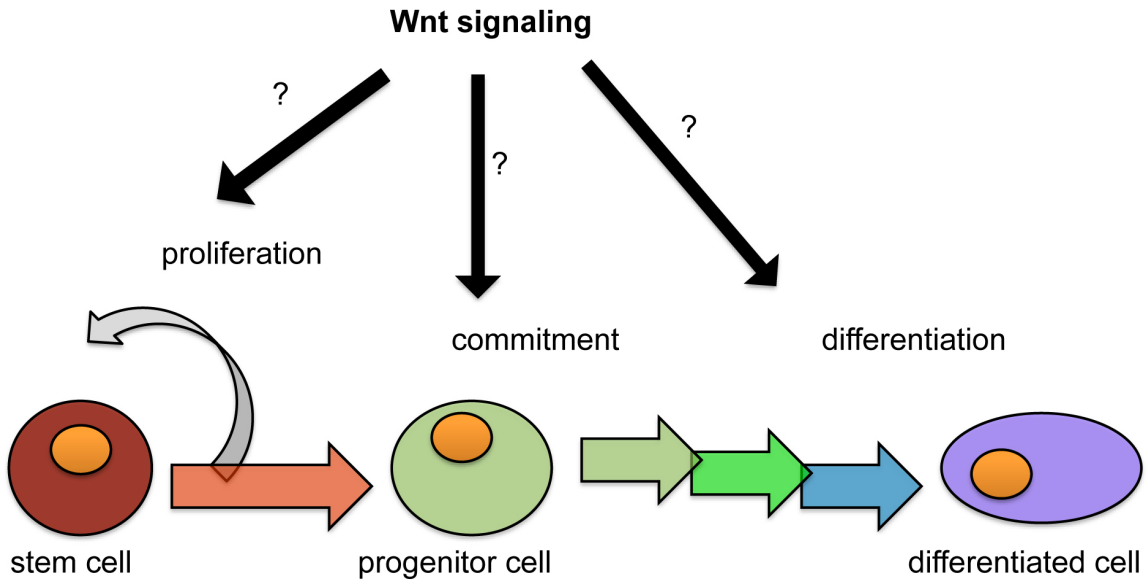

Figure 10. How does Wnt signalling affect the stem and progenitor cell lineage? The aim of this thesis is to dissect the role(s) of Wnt signalling within the CMZ, from stem cells via progenitor cells down to differentiated cells. Which effects does Wnt have on proliferation, commitment and differentiation?

Thus, the general aim of this thesis is to dissect the role of Wnt signalling within the CMZ of the teleost retina (Figure 10). I divide this aim into two goals:

First, map the exact localisation of several Wnt signalling components to reveal which cells in the CMZ show active signalling.

Second, manipulate the CMZ cell function to specifically study the role of Wnt signalling in the lineage of retinal precursors. I will take advantage of the tight spatiotemporal organization of the fish retina to follow complete lineages of single cells featuring modified Wnt signalling during the postembryonic life. Our conditional tools allow testing the impact of altered Wnt signalling features on different levels along the well described and highly stereotypic retinal cell type specification. Different Cre drivers (*rx2*,

tlx & *atoh7*) specifically active in distinct stages along the line of terminal differentiation in the retina will be used to clonally trigger perturbations in the Wnt signalling cascade. Fluorescent reporters highlight cells with altered Wnt signalling which will facilitate analysis by advanced microscopy.

2 Materials and methods

2.1 Materials

2.1.1 Kits

Description	Source of supply
innuPREP DOUBLEpure Kit	Analytik Jena
mMESSAGE mMACHINE Sp6 Kit	Invitrogen
Plasmid Midi Kit	Qiagen
RNeasy Mini Kit	Qiagen
Click-iT EdU Alexa Fluor 647 Imaging Kit	Thermo Fisher
In Situ Cell Death Detection Kit, TMR red	Sigma

2.1.2 Enzymes

Restriction endonucleases	Source of supply
EcoRI-HF (20 $^{U}/_{\mu l}$)	NEB
SacII (20 $^{U}/_{\mu l}$)	NEB
SpeI-HF (20 $^{U}/_{\mu l}$)	NEB
Ligase	
T4 DNA Ligase (5 $^{U}/_{\mu l}$)	Thermo Fisher
Polymerases	
T4 DNA Polymerase (5 $^{U}/_{\mu l}$)	Thermo Fisher
Q5 High-Fidelity DNA Polymerase (2 $^{U}/_{\mu l}$)	NEB
Taq DNA Polymerase Roboklon (5 $^{U}/_{\mu l}$)	Roboklon
T7 RNA Polymerase (20 $^{U}/_{\mu l}$)	Roche
Sp6 RNA Polymerase (20 $^{U}/_{\mu l}$)	Roche
Miscellaneous	
Proteinase K (20 $^{mg}/_{ml}$)	Merck
RNasin Ribonuclease Inhibitor (20 $^{U}/_{\mu l}$)	Promega
RiboLock RNase Inhibitor (40 $^{U}/_{\mu l}$)	Thermo Fisher
SuperscriptII (200 $^{U}/_{\mu l}$)	Invitrogen
Turbo DNase (2 $^{U}/_{\mu l}$)	Thermo Fisher
Hatching enzyme	Homemade
ISceI Meganuclease (5 $^{U}/_{\mu l}$)	NEB

2.1.3 DNA ladders

Description	Source of supply
GeneRuler 1 kb Plus DNA Ladder	Thermo Fisher
GeneRuler DNA Ladder Mix	Thermo Fisher

2.1.4 Antibodies

Antibodies used on sections (pT-LRP6 & ABC)	Host species	Dilution	Source of supply
Anti-pT-LRP6	Rabbit	1:50	Gift from Christof Niehrs lab
Anti-ABC	Mouse	1:30	Millipore
Anti-Rx2	Rabbit	1:300	Homemade
AlexaFluor 633 anti-mouse	Goat	1:400	Thermo Fisher
AlexaFluor 546 anti-rabbit	Goat	1:400	Thermo Fisher
Antibodies used on sections (EdU & TUNEL)			
Anti-GFP	Chicken	1:200	Thermo Fisher
Anti-Rx2	Rabbit	1:300	Homemade
AlexaFluor 488 anti-chicken	Donkey	1:300	Jackson
Dylight 549 anti-rabbit	Goat	1:300	Dynomics
AlexaFluor 647 anti-rabbit	Goat	1:300	Thermo Fisher
Antibodies used on whole mounts			
Anti-mCherry	Rabbit	1:200	Abcam
Anti-GFP	Chicken	1:200	Thermo Fisher
Anti-Rx2	Rabbit	1:200	Homemade
AlexaFluor 488 anti-chicken	Donkey	1:200	Jackson
AlexaFluor 647 anti-rabbit	Goat	1:300	Thermo Fisher
Antibodies used for *in situ* hybridisation			
Anti-Digoxigenin-AP Fab fragments	Sheep	1:1000	Roche
Anti-Digoxigenin-POD Fab fragments	Sheep	1:50	Sigma
Anti-Fluorescein-POD Fab fragments	Sheep	1:50	Sigma

2.1.5 Chemicals

Description	Source of supply
Acetone	Sigma
Agar	Gibco
Agarose	Biozym
Agarose (low melting)	Biozym
Ampicillin	Sigma
Bacto-Tryptone	Gibco
BCIP	Roche
Blocking reagent	Roche
Bovine serum albumin (BSA, 10 $^{mg}/_{ml}$)	NEB
Calcium chloride dehydrate	Sigma
Chloroform	Sigma
Cy5 Fluorophore Tyramide	PerkinElmer
DAPI	Sigma
dATPs (2 mM)	Thermo Fisher
digUTPs	Roche
DMSO	NEB
dNTPs (2.5 or 5 mM each)	Sigma

DTT	Thermo Fisher
EDTA	Roth
EdU	Thermo Fisher
EGTA	Sigma
Ethanol	Merck
Ethidium bromide (EtBr)	Sigma
Fluorescein Fluorophore Tyramide	PerkinElmer
Formamide	Sigma
Glacial acetic acid	Merck
Glucose	Sigma
Glycerol	Grüssing
Glycine	Sigma
Heparin	Gibco
Hoechst	Thermo Fisher
Horse serum	Sigma
Hydrogen chloride (HCl)	Merck
Hydrogen peroxide (H_2O_2)	Sigma
IPTG	Thermo Fisher
Isopropanol	Sigma
Kanamycin	Roth
Magnesium chloride ($MgCl_2$, 50 mM)	Invitrogen
Magnesium chloride ($MgCl_2$)	Merck
Magnesium Sulphate Heptahydrate	Grüssing
Methanol (MeOH)	Roth
Natural goat serum (Donor Herd)	Sigma
NBT	Roche
Orange Loading Dye	Thermo Fisher
Paraformaldehyde (PFA)	Sigma
Penicillin-Streptomycin-Glutamine (Pen/Strep)	Invitrogen
Polyethylene glycol (PEG)	Thermo Fisher
Potassium acetate	Sigma
Potassium chloride	AppliChem
Potassium dihydrogen phosphate	Merck
Potassium hydrogen phosphate	Merck
Potassium hydroxide (KOH)	Merck
Ribonucleic acid from Torula yeast type VI	Sigma
RNase-free H_2O	Gibco
rNTPs (ATP, CTP, GTP 15.4 mM, UTP 10.0 mM)	Roche
Sheep serum	Sigma
Sodium chloride (NaCl)	Sigma
Sodium citrate	Sigma
Sodium dodecyl sulfate (SDS)	Sigma
Sodium hydrogen carbonate	Merck
Sodium hydrogen phosphate	AppliChem
Sodium hydroxide	Merck
Sucrose	Roth
Tamoxifen	Sigma

Tricaine mesylate	Sigma
Tris base	Sigma
Trisodium citrate	Sigma
Triton X100	Roth
TRIzol reagent	Invitrogen
Tween 20	Sigma
X-Gal	Thermo Fisher
Yeast Extract	Roth

2.1.6 Media, solutions and buffer

Description	**Source of supply**
Elution Buffer (EB)	Analytik Jena
FastDigest Green Buffer (10x)	Thermo Fisher
FastDigest Buffer (10x)	Thermo Fisher
Gel Loading Buffer II (5x)	Invitrogen
T4 DNA Ligase Buffer (10x)	Thermo Fisher
T4 DNA Pol Buffer (5x)	Thermo Fisher
Transcription-Buffer (10x)	Roche
TSA Amplification Diluent	PerkinElmer
Tissue freezing medium	Leica
RNA Loading Dye (2x)	Thermo Fisher
Rapid Ligation Buffer (2x)	Promega
Q5 Reaction Buffer (5x)	NEB
Probes master mix (2x)	Roche
PolBuffer B (10x)	Roboklon
ISceI Buffer	NEB
Fluoromount	Roth
First-Strand Buffer (5x)	Invitrogen

Description	**Ingredients**	**Composition**
TB-Medium	Bacto-Tryptone	12 $^{g}/_{l}$
	Yeast Extract	24 $^{g}/_{l}$
	Glycerol	0.4%
	Potassium dihydrogen phosphate	2.13 $^{g}/_{l}$
	Potassium hydrogen phosphate	12.54 $^{g}/_{l}$
LB-Medium	Bacto-Tryptone	10 $^{g}/_{l}$
	Yeast Extract	5 $^{g}/_{l}$
	Sodium chloride	10 $^{g}/_{l}$
LB-Plates	Bacto-Tryptone	10 $^{g}/_{l}$
	Yeast Extract	5 $^{g}/_{l}$
	Sodium chloride	10 $^{g}/_{l}$
	Agar	15 $^{g}/_{l}$
P1	Glucose	50 mM
	Tris-HCl	25 mM
	EDTA	10 mM
	pH 8, stored at 4°C	

P2	Sodium hydroxide	0.2 N
	SDS	1%
P3	Potassium acetate	5 M
	stored at 4°C	
TE	Tris-HCl	10 mM
	EDTA	1 mM
	pH 8.0	
TAE	Tris base	242 $^{g}/_{l}$
	Glacial acetic acid	5.71%
	EDTA	50 mM
	pH 8.5	
PBS	Sodium chloride	137 mM
	Potassium chloride	2.7 mM
	Potassium dihydrogen phosphate	240 $^{mg}/_{l}$
	Sodium hydrogen phosphate	1.44 $^{g}/_{l}$
	pH 7,4	
PBTS	Sodium chloride	137 mM
	Potassium chloride	2.7 mM
	Potassium dihydrogen phosphate	240 $^{mg}/_{l}$
	Sodium hydrogen phosphate	1.44 $^{g}/_{l}$
	Triton X100	0.1%
	pH 7,4	
2x PTW	Sodium chloride	274 mM
	Potassium chloride	5.4 mM
	Potassium dihydrogen phosphate	480 $^{mg}/_{l}$
	Sodium hydrogen phosphate	2.88 $^{g}/_{l}$
	Tween 20	0.1%
	pH 7,4	
PTW	Sodium chloride	137 mM
	Potassium chloride	2.7 mM
	Potassium dihydrogen phosphate	240 $^{mg}/_{l}$
	Sodium hydrogen phosphate	1.44 $^{g}/_{l}$
	Tween 20	0.1%
	pH 7,4	
ERM	Sodium chloride	17 mM
	Potassium chloride	0.4 mM
	Calcium chloride dihydrate	0.27 mM
	Magnesium Sulphate Heptahydrate	0.66 mM
	pH 7	
Hatching medium	Sodium chloride	17 mM
	Potassium chloride	0.4 mM
	Calcium chloride dihydrate	0.27 mM
	Magnesium Sulphate Heptahydrate	0.66 mM
	Methylen blue	0.0001%
	pH 7.2	
Tricaine 20x	Tricaine mesylate	4 $^{g}/_{l}$
	Sodium hydrogen phosphate	10 $^{g}/_{l}$

	pH 7 – 7.5	
Yamamoto-Mix 10x	Sodium chloride	7.5 $^{g}/_{ml}$
	Potassium chloride	0.2 $^{g}/_{ml}$
	Calcium chloride dihydrate	0.2 $^{g}/_{ml}$
	Sodium hydrogen carbonate	0.02 $^{g}/_{ml}$
	pH 7.3	
20x SSC	Sodium chloride	3 M
	Trisodium citrate	300 mM
	pH 7	
Hyb-Mix	Formamide	50%
	SSC	5x
	Heparin	150 $^{\mu g}/_{ml}$
	Ribonucleic acid from Torula yeast Typ VI	5 $^{mg}/_{ml}$
	Tween 20	0.1%
4x SSCT	SSC	4x
	Tween 20	0.1%
2x SSCT	SSC	2x
	Tween 20	0.1%
0.2 SSCT	SSC	0.2x
	Tween 20	0.1%
Staining buffer	Tris-HCl pH 9.5	100 mM
	Sodium chloride	100 mM
	$MgCl_2$	50 mM
	Tween 20	0.1%
TN	Tris-HCl	100 mM
	Sodium chloride	150 mM
	pH 7.5	
TNT	Tris-HCl	100 mM
	Sodium chloride	150 mM
	Tween 20	0.1%
	pH 7.5	
TNB	Tris-HCl	100 mM
	Sodium chloride	150 mM
	Tween 20	0.1%
	Blocking reagent	2%
	pH 7.5	

2.1.7 Equipment

Description	**Source of supply**
Bacterial Shaker INNOVA 44	New Brunswick scientific
Borosilicale glass capillars GC100T(F)	ClarcElectromedical Instruments
Centrifuge 5417C	Eppendorf
Cryostat CM3050S	Leica
Embryo incubators	Heraeus instruments and RuMed
FemtoJet express or Microinjector 5242	Eppendorf

Freezer (-20°C)	Liebherr
Freezer (-80°C)	Thermo Fisher
Fridge (4°C)	Liebherr
InjectMan NI2	Eppendorf
Leica TCS Sp8	Leica
Leica TCS SpE	Leica
Microinjector 5242	Eppendorf
Microwave	Sharp
Mini-centrifuge	Starstedt
NanoDrop ND-1000 Spectrophotometer	Thermo Fisher Fisher
Needle puller P-30	Sutter Instrument Co USA
Nikon AZ100 Multizoom	Nikon
Nikon SMZ18 stereomicroscope	Nikon
pH-Meter	Sartorius
Power supply Power-PAC Basic	Bio RAD
Roche Lightcycler480	Roche
Scales	Saturius
Shaker CAT S 20	NeoLab
Shaker GFL 3005	HILAB
Stereomicroscope Zeiss Stemi 2000	Zeiss
Thermocycler	Bio Rad
Thermomixer 5436	Eppendorf
Vibratom Leica VT 1000S	Leica
Vortex	Scientific Industries
Water bath	GFL (Gesellschaft für Labortechnik)
Zeiss Axio imager M1	Zeiss

2.1.8 Miscellaneous material

Description	**Source of supply**
Forceps (110 mm, straight)	NeoLab
Glass cover slips	Thermo Fisher
Glass slides	Menzel Gläser
LC480-PCR-plate	Roche
Mach1 T1 Phage-resistant Chemically Competent *E. coli*	Homemade
MaTek dishes	MaTek
Nail polish	Essence
Parafilm	Pechiney
Paramecia	Homemade
PCR tubes (0.2, 0.5 ml, thin walled)	Eppendorf
Random primer ($3^{\mu g}/_{\mu l}$)	Thermo Fisher
Reaction tubes (1.5, 2 ml)	Eppendorf
Sandpaper 180	Bauhaus
Superglue	UHU
Universal probe library	Roche

2.1.9 Oligonucleotides

All oligonucleotides were acquired from Eurofins. The RT-qPCR primer for GAPDH and axin2 were ordered by Sergio P. Acebron and thus do not have an internal stock number.

Primer used to generate probes for *in situ* hybridisation	**5'→ 3' Sequence**	**Internal number**
lef1.1_fwd	GAAGAGGAGGGAGACTTGGC	JW6175
lef1.1_rev	CAGTGGTGGTGTGATTTGCC	JW6176
lef1.2_ fwd	AACAGCAACAACCACGATGC	JW6177
lef1.2_ rev	GAATCCCAGTTGCGTGAGGA	JW6178
myc_ fwd	CCTGCAGGATCTGAACACGT	JW6181
myc_ rev	GTCGGACTGCATGCTGTAGA	JW6182
myca_ fwd	ATCCCGAGTACCTACGGGAC	JW6179
myca_ rev	TCAAGTCGTCGCTTCAGCTC	JW6180
sox2_ fwd	CTTCATGGTGTGGTCCCGAG	JW6183
sox2_ rev	CATGTCCCTCAGATCACCGC	JW6184
sp5a_ fwd	TGAAACACTGCAAGCTTTTCTAC	JW6185
sp5a_ rev	GGACACCTGCACCTCCTG	JW6186
sp5l_ fwd	GCTCTTTCCTTCCTGGCCAC	JW6187
sp5l_ rev	GTGCCTTCAGGTGAGAGGTC	JW6188
Sequencing primer		
M13uni(-21):	TGTAAAACGACGGCCAGT	
M13rev(-29)	CAGGAAACAGCTATGACC	
Cre/loxP construct (after 2nd loxP)_fwd	GCTTGATATCGAATTCCTGCAGCCC	JW0832
RT-qPCR primer (+ UPL probes)		
gapdh_fwd (probe #87)	CATTGTTGAGGGCCTGATG	
gapdh_rev (probe #87)	GGGTCCGTCCACAGTCTTC	
axin2_fwd (probe #25)	TCTGGCCCAGCTAGAGGAG	
axin2_rev (probe #25)	TGGATCCCAGACAGTAAATGC	
dn-gsk3_fwd (probe #121)	GCATGAAAGTCAGCCGAGAT	JW4752
dn-gsk3_rev (probe #121)	CCTGGGGTCGCTACTACTGT	JW4753
wnt3a_fwd (probe #131)	CTGGCAGCTGTGAAGTGAAG	JW4756
wnt3a_fwd (probe #131)	GAGGAAATCCCCGATGGT	JW4757

2.1.10 Plasmids

Plasmids	**Source/Internal stock number**
pGEM-T Easy	Promega
Sc(*ubi*::loxP_mCherry_loxP_eGFP-DN-GSK3)	3753
Sc(*ubi*::loxP_mCherry_loxP_CA-LRP6-eGFP)	3752
Sc(*ubi*::loxP_mCherry_loxP_FLAG-CK1γ)	3755
Sc(*ubi*::loxP_mCherry_loxP_FLAG-DN-CK1γ)	3796
Sc(*ubi*::loxP_mCherry_loxP_Wnt3a-His)	3759
Sc(ubi::loxP_mCherry_loxP_FLAG-Dkk1)	4118

Tol2(7xTCF-*Xla.Siam*::GFP)	4131
Tol2(7xTCF-*Xla.Siam*::nlsmCherry)	4208
Sc(7xTCF-*Xla.Siam*::CreERT2 *cmlc2*::GFP)	6492
Axin2.1 cDNA in pGEM®	3698
Axin2.2 cDNA in pGEM®	3699

All plasmids described exhibit a bacterial origin of replication. In the following the vector features relevant to this thesis shall be described.

2.1.10.1 pGEM-T Easy vector

The pGEM-T Easy vector was acquired from Promega. It features an ampicillin resistance gene and a lacZ gene for blue/white selection with IPTG and X-Gal. The vector had been linearized within the lacZ gene and a thymidine had been added to both 3´-ends by Promega. Hence, this vector is suitable for ligation with inserts that feature A-overhangs. The pGEM-T Easy vector was used to clone the cDNA fragments used for *in situ* probe generation. For this, PCR products generated from cDNA were purified and A-tailed before they were ligated to the pGEM-T Easy vector. Inserts cloned into pGEM-T Easy were sequenced using M13uni(-21) and M14rev(-29).

2.1.10.2 Functional lineage tracing constructs

All constructs for generating the transgenic lines used for functional lineage tracing are identical except for the gene expressed after recombination. Additionally, all constructs feature an ampicillin resistance gene and ISceI sites flanking the functional lineage tracing construct. Wnt signalling components were cloned from: pCS2 CA-LRP6-GFP and pSC2 DN-GSK3-eGFP were gifts from Edward De Robertis (Addgene plasmid #29682 & #29681) (Taelman et al., 2010), pCS2- Wnt3a-His was a gift from Thomas Holstein and pCS2 FLAG-DN-CK1γ was a gift from Christof Niehrs, which was used to produce pCS2 FLAG-CK1γ by Daigo Inoue via mutagenesis PCR.

2.1.10.3 Vectors used for mRNA production

Vectors used for mRNA production were pSC2 DN-GSK3-eGFP and pCS2- Wnt3a-His. They were linearized, purified and then transcribed with Sp6. GFP and Cre mRNAs were gifts from Beate Wittbrodt.

2.1.11 Medaka lines

Medaka lines used	**Internal stock number**
Cab F60-64	4564, 5266, 5692, 6097, 6480
Heino H F28	6735
Sc(*rx2*::H2B-eGFP)	6626
Sc(*tlx*(3.5kb)::GFP), Sc(*rx2*::H2B-RFP)	6622
Sc(*atoh7*::GFP)	6028
GaudiRSG	6801
GaudiLxBBW	5390
Sc(*hsp*70::Cre *cmlc2*::GFP)	6921
Sc(*rx2*::CreERT2 *cmlc2*::CFP)	6165
Sc(*tlx*::CreERT2 *cmlc2*::CFP)	5759
Sc(*atoh7*::CreERT2 *cmlc2*::CFP)	6864
Sc(ubi::loxP_mCherry_loxP_FLAG-Dkk1)	Not active
Medaka lines created	
Sc(*ubi*::loxP_mCherry_loxP_eGFP-DN-GSK3)	Line1: 6976, Line2: 7104
Sc(*ubi*::loxP_mCherry_loxP_CA-LRP6-eGFP)	Not active
Sc(*ubi*::loxP_mCherry_loxP_FLAG-CK1γ)	Line1: 6458, Line2: 7107
Sc(*ubi*::loxP_mCherry_loxP_FLAG-DN-CK1γ)	Line3: 7074, Line4: 7058, Line5: 7057
Sc(*ubi*::loxP_mCherry_loxP_Wnt3a-His)	Line1: 7121, Line2: 7105
Tol2(7xTCF-*Xla.Siam*::GFP)	Line1: 6978, Line4: 7018
Tol2(7xTCF-*Xla.Siam*::nlsmCherry)	Line3: 7055
Sc(7xTCF-*Xla.Siam*::CreERT2 *cmlc2*::GFP)	Line1: 6977, Line2: 7025

The inbred medaka Cab strain was used for *in situ* hybridisation, immunostainings and generation of transgenic animals. The inbred Heino H stain was used for double fluorescent *in situ* hybridisation. All transgenic lines were created either by Meganuclease (Sc) or Tol2 mediated integration. The fluorescent reporter lines feature expression of histone-associated GFP/ RFP (*rx2*) or cytosolic GFP (*tlx* and *atoh7*) under the respective promoters. Transgenic lines of the Cre/loxP based toolkit are described in detail in sections 1.3.1 and 3.2.1. The Cre driver lines additionally feature GFP or CFP expression in the heart used for screening. The Wnt reporter lines (data not shown) feature seven

repeats of the TCF binding site followed by the *siamois* minimal promoter from *Xenopus laevis* and either cytosolic GFP or nuclear mCherry as fluorescent reporters. The Wnt responsive Cre lines (data not shown) contain the seven TCF sites followed by the *siamois* minimal promoter driving expression of CreERT2 and additional expression of GFP in the heart.

2.2 Molecular biology methods

2.2.1 Heat shock transformation

Mach1 T1 Phage-resistant chemically competent *E. coli* were thawed on ice before 5 µl ligation reaction mixture were added to 50 µl competent cells, gently mixed by stirring and incubated for 5 additional minutes on ice. The heat shock was performed for 30 - 45 s at 42°C. Then the mix was incubated on ice for 2 min, 250 µl TB-medium were added and the mix was incubated again for 45 – 60 min at 37°C and approximately 200 rpm. Afterwards, the bacteria were plated on pre-warmed bacterial LB-agar plates, supplemented with the appropriate antibiotic (100 $^{\mu g}/_{ml}$ ampicillin or 50 $^{\mu g}/_{ml}$ kanamycin), IPTG (100 µM) and X-Gal (20 $^{\mu g}/_{ml}$) if needed and incubated overnight at 37°C.

2.2.2 Plasmid preparation (Mini & Midi)

For small-scale plasmid preparations, 2 ml LB medium supplemented with the appropriate antibiotic (100 $^{\mu g}/_{ml}$ ampicillin or 50 $^{\mu g}/_{ml}$ kanamycin) were inoculated with a single colony and incubated for 6 – 16 h at 37°C and 200 rpm. The suspension was then transferred to a 2 ml tube, centrifuged for 1 min at 14 000 rpm and the supernatant was discarded. 250 µl P1 were added and the pellet was dissolved completely by vortexing. Then, 250 µl P2 were added, the solution was mixed by inverting the tube 4 - 6 times and the mixture was incubated for 3 - 5 min at room temperature. In the following step, 250 µl P3 were added, the solution was mixed by inverting the tube 4 - 6 times before the mixture was centrifuged for 10 min at 14000 rpm. The supernatant was carefully transferred to a 1.5 ml tube avoiding any transfer of the precipitant. 500 µl isopropanol were added to the supernatant, the tube was inverted 4 - 6 times and then centrifuged for

20 min at 14 000 rpm. Subsequently, the supernatant was removed, 500 µl 70% ethanol were added and the tube was centrifuged again for 10 min at 14 000 rpm. Finally, the supernatant was removed as completely as possible; the precipitated DNA was dried on air for 5 min and dissolved in 50 µl Elution buffer (EB) or dH_2O. The purified plasmid DNA was stored at -20°C.

For medium scale plasmid preparations 50 ml LB medium supplemented with the appropriate antibiotic (100 $^{\mu g}/_{ml}$ ampicillin or 50 $^{\mu g}/_{ml}$ kanamycin) were inoculated with 3 µl bacterial culture and incubated overnight at 37°C and 200 rpm. The plasmid purification was performed using the Plasmid Midi Kit with the following alterations to the manufacturer's protocol: First, the bacterial overnight culture was harvested by centrifugation at 4 000 rpm for 30 min. Second, the centrifugation step after addition of buffer P3 was replaced by filtration of the solution using filter paper before applying the solution to the column. Third, DNA precipitation was performed using 4 instead of 3.5 ml isopropanol and the subsequent centrifugation was done at 4 000 rpm for 60 min instead of 15 000 rpm for 30 min. Finally, the isopropanol was not decanted completely, but the pellet was resuspended in the remaining approximately 500 µl liquid, transferred into a 1.5 ml tube and 70% ethanol was added to yield a total volume of 1.5 ml.

2.2.3 Restriction digest

For analytic restriction digests, 1 µl FastDigest Green Buffer (10x), 0.2 µl of the desired restriction enzymes and 2.5 µl plasmid DNA (200 – 700 $^{ng}/_{\mu l}$) in a total volume of 10 µl were incubated for 0.5 – 1 h at 37°C and subsequently analysed by gel electrophoresis.

For preparative digests 5 µl FastDigest Buffer (10x), 0.5 - 1 µl of the desired restriction enzymes and either 2 - 4 µg plasmid DNA or 30 µl PCR product in a total volume of 50 µl were incubated for 2 h or overnight at 37°C and subsequently the desired DNA fragment was isolated by gel electrophoresis.

2.2.4 Blunting

Blunting reactions were performed using 2 µl T4 DNA Polymerase (5 $^{U}/_{\mu l}$), 0.66 µl dNTPs (2.5 mM), 30 µl linearized and purified plasmid and 10 µl T4 DNA Pol Buffer in

a total reaction volume of 50 µl. The reaction mixture was incubated for 30 min at room temperature and subsequently purified.

2.2.5 Ligation

Ligation reactions were performed using 1 µl T4 DNA Ligase (5 $^{U}/_{µl}$), 1 µl 10x T4 DNA Ligase Buffer and 20 – 100 ng linear vector DNA in a 3:1 molar ratio of insert over vector DNA in a total reaction volume of 10 µl. The reaction mix was incubated for 20 min - 1 h at 22°C. 5 µl were used in a subsequent transformation.

For ligations with pGEM-T Easy, 1 µl T4 DNA Ligase (5 $^{U}/_{µl}$), 5 µl 2x Rapid Ligation Buffer, 0.5 µl (25 ng) pGEM-T Easy Vector and 3.5 µl linear insert DNA (amplified via PCR, purified via DNA clean-up and A-tailed) were mixed and incubated overnight at 4°C. 5 µl were used in a subsequent transformation.

2.2.6 Polymerase chain reaction (PCR)

To amplify a DNA fragment from plasmid template DNA in order to clone those fragments, a PCR reaction was assembled according to Table 1. The PCR programme is shown in Table 2.

Table 1. PCR reaction mixture to amplify fragments from plasmid DNA.

Volume [µl]	Reagent
10	5x Q5 Reaction Buffer
4	dNTPs (2.5 mM)
2.5	Primer forward (10 µM)
2.5	Primer reverse (10 µM)
2	Template DNA (50 $^{ng}/_{µl}$)
0.5	Q5 High-Fidelity DNA Polymerase
Ad. 50 µl	ddH_2O

Table 2. PCR programme to amplify fragments from plasmid DNA.

Step no.	Programme
1	98°C for 30 s
2	98°C for 10 s
3	Annealing temperature of the primers (calculated with NEB T_m Calculator) for 30 s
4	72°C for 20 - 30 s per 1 kb PCR product
5	Go to step 2 for 30 times
6	72°C for 2 min

To amplify DNA fragments from cDNA for cloning into pGEM-T Easy and generation of probes for *in situ* hybridisation, PCR was performed according to Table 3 and Table 4.

Table 3. Reaction mixture to amplify fragments from cDNA.

Volume/mass	Reagent
10 µl	5x Q5 Reaction Buffer
4 µl	dNTPs (2.5 mM)
1 µl	Primer forward (10 µM)
1 µl	Primer reverse (10 µM)
5 µl	cDNA from Stage 36/38 embryos (< 200 $^{ng}/_{µl}$)
0.5 µl	Q5® High-Fidelity DNA Polymerase
Ad. 50 µl	ddH_2O

Table 4. PCR programme to amplify fragments from cDNA.

Step no.	Programme
1	98°C for 30 s
2	98°C for 10 s
3	Annealing temperature of the primers (calculated with NEB T_m Calculator) for 30 s
4	72°C for 20 s
5	Go to step 2 for 34 times
6	72°C for 2 min

Subsequently PCR products were purified by gel electrophoresis if needed followed by a DNA clean-up.

2.2.7 Gel electrophoresis

Gel electrophoresis was performed using a 0.8 or 1% agarose gel in TAE buffer in an electrophoresis chamber filled with TAE. Orange Loading Dye (6x) was added to PCR products or preparative restriction digests of plasmids (analytic digests and denatured mRNA already contained loading dye). A DNA ladder and the samples were loaded into the pouches of the agarose gel and a voltage of 130 V was applied to the gel electrophoresis chamber for 0.5 - 1 h depending on the sizes of the DNA fragments. The gel was stained in an EtBr bath (2 $^{\mu g}/_{ml}$ in TAE) for 20 min and captured with a gel documentation system using a UV lamp. The desired fragments created by preparative restriction digests or PCRs were cut out of the gel with a scalpel. Subsequently, a DNA clean-up was performed.

2.2.8 A-tailing

For addition of an A-tail to DNA fragments featuring blunt ends, purified PCR products were used. The reaction was assembled according to Table 5, incubated at 72°C for 25 min and subsequently used in a ligation reaction.

Table 5. Reaction mixture for A-tailing.

Volume [µl]	Reagent
7.25	Eluate from gel purification
1	PolBuffer B (10x)
1	dATPs (2 mM)
0.25	Taq DNA Polymerase Roboklon (5 $^{U}/_{\mu l}$)

2.2.9 DNA clean-up

The clean-up of PCR products or DNA fragments cut out of an agarose gel was performed using the innuPREP DOUBLEpure Kit according to the provided protocol. In the elution step 15 - 30 µl Elution Buffer or ddH_2O were used.

2.2.10 Quantitative Real-time PCR (RT-qPCR)

For quantification of gene transcription, the RNA of medaka embryos was extracted, reverse transcribed to yield cDNA and finally quantified by qRT-PCR with the Roche Lightcycler480 and universal probe library (UPL) mono-colour hydrolysis probes as described below. All primers and the corresponding UPL-probes are listed in section 2.1.9.

2.2.10.1 RNA extraction

For extraction of total RNA, medaka embryos were washed with ERM, the medium was removed completely and 1 ml TRIzol reagent was added. Lysis was performed by destroying the chorions with pestles and vortexing for 1 min. Afterwards, the samples were frozen at -80°C for at least 1 h. Samples were thawed at 37°C on a shaker for 1 min and put on ice immediately. Next, 200 µl chloroform ($^1/_5^{th}$ of the volume) was added and mixed for 30 s by vortexing. The solution was centrifuged at 14 000 rpm for 30 min at 4°C, the aqueous (upper) phase (usually 350 µl) was transferred into a new tube and mixed with the same volume of isopropanol. RNA was precipitated for at least 1 h at -80°C followed by another centrifugation step at 14 000 rpm for 25 min at 4°C. The supernatant was discarded, the pellet was washed with 1 ml 70% ice-cold ethanol (with RNase-free H_2O), incubated on ice for 5 min, centrifuged at 14 000 rpm for 5 min and the supernatant was removed completely. The RNA pellet was dried on ice for 5 min, dissolved in 11 µl RNase-free H_2O and residual ethanol was evaporated at 50°C for 2 min. Finally, the RNA concentration was determined and the samples were stored at -80°C.

2.2.10.2 Reverse transcription

For reverse transcription, reaction mixture I was prepared on ice according to Table 6, incubated at 65°C for 5 min and then chilled on ice for 5 min.

Table 6. Reaction mixture I for reverse transcription.

Volume/mass	Reagent
1 µl	Random primer ($3^{\mu g}/_{\mu l}$)
0,5 – 1 µg	RNA
2 µl	dNTPs (5 mM)
Ad. 12 µl	ddH_2O (RNAse-free)

Next, reaction mixture II (Table 7) was added on ice, mixed and centrifuged briefly.

Table 7. Reaction mixture II for reverse transcription.

Volume [µl]	Reagent
4	5x First-Strand Buffer
2	0,1 M DTT
1	RiboLock RNase Inhibitor ($40\ ^{U}/_{\mu l}$)

The mixture was incubated at 25°C for 10 min and then at 42°C for 2 min. Now, 0.5 µl SuperscriptII was added by pipetting up and down (except for –RT controls) and another incubation step at 42°C for 90 min followed. Finally, the reaction was inactivated at 70°C for 15 min and the resulting cDNA was stored at -20°C.

2.2.10.3 Quantitative PCR

The cDNA was diluted 1:5 with RNase-free H_2O and 5 µl were used in an 11 µl PCR reaction. The primer/probe mixture was prepared according to Table 8. Excess primer/probe mixture was stored at -20°C for further use.

Table 8. Primer/probe mixture.

Volume [µl]	Reagent
5	Primer forward (100 µM)
5	Primer reverse (100 µM)
10	UPL-probe (10 µM)
30	ddH_2O

Next, the PCR mixture was assembled according to Table 9 in one well of an LC480-PCR-plate, mixed and centrifuged briefly.

Table 9. Reaction mixture for quantitative PCR.

Volume [µl]	Reagent
5.5	2x PROBES master mix
0.5	primer/probe mix
5	cDNA template

PCR amplification was performed with the mono colour hydrolysis probe template. The programme consisted of a pre-incubation step at 95°C, then 50 amplification cycles (95ºC for 10 s, 60ºC for 20 s, 72ºC for 1 s) and a final cooling step at 40ºC for 30 s. All samples were measured in duplicates. Differences in gene expression were analysed by normalising the expression levels of the genes of interest to the housekeeping gene GAPDH.

2.2.11 *In vitro* transcription

Transcription reactions were performed using the mMESSAGE mMACHINE Sp6 Kit. 1 µg linearized, purified DNA was used as transcription template and the "Capped Transcription Reaction Assembly" including the digestion of template DNA by Turbo DNase was performed according to the protocol. The recovery of RNA produced by transcription reactions was performed using the RNeasy Mini Kit according to the provided protocol and the elution was done with 30 µl RNase-free H_2O. After elution, the RNA was placed on ice immediately, 1 µl was transferred to a new tube for analysis of the RNA quality and the remaining RNA was stored at -80°C. The RNA was denatured in a mixture of 1 µl RNA, 2 µl Gel Loading Buffer II and 7 µl ddH_2O at 80°C for 5 min and then immediately applied onto an agarose gel for gel electrophoresis.

2.2.12 Probe generation for *in situ* hybridisation

Prior to probe generation the desired DNA fragment (~700 bp) was amplified from cDNA via PCR using primers flanking the sequence of interest, purified by gel electrophoresis

and DNA clean-up. Then, the DNA fragments were cloned into pGEM-T Easy, either amplified again using the primers M13for and M13rev or linearized (with EcoRI, SacII or SpeI) and finally purified again via gel electrophoresis and DNA clean-up. Probe generation was performed as previously described (Loosli et al., 1998). To generate an RNA probe labelled with digoxigenin, a reaction mix was assembled according to Table 10 and incubated at 37°C for 2 h.

Table 10. Digoxigenin probe generation mixture.

Volume/mass	Reagent
1 µg	Linear template DNA
2 µl	DTT (100 mM)
1.3 µl	rNTPs (ATP, CTP, GTP 15.4 mM, UTP 10.0 mM)
0.7 µl	digUTP (10 mM)
0.5 µl	RNasin® Ribonuclease Inhibitor
2 µl	Transcription-Buffer (10x)
Ad. 18 µl	ddH_2O
2 µl	RNA polymerase (Sp6 or T7)

After incubation, 1 µl Turbo DNase was added to the reaction mix and incubated at 37°C for 15 min. The recovery of the digoxigenin probe was performed using the RNeasy Mini Kit according to the provided protocol and the elution was done with 25 µl RNase-free H_2O. After elution, the digoxigenin probe was placed on ice immediately, 2 µl were transferred to a new tube for analysis of the RNA quality, 150 µl Hyb-Mix was added to the remaining digoxigenin probe and the mix was stored at -20°C. For analysis, the digoxigenin probe was denatured in a mixture of 2 µl digoxigenin probe, 5 µl 2x RNA Loading Dye and 1 µl ddH_2O at 80°C for 10 min and then immediately applied to an agarose gel for gel electrophoresis.

2.2.13 Sequencing

Sequencing of DNA was done by Eurofins MWG Operon with 15 µl of plasmid DNA (~ 250 $^{ng}/_{µl}$) or purified PCR products (2 $^{ng}/_{µl}$ for 150 – 300 bp or 5 $^{ng}/_{µl}$ for 300 – 1 000 bp) either including 10 pmol of the desired primer or a primer from Eurofins MWG Operon was selected.

2.3 Medaka experiments

2.3.1 Medaka maintenance and mating

Medaka fish colony was maintained as closed stock as described previously (Koster et al., 1997; Wittbrodt et al., 2002) under standard recirculating aquaculture conditions for medaka (28°C, 14 h light/10 h dark cycle). One night prior to mating, the males were removed from the tanks (3 females and one male each) and pooled in a separate tank. In the morning, the male fish were put back into the tanks with the females, eggs were collected after 25 – 35 min and placed into a petri dish filled with embryo rearing medium (ERM; ice cold in case they were injected subsequently). The embryos were extricated from the filament. After that they were transferred to ERM (ice cold in case they were injected) again and either injected or directly incubated at 28°C. The medium was changed every second day and infected eggs were removed from the dish. The medium was changed to hatching medium once the screening was completed.

2.3.2 RNA/DNA microinjection into zygotes

Microinjection was performed as described previously (Rembold et al., 2006a; Thermes et al., 2002). The injection mix was prepared on ice according to Table 11, centrifuged at 14 000 rpm for 5 min and placed on ice again until the injection. Injection concentrations for mRNAs were: Cre NLS 20 $^{ng}/_{\mu l}$, eGFP 20 $^{ng}/_{\mu l}$ (130 nM), eGFP-DN-GSK3 20 $^{ng}/_{\mu l}$ (130 nM) and Wnt3a 20 $^{ng}/_{\mu l}$ (45 nM).

Table 11. Injection mixtures for medaka.

mRNA injection		**DNA injection**	
Quantity	Reagent	Quantity	Reagent
0.75 µl	Yamamoto mix 10x	0.75 µl	Yamamoto mix 10x
20 - 100 $^{ng}/_{\mu l}$	mRNA	0.75 µl	ISceI Buffer
		10 $^{ng}/_{\mu l}$	Plasmid DNA
		1 µl	Meganuclease ISceI
Ad. 15 µl	ddH_2O	Ad. 15 µl	ddH_2O

Medaka zygotes were placed into the columns of an injection-plate (1.5% agarose in ddH_2O) filled with ice-cold ERM. The injection needle was filled with injection mixture, which was subsequently injected into each zygote (10 % of the visually estimated zygote volume). After injection of all zygotes was finished, they were incubated at 28°C.

2.3.3 Transplantation of cells at blastula stage

Transplantations were done as previously described (Ho and Kane, 1990; Rembold et al., 2006b). Before transplantation, the chorion of the embryos was removed. Therefore, eggs were collected and rolled on filter paper to remove the long attaching filaments that hold the eggs together. Then, the short villi on the surface of the chorion were removed by one of two alternatives. The first alternative is rolling the eggs on sandpaper until the villi are gone and the chorion surface appears roughened. The other alternative is digesting the villi with proteinase K. Therefore, eggs were incubated in a 1:1 mixture of proteinase K ($20^{mg}/_{ml}$) and ddH_2O for roughly 1 h 20 min in 2 ml tubes at 30°C shaking at 850 rpm until the villi were not visible any more. Then the eggs were washed with ERM 3x for 10 min each and maintained in ERM at 28 – 32°C. Once the embryos had reached stage 7, they were transferred to glass vials, the medium was removed completely, the embryos were covered with hatching enzyme and incubated at 28°C for 1 – 2.5 h. From this step on it is essential that the embryos do not get in contact with air. The hatching process was monitored by regular assessment under the bright field binocular. Once few embryos escaped their chorions, the hatching solution was diluted by careful addition of ERM and 3 further washes with ERM. The embryos were carefully transferred to either a dish coated with 1.5% agarose or a glass dish, both filled with ERM supplemented with Pen/Strep by a glass pipette and always surrounded by medium. For the actual transplantation, blastula stage embryos (stage 10 - 11) were transferred into the slots of a transplantation plate (1.5% agarose in ddH_2O) filled with ERM supplemented with Pen/Strep again with a glass pipette and surrounded by medium. The donor and acceptor embryos were positioned in a way that allows both to be distinguished and to assign the corresponding acceptors to a donor. After calibration of the transplantation needle, it was filled with ERM supplemented with Pen/Strep. Blastomeres were aspirated from the central-most and superficial-most region (future eye field) of a donor embryo and transferred to the same position in the corresponding host embryos. Each donor was used

to transplant cells into 3 – 5 hosts. Only 5 – 10 cells were transplanted into each host embryo. After transplantation, the embryos were maintained at 28°C in a fresh plate filled with 1% PEG in ERM supplemented with Pen/Strep. The medium was replaced every day. After 5 days, the medium was changed to ERM supplemented with Pen/Strep, which was also changed every day until hatch. Once the fish hatched, they were screened for red fluorescence in the eye and raised under standard conditions.

2.3.4 Cre/loxP mediated recombination

Cre/loxP mediated recombination in the transgenic lines used in this thesis is illustrated in Figure 11. Cre recombinase mediates the recombination of loxP sites. This leads to excision of the fragment flanked by loxP sites in case they are oriented head-to-tail or inversion in case they are oriented tail-to-tail. Hence, recombination leads to expression of nuclear GFP for GaudiRSG, eGFP fused to DN-GSK3 for eGFP-DN-GSK3 and membrane-bound CFP, cytosolic dTomato, cytosolic YFP or nuclear GFP for GaudiLxBBW. Recombination was either performed via heat shock (*hsp70*::Cre) or incubation in tamoxifen (*rx2*::CreERT2, *tlx*::CreERT2, *atoh7*::CreERT2) as described in the following.

2.3.4.1 Heat shock

Stage 34 – 37 embryos were moved to room temperature at least 2 h prior to the heat shock to allow them to equilibrate. Then, the medium was removed completely, the plastic dish was carefully dried without harming the embryos and filled with 43°C ERM. The embryos were placed in a 37°C incubator directly afterwards for 2 h. Finally, they were returned to 28°C.

2.3.4.2 Tamoxifen treatment

Tamoxifen treatment was performed just after the fish hatched. Therefore, they were incubated in 5 µM tamoxifen (Stock: 50 mM in DMSO stored at -20°C) in ERM supplemented with paramecia overnight at room temperature and protected from light.

Afterwards, the hatchlings were washed 5x for 10 min at room temperature prior to returning them to 28°C.

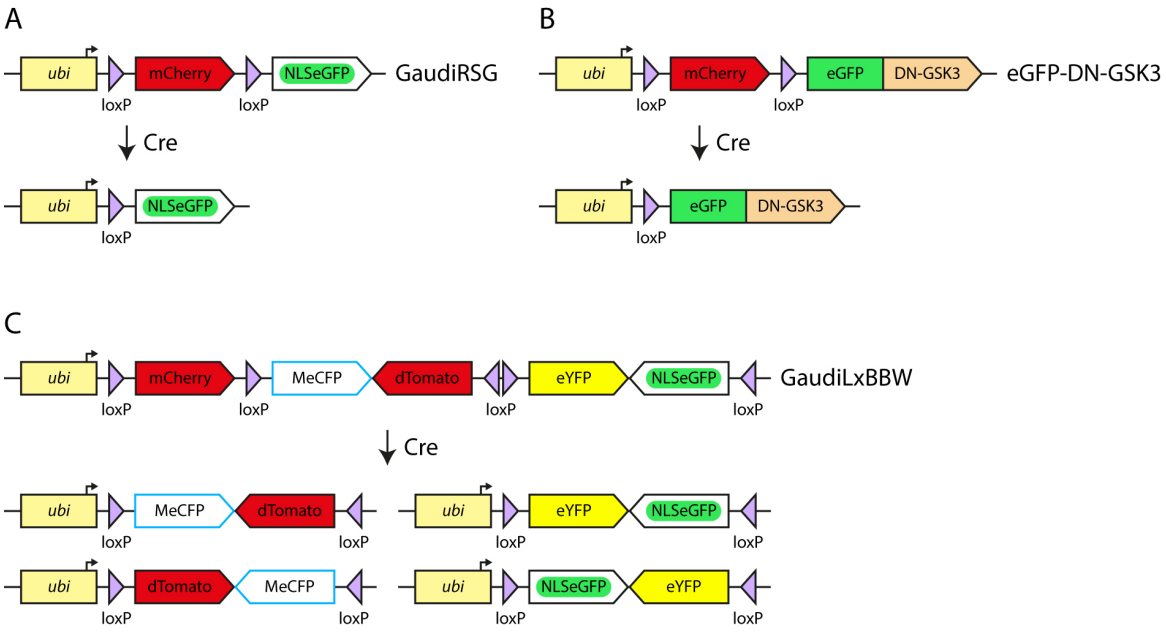

Figure 11. Cre/loxP mediated recombination in Gaudi and eGFP-DN-GSK3 lines. Cre recombinase mediates recombination of loxP sites. This leads to excision of the fragment flanked by loxP sites in case they are oriented head-to-tail or inversion in case they are oriented tail-to-tail. (A) GaudiRSG, (B) eGFP-DN-GSK3 and (C) GaudiLxBBW.

2.3.5 EdU treatment

When EdU treatment was performed after heat shock induction, the embryos were dechorionated prior to the heat shock as described in section 2.3.3. EdU treatment was performed by incubating the fish in 50 µM EdU (Stock: 10 mM in DMSO stored at -20°C) in ERM for 2.5 days at 28°C. Afterwards, the hatchlings were washed 5x for 10 min prior to fixation.

2.3.6 Fixation

Fixation was performed with formaldehyde. For this, fish were euthanized with 20x tricaine in ERM, briefly washed with 1xPTW and them incubated in 4% paraformaldehyde (PFA) in 2xPTW at 4°C overnight for hatchlings or over 3 days for adult fish. Afterwards, the fish were washed 5x for 10 min prior to cryosectioning, whole mount immunohistochemistry or *in situ* hybridisation.

2.3.7 Cryosectioning

For cryosectioning, fixed medaka hatchlings were transferred to 30% sucrose in PTW and kept at 4°C over night. Then, the medium was replaced by a mixture of 1:1 30% sucrose in PTW and tissue freezing medium and the hatchlings were incubated at least 5 days at 4°C. Next, the trunk was removed just posterior to the brain, the heads were transferred to plastic moulds, the moulds were filled with tissue freezing medium and the heads were positioned with the dorsal side facing the bottom of the plastic mould. The moulds were shock-frozen in liquid nitrogen and then stored at -80°C until further use. 20 min before sectioning, the moulds were transferred to the cryostat (-25°C) to allow them to equilibrate in temperature. The fish embedded in tissue freezing medium were removed from the plastic moulds, mounted in the cryostat, sectioned into 16 µm thin sections and transferred to glass slides. The glass slides were dried for 1 – 2 h at room temperature and stored at -80°C until further use.

2.3.8 Immunohistochemistry on sections

For immunohistochemistry on sections, three different protocols were used: Staining for pT-LRP6 was performed according to Table 12, staining for active β-catenin (ABC) according to Table 13 and staining for TUNEL/EdU according to Table 14. All steps were done at room temperature if not stated otherwise. For the pT-LRP6 staining, endogenous fluorescence of the reporter lines was preserved by performing all steps in the dark. Antigen retrieval was performed in a water bath. Blocking and antibody incubations were performed in humid chambers and the glass slides were covered with parafilm to prevent evaporation. All other steps were performed on a horizontal shaker.

Table 12. Steps for immunocytochemical labelling – pT-LRP6.

Step	Incubation conditions	Incubation reagent
Washing	1x 5 min	PBS
Opening	1x 10 min	0.1% Triton X100 in PBS
Washing	1x 5 min	PBS
Blocking	1 h	Blocking solution A (4% horse serum, 1 mM EGTA, 5 mM EDTA in PBST)
Primary antibody	Over night at 4°C	Primary antibody (anti-pT-LRP6 1:50) in

		blocking solution A
Washing	5x 5 min	PBST
Secondary antibody & DAPI	4 h at room temperature	Secondary antibody 1:400, Hoechst 1:400 in blocking solution A
Washing	3x 5 min	PBST
Washing	1x 5 min	PBS
Rinsing		H_2O
Mounting	Cover with coverslip, let dry at 37°C over night	Fluoromount
Storage	At 4°C for several days	

Table 13. Steps for immunocytochemical labelling – ABC.

Step	**Incubation conditions**	**Incubation reagent**
Washing	1x 5 min	PBS
Opening	1x 10 min	0.1% Triton X100 in PBS
Antigen retrieval	20 min at 95°C	10 mM sodium citrate (pH 6.0), 0.05% Tween 20 in PBS
Washing	1x 5 min	PBS
Blocking	1 h	Blocking solution B (4% natural goat serum, 1 mM EGTA, 5 mM EDTA in PBST)
Primary antibodies	Over night at 4°C	Primary antibodies (anti-ABC 1:30 & anti-Rx2 1:300) in blocking solution B
Washing	5x 5 min	PBST
Secondary antibodies & DAPI	4 h at room temperature, protected from light	Secondary antibodies 1:400, Hoechst 1:400 in blocking solution B
Washing	3x 5 min, protected from light	PBST
Washing	1x 5 min, protected from light	PBS
Rinsing		H_2O
Mounting	Cover with coverslip, let dry at 37°C over night, protected from light	Fluoromount
Storage	At 4°C for several days,	

	protected from light

Table 14. Steps for immunocytochemical labelling – EdU/TUNEL.

Step	Incubation conditions	Incubation reagent
Washing	3x 5 min	PTW
Blocking	1 - 2 h	10% horse serum in PTW
Washing	3x 5 min	PTW
Primary antibodies	Over night at 4°C	Primary antibodies (anti-GFP 1:200 & anti-Rx2 1:300), 1% horse serum in PTW
Washing	5x 5 min	PTW
Secondary antibodies & DAPI	2 - 3 h at 37°C, protected from light	Secondary antibodies 1:300, DAPI 1:1000, 1% horse serum in PTW
Washing	4x 5 min, protected from light	PTW
EdU/TUNEL detection	Described below	Described below
Washing	5x 5 min, protected from light	PTW
Mounting	Cover with coverslip, seal with nail polish	60% glycerol in PBS
Storage	At 4°C for several days, protected from light	

For detection of proliferation or apoptotic cells immunohistochemistry was followed by EdU detection or TUNEL staining respectively. EdU detection was performed with the Click-iT EdU Alexa Fluor 647 Imaging Kit. For this, Click-iT reaction cocktail was prepared according to the manufacturer's protocol (75 µl per slide). The slides were then incubated with the reaction cocktail covered with parafilm for 45 min at room temperature in a humidified chamber. The TUNEL staining was performed with the *In Situ* Cell Death Detection Kit, TMR red. Prior to TUNEL detection, the slides were fixed with 4% PFA in PTW (pH 7.4) covered with parafilm for 20 min at 18°C in a humidified chamber. Then the slides were permeabilised by incubating them in 0.1% Triton X100 and 0.1% sodium citrate in PBS (precooled) on ice for 2 min. Next, the TUNEL reaction mixture was prepared according to the manufacturer's protocol (75 µl per slide) and the slides were incubated for 1 h at 37°C covered with parafilm in a humidified chamber.

2.3.9 Whole mount immunocytochemistry

Whole mount immunohistochemistry on adult retinae was performed according to Table 15. The incubation steps were done at room temperature on a horizontal shaker if not stated otherwise. In case the staining was not done directly after fixation, the fish were incubated in 50% methanol in PTW for 10 min twice, then in 100% methanol for 10 min, the methanol was exchanged again and the fish were stored at -20°C. Just prior to the staining protocol the fish were rehydrated by incubating them in 50% methanol twice for 10 min and washing them three times in PTW for 10 min. Regardless whether the fish were stored in methanol or not, the retinae were dissected prior to the staining. For this, the eyes were removed from the head with pincers, then the choroid was carefully peeled off starting from the optic nerve head and lastly the lens was removed leaving only the retina, which was used for the staining. The acetone permeabilisation was performed in glass vials without shaking and the blocking and antibody incubation steps were done in tubes on a rotator (so that the tubes rotated sideways and not over head). All other steps were performed in petri dishes on a horizontal shaker.

Table 15. Steps for whole mount immunocytochemical labelling.

Step	Incubation conditions	Incubation reagent
Bleaching	Approx. 3 h, until no pigmentation remains	0.5% KOH, 3% H_2O_2 in H_2O
Washing	2x 5 min on rotator	PTW
Permeabilisation	15 min at -20°C	100% Acetone (precooled on ice)
Rinse	2x	PTW
Washing	2x 5 min	PTW
Blocking	1 - 2 h	Blocking solution C (1% BSA; 1% DMSO; 4% Sheep serum in PTW)
Primary antibodies	3 days at 4°C	Primary antibodies 1:200 in blocking solution C
Washing	5x 30 min	PTW
Secondary antibodies & DAPI	2 days at 4°C, protected from light	Secondary antibodies 1:200, DAPI 1:500 in blocking solution C
Washing	5x 30 min, protected from light	PTW
Storage	At 4°C for several days, protected from light	PTW

For imaging, the retinae where either mounted in MaTek dishes in a 1% low melting agarose mould or in 1% low melting agarose directly as illustrated in Figure 12. The bigger the retinae are, the more likely will the agarose deform the retinae. Hence, bigger retinae (2 – 2.5 month) were mounted in agarose moulds, whereas smaller retinae (2.5 weeks – 1.5 month) were mounted directly in agarose. After the agarose solidified, the dishes were filled with PTW.

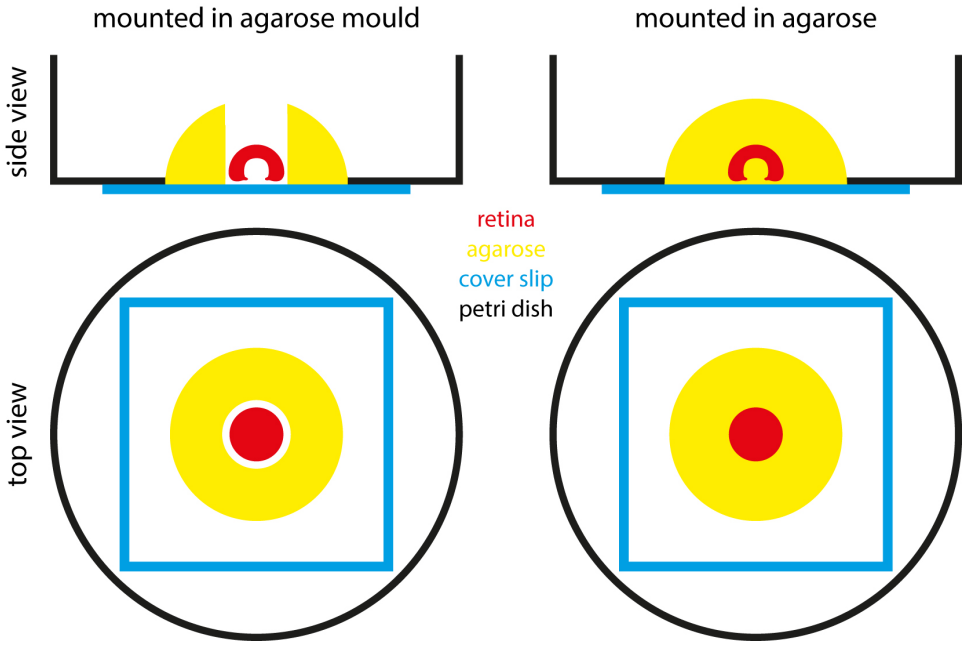

Figure 12. Mounting techniques for whole retinae. Retinae were either mounted in a 1% low melting agarose mould (2 – 2.5 month old fish) or in 1% low melting agarose directly (2.5 weeks – 1.5 month old fish).

2.3.10 Whole mount *in situ* hybridisation

Whole mount *in situ* hybridisation was performed as previously described (Loosli et al., 1998) according to Table 16 either on Cab or Heino H medaka stains. The incubation steps were done at room temperature in tubes on a rotator (so that the tubes rotated sideways and not over head) if not stated otherwise. The steps at 65°C were done in a water bath without rotation.

Table 16. Steps for whole mount *in situ* hybridisation.

Step	Incubation conditions	Incubation reagent
Dehydration	5 min each	25, 50, 100 and then 100% MeOH (in PTW)

Freezing	At least 3 days at -20°C in a glass vial, without rotation	100% MeOH
Rehydration	5 min each	75, 50 and then 25% MeOH in PTW
Washing	2x 5 min	PTW
Permeabilisation	2 h, without rotation	100 $^{ng}/_{µl}$ proteinase K in PTW
Proteinase inactivation	Rinse 2x	2 $^{mg}/_{ml}$ glycine in PTW
Fixation	20 min	4% PFA in PTW
Washing	5x 5 min	PTW
Equilibration	Few minutes, until fish sink to bottom, without rotation	Hyb-Mix
Prehybridisation	2 h at 65°C	Hyb-Mix
Hybridisation	Overnight at 65°C	6 µl Dioxygenin-probe + 150 µl Hyb-Mix preheated to 80°C
Washing	2 x 30 min at 65°C	50% formamide, 2x SSCT preheated to 65°C
Washing	15 min at 65°C	2x SSCT preheated to 65°C
Washing	2 x 30 min at 65°C	0.2x SSCT preheated to 65°C
Washing	3x 5 min	PTW
Blocking	2 h	5% sheep serum in PTW
Antibody incubation	Overnight at 4°C	Anti-Dioxigenin-AP Fab fragment 1:1000, 5% sheep serum in PTW
Washing	5x 10 min in dishes on shaker	PTW
Equilibration	2x 5 min in dishes on shaker	Staining buffer (SB)
Staining	Approx. 7 h, in dishes, protected from light	337.5 $^{µg}/_{ml}$ NBT, 175 $^{µg}/_{ml}$ BCIP in SB
Washing	3x 5 min, protected from light	PTW
Fixation	5 min, protected from light	4% PFA in 2x PTW
Washing	3x 5 min, protected from light	PTW
Storage	At 4°C for several days,	PTW

	protected from light

After whole mount *in situ* hybridisation, hatchlings where sectioned with the cryostat as described in section 2.3.7. Afterwards, the sections were coated with 60% glycerol in PBS, covered with a coverslip and sealed with nail polish prior to imaging.

2.3.11 Whole mount double fluorescent *in situ* hybridisation (WM-dFISH)

Whole mount double fluorescent *in situ* hybridisation was performed as described previously (Souren et al., 2009) according to Table 17 on Heino H medaka. The incubation steps were done at room temperature in tubes on a rotator (so that the tubes rotated sideways and not over head) if not stated otherwise. The steps at 65°C were done in a water bath without rotation. From the first staining reaction on (step 20) all steps were performed protected from light. Probes for Wnt reporter genes were digoxigenin-labelled and the *rx2* probe was fluorescein-labelled. The latter was kindly provided by Beate Wittbrodt.

Table 17. Steps for whole mount double fluorescent *in situ* hybridisation.

Step	Incubation conditions	Incubation reagent
Dehydration	5 min each	25, 50, 100 and then 100% MeOH (in PTW)
Freezing	At least 3 days at -20°C in a glass vial, without rotation	100% MeOH
Rehydration	5 min each	75, 50 and then 25% MeOH in PTW
Washing	2x 5 min	PTW
Permeabilisation	2 h, without rotation	100 $^{ng}/_{\mu l}$ proteinase K in PTW
Proteinase inactivation	Rinse 2x	2 $^{mg}/_{ml}$ glycine in PTW
Fixation	20 min	4% PFA in PTW
Washing	5x 5 min	PTW
Equilibration	Few minutes, until fish sink to bottom, without rotation	Hyb-Mix
Prehybridisation	2 h at 65°C	Hyb-Mix

Hybridisation	Overnight at 65°C	5 µl Dioxygenin-Wnt reporter-probe + 11 µl Fluorescein-*rx2*-probe + 100 µl Hyb-Mix preheated to 80°C
Washing	2 x 30 min at 65°C	50% formamide, 2x SSCT preheated to 65°C
Washing	15 min at 65°C	2x SSCT preheated to 65°C
Washing	2 x 30 min at 65°C	0.2x SSCT preheated to 65°C
Washing	3x 5 min	TNT, freshly prepared
Blocking	2 h	TNB
Antibody incubation	Overnight at 4°C	100 µl Anti-fluorescein-POD Fab fragment 1:50 in TNB
Washing	5x 10 min in dishes on shaker	TNT
Equilibration	5 min	TSA Amplification Diluent
Staining	2h, without rotation	100 µl Fluorescein Fluorophore Tyramide 1:50 in TSA Amplification Diluent
Washing	4x 10 min in dishes on shaker	TNT
Peroxidase inactivation	20 min in dishes, without shaking	1% H_2O_2 in TNT
Washing	5x 5 min	TNT
Blocking	1 h	TNB
Antibody incubation	Overnight at 4°C	100 µl Anti-digoxigenin-POD Fab fragment 1:50, DAPI 1:1000 in TNB
Washing	5x 10 min in dishes on shaker	TNT
Equilibration	5 min	TSA Amplification Diluent
Staining	2h, without rotation	100 µl Cy5 Fluorophore Tyramide 1:50 in TSA Amplification Diluent
Washing	3x 10 min in dishes on shaker	TNT
Washing	10 min in dishes on shaker	TN
Storage	At 4°C for several days	TN

After whole mount double fluorescent *in situ* hybridisation, hatchlings where sectioned with the vibratome.

2.3.12 Vibratome sectioning

Vibratome sectioning was either done with hatchlings after WM-dFISH or with immunostained whole retinae to reveal the retinal layers. For hatchlings, the trunk was removed just posterior to the brain. The heads or retinae were transferred to 6-well plates, medium was removed and the wells were filled with 4% agarose in TN or PTW, respectively. The heads were positioned with the dorsal side facing the bottom of the well. The retinae were positioned so that the CMZ faced the bottom of the well (except for the *atoh7*::CreERT2 induced retinae, where the CMZ faced the side of the well). Once the agarose had solidified, a small block of agarose including the specimen was cut out of the well with a scalpel and fixed upside down on the specimen mount using superglue. Then the specimen mount was fixed within the buffer tray and filled with TN or PTW, respectively. Hatchlings and *atoh7*::CreERT2 induced retinae were sectioned into 40 - 50 µm thin sections, the sections were collected in a 24-well plate filled with TN or PTW respectively. Finally, the sections were mounted on a glass slide, coated with 60% glycerol in PBS, covered with a coverslip and sealed with nail polish followed by imaging. For the other retinae, the CMZ was sectioned off in 45 µm thin sections. The sections were examined under a bright field binocular and as soon as clear retinal layers appeared on the sections, sectioning was stopped and the remaining part of the retinae was used for imaging. Therefore, the agarose block containing the remaining part of the retinae was fixed on a MaTek dish using 1% agarose with the retinae facing the bottom. After the agarose had solidified, the MaTek dish was filled with PTW and imaged directly.

2.3.13 Microscopy and Image analysis

General screening was performed using the Stereomicroscope Zeiss Stemi 2000 and screening for fluorescence was executed with the Nikon SMZ18 stereomicroscope. Hatchlings were anaesthetised with 1x tricaine in ERM prior to screening.

The colorimetric *in situ* hybridisations were imaged with the upright Zeiss Axio imager M1 (Plan-Apochromat lenses: 10x/0.45, 20x/0.8; DIC filter). The back views of the whole retinae were acquired with the upright Nikon AZ100 Multizoom confocal laser scanning microscope (5x Objective Plan Fluor Dry 0.5). The front views of whole retinae and all fluorescently labelled sections were imaged with the inverted confocal laser scanning microscopes Leica TCS SpE (ACS APO objective lenses: 10x/0.30 dry, 20x/0.60 multi-immersion, 40x/1.15 and 63x/1.30 oil; laser lines: 405 nm, 488 nm, 532 nm and 635 nm) and Leica TCS Sp8 (ACS APO objective lenses: 10x/0.30 dry, 20x/0.75 multi-immersion, 40x/1.2 oil and 63x/1.30 glycerol; laser lines: 405 nm, 488 nm, 532 nm and 638 nm) both equipped with one/several PMTs. Confocal imaging was performed in the sequential mode to minimize bleed through. Images of the Gaudi and eGFP-DN-GSK3 lines were not acquired with the same settings for laser intensity/PMT sensitivity, as the fluorescence signal for those lines varied considerably.

Images were processed using Fiji image processing software to adjust brightness and contrast, followed the PureDenoise plugin (standard automated settings, six cycles) (Luisier et al., 2010) for images acquired with the Leica TCS SpE/Sp8 or background subtraction by application of a rolling ball filter for images acquired with the Nikon AZ100.

Images of whole retinae are always shown so that the dorsal side is oriented to the top and ventral to the bottom.

3 Results

3.1 Wnt signalling is active in the medaka CMZ

In order to reveal which function Wnt signalling has in the CMZ, it is necessary to first describe where its components are present. Therefore, we tested key components of the Wnt/β-catenin signalling cascade, namely expression of Wnt ligands, phosphorylation of LRP6, presence of non-phosphorylated (active) β-catenin (ABC) and expression of canonical Wnt signalling target genes. We found that all of those components are present within or directly adjacent to the CMZ. The results for each of the experiments are described in this paragraph.

3.1.1 Wnt ligands are expressed by cells adjacent to the CMZ

First, we wanted to unravel where the source of Wnt signalling is located in the postembryonic retina, meaning which cells express Wnt ligands. Therefore, we performed whole mount *in situ* hybridisation for *wnt3a*, *wnt2*, *wnt2ba* and *wnt2bb* (4 out of approximately 28 Wnt paralogs found in teleost fish (Mwafi et al., 2014)) on medaka hatchlings, cryo-sectioned the fish afterwards and analysed the expression in the eyes (Figure 13). The signal for the mRNAs (violet) is located at the periphery of the eye (Figure 13 A-D). All Wnts tested show a very similar expression pattern. More specifically, they are located within the RPE directly adjacent to the CMZ (Figure 13 A'-D'). Hence, cells within the CMZ may be exposed to Wnt ligands produced by cells of the neighbouring RPE.

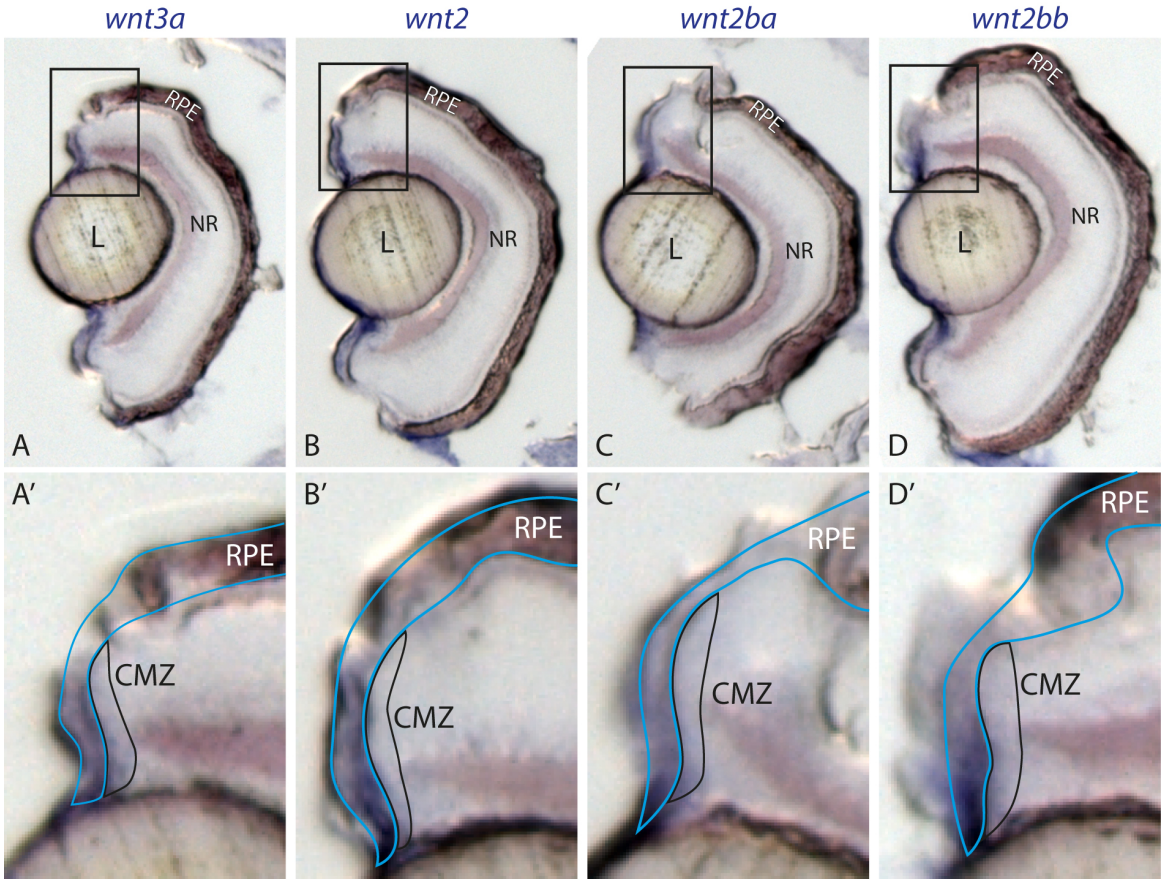

Figure 13. Wnt ligands are expressed in cells directly adjacent to the CMZ. (A-D) *in situ* hybridisation for *wnt3a*, *wnt2*, *wnt2ba* and *wnt2bb* on medaka hatchlings, shown are only the retinae. Signal is shown in violet (not pink). The mRNA of Wnts is detected in the periphery of the eye. (A'-D') show close-ups. Here, RPE is outlined in light blue and the CMZ in black (outlines drawn according to retinal anatomy). The violet signal is present within the RPE directly adjacent to the CMZ. RPE – retinal pigment epithelium, L – lens, NR – neural retina, CMZ – ciliary marginal zone. *In situ* hybridisations performed by Daigo Inoue.

3.1.2 LRP6 is phosphorylated in cells throughout the CMZ

Next, we asked which cells show phosphorylated LRP6 in the retina. As described above LRP6 has several phosphorylation sites. We chose to test for the phosphorylation at T1479, as this site is phosphorylated in a strictly Wnt dependent manner and an antibody exists which detects phosphorylated T1479, namely pT1479-LRP6 (in the following called pT-LRP6) (Davidson et al., 2005; Niehrs and Shen, 2010; Zeng et al., 2005). As the stainings for pT-LRP6 were very weak in medaka hatchlings when used in combination with other antibodies, we decided to perform the staining on three fish lines expressing fluorescent reporters under the promoters *rx2*, *tlx* and *atoh7*, respectively. This enabled us to get more specific information on the identities of the cells featuring LRP6 phosphorylation beyond knowing their location within the CMZ.

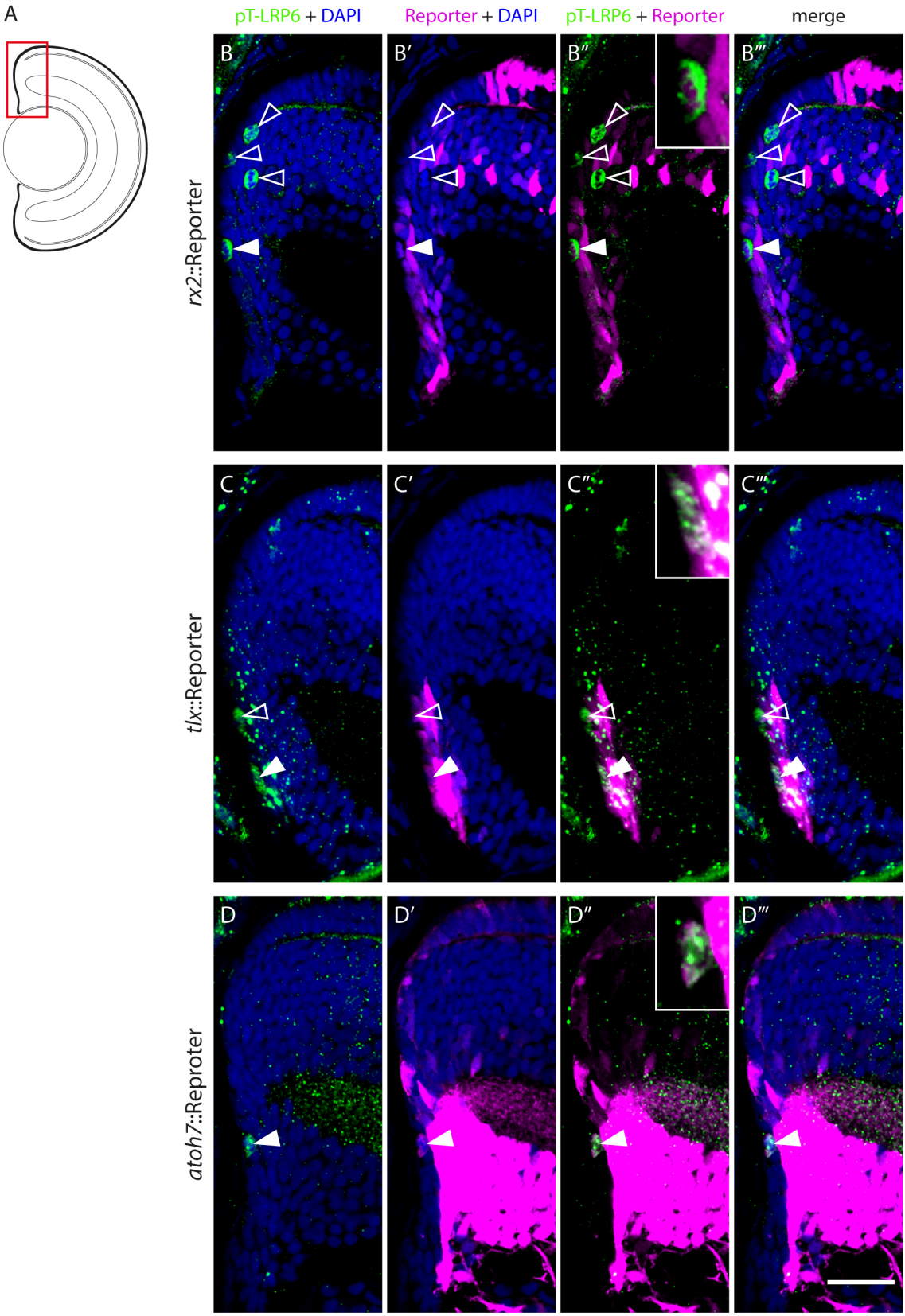

Figure 14. pT-LRP6 localises to cells throughout the CMZ. (A) Scheme of the eye highlighting the area (red) that is depicted in B-D’’’. (B-D’’’) Confocal stacks of immunostainings against pT-LRP6 (green) on *rx2* (B-B’’’), *tlx* (C-C’’’) and *atoh7* (D-D’’’) reporter lines (magenta). Cells in which the pT-LRP6 signal co-localises with the respective reporter are marked with filled arrowheads. Empty arrowheads mark cells featuring only the pT-LRP6 signal. pT-LRP6 positive cells were found within the *rx2*-, the *tlx* and the apical most part of the *atoh7*-domain but also outside of those domains. B’’-D’’ include close-ups of cells labelled by pT-LRP6 and the respective reporter. Immunohistochemistry performed by Ann Kathrin Heilig with suggestions for the protocol by Sergio P. Acebron. Scale bar 20 µm.

At the most peripheral part of the retina in which the CMZ is located (Figure 14 A), pT-LRP6 localises to *rx2* (B-B’’’), *tlx* (C-C’’’) or *atoh7* (D-D’’’) positive cells (filled arrowheads), but also to cells outside of the respective domains (empty arrowheads). The cells positive for pT-LRP6 are localised very close to the RPE in most cases and feature condensed DAPI staining, indicating that they are undergoing mitosis. The additional spotty pattern visible most notably in C-C’’’ is most probably due to precipitation of the antibody and occurred to a variable degree in all of the stainings with this antibody. Thus, LRP6 is phosphorylated in mitotic cells throughout the CMZ, meaning that it is active in both stem and progenitor cells.

3.1.3 Non-phosphorylated β-catenin is present in Rx2 positive cells

In order to determine in which cells of the CMZ β-catenin is not phosphorylated and thus degraded, we performed immunostainings on sections of medaka hatchlings against the active, non-phosphorylated, form of β-catenin (ABC, dephosphorylated on Ser33, Ser37 and Thr41). We analysed the staining in the CMZ (Figure 15 A). The signal for ABC (green) is localised to the cytosol of most Rx2 positive cells (dashed line) (B-B’’’ and C-C’’’). Only few cells in the Rx2-domain do not show ABC staining. Those are located at the peripheral tip of the Rx2 domain where the slow cycling cells reside (continuous line) (Wan et al., 2016). However, we were not able to detect clear ABC staining in the nuclei of cells, which may be due to low accessibility even with the use of the detergent Triton X100 or to a low signal-to-noise ratio. Consequently, non-phosphorylated β-catenin is restricted to Rx2 positive stem cells, although it is not visible in the peripheral-most tip cells.

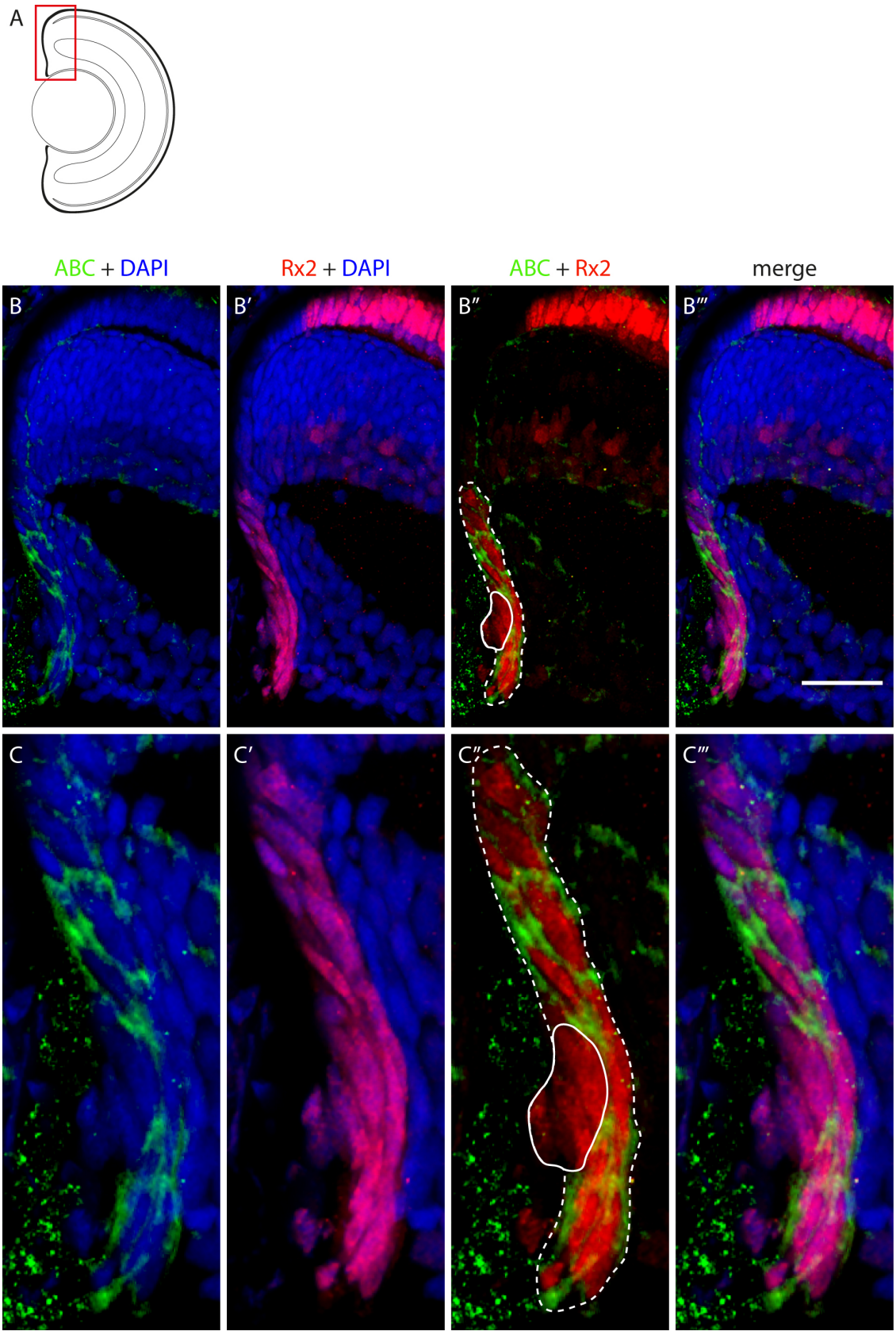

Figure 15. Non-phosphorylated β-catenin localises to Rx2 positive cells. (A) Scheme of the eye highlighting the area (red) that is depicted in B-B’’’. (B-B’’’) Confocal stacks of immunostainings on sections of medaka hatchlings against active β-catenin (ABC, green) and the Rx2 protein (red). (C-C’’’) Close-ups of the images above. The ABC staining is present in most Rx2 positive cells (dashed line) except for very few cells at the tip of the Rx2 domain (continuous line). Immunohistochemistry performed by Ann Kathrin Heilig with suggestions for the protocol by Sergio P. Acebron. Scale bar 20 µm.

3.1.4 Wnt/β-catenin target genes are expressed in *rx2* positive cells

The final components of the Wnt/β-catenin signalling cascade we studied where Wnt/β-catenin target genes. To this end, we produced probes against the transcripts of the following genes: *axin2.1*; *axin2.2*; *lef1.1*; *lef1.2*; *myc*; *myca*; *sp5l*; *sp5a* and *sox2*. We subsequently performed WM-dFISH for each Wnt target gene and *rx2* to compare the exact expression patterns, sectioned the embryos afterwards and analysed the signal in the CMZ (Figure 16). The majority of the Wnt target genes show a very similar expression pattern to *rx2*, namely *axin2.1*; *lef1.1*; *lef1.2*; *myca*; *sp5l* and *sp5a* (A-F'''). Only two genes were expressed in a subset of the *rx2* domain: *axin2.2* and *myc* (G-H'''). The mRNA of those genes is more restricted to the tip of the CMZ and is not present in as many cells towards the apical side compared to the *rx2* mRNA. On the other hand, *sox2* is the only gene we tested that features an expression domain which is larger than the *rx2* domain (I-I'''). Here, the domain reaches more cells towards the apical side than *rx2*. However the deviations from the *rx2* expression pattern are only few cells for each of the Wnt target genes, as highlighted with a dashed line (G'', H'' & I''). The bright green signal at the bottom right corner in most images is probably caused by probe trapping in the lens. The described expression patterns of all Wnt target genes in respect to *rx2* is summarised schematically in J. In summary, the expression of Wnt/β-catenin target genes (with one exception: *sox2*) is restricted to the *rx2* positive stem cells of the CMZ.

3.1.5 Summary: Localisation of Wnt/β-catenin signalling components in the CMZ

As described in the previous paragraphs, all analysed components of the Wnt/β-catenin signalling cascade localise to the CMZ. This paragraph summarises and consolidates the exact expression/localisation patterns of those components (Figure 17). Wnt ligands are expressed within the RPE in close proximity to the stem and progenitor cells of the CMZ (blue). Phosphorylated LRP6 (horizontal lines) is present in few, presumably mitotic, cells throughout the whole CMZ. To be specific those cells are located within the *rx2* (magenta), *tlx* (green) and *atoh7* (yellow) domains, beyond that they are also located more towards the apical side of the retina. However, active β-catenin (backward diagonal lines) and the expression of most Wnt target genes (forward diagonal lines) are restricted to *rx2* positive stem cells.

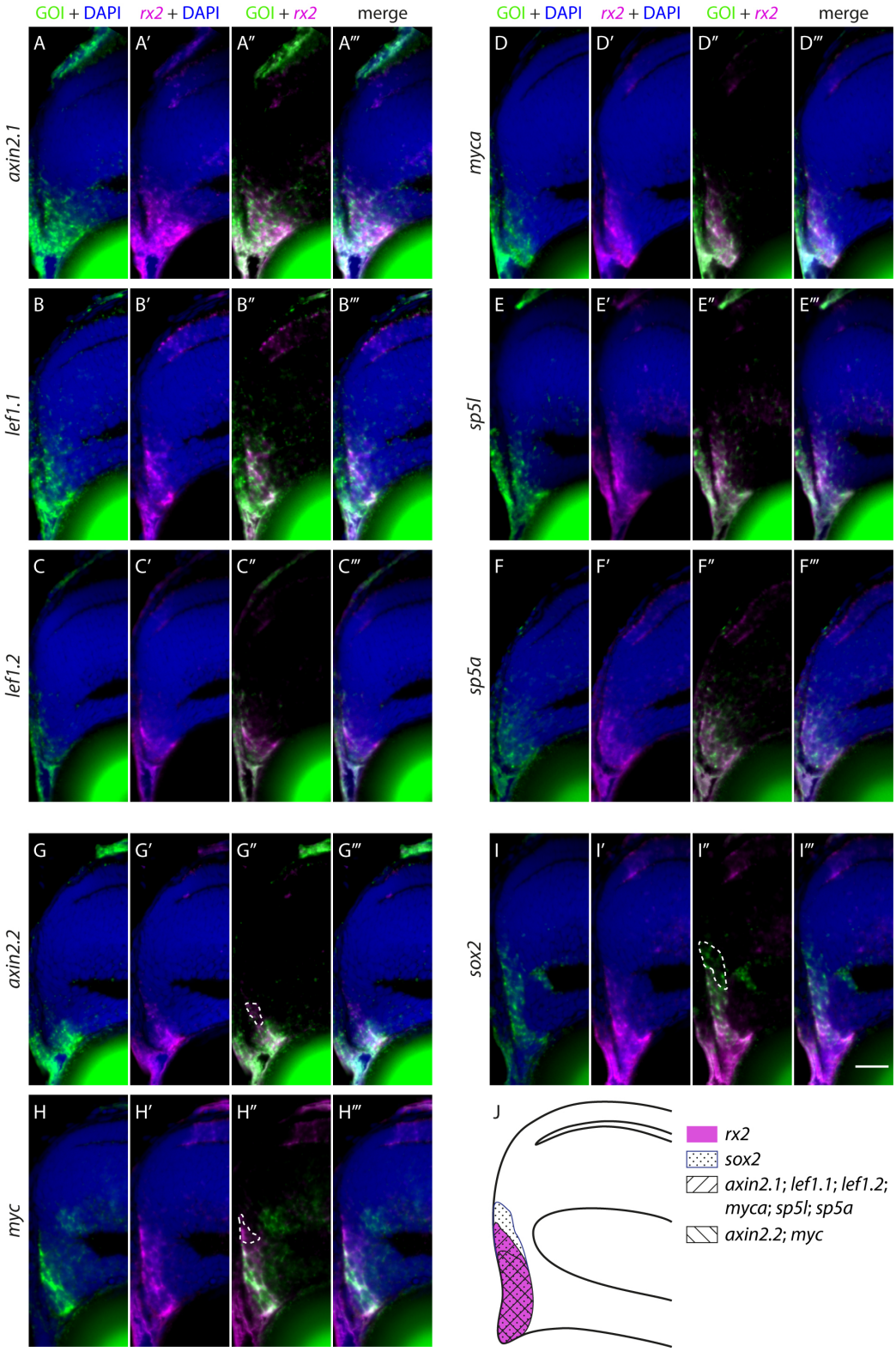

Figure 16. Wnt/β-catenin target genes are expressed mainly in the *rx2* domain. (A-I‘’’) Confocal images of sectioned WM-dFISH on medaka hatchlings. The region of the CMZ is shown as in the previous figures. The probes were designed against several Wnt target genes (*axin2.1*; *axin2.2*; *lef1.1*; *lef1.2*; *myc*; *myca*; *sp5l*; *sp5a* and *sox2*) shown in green and *rx2* shown in magenta. (J) Scheme summarizing expression patterns of Wnt target genes in respect to *rx2*. Most Wnt target genes are expressed in the same area as *rx2* (magenta), namely *axin2.1*, *lef1.1*, *lef1.2*, *myca*, *sp5l* and *sp5a* (forward diagonal lines). However, *axin2.2* and *myc* (backward diagonal lines) are expressed only in a subset of *rx2* positive cells. The expression domain of *sox2* (dotted pattern) on the other hand is larger than the *rx2* domain. The expression patterns deviating from the *rx2* domain are outlined with dashed lines (G’’, H’’, I’’). Note that the oversaturated green signal in the bottom right corner of most images is probably due to probe trapped in the lens. WM-dFISH performed by Ann Kathrin Heilig. Scale bar 20 µm.

Furthermore, there are even few cells at the tip of the *rx2* domain that lack active β-catenin. Hence, only *rx2* positive stem cells feature Wnt/β-catenin signalling, but additionally progenitor cells show activation of Wnt signalling on the level of phosphorylated LRP6.

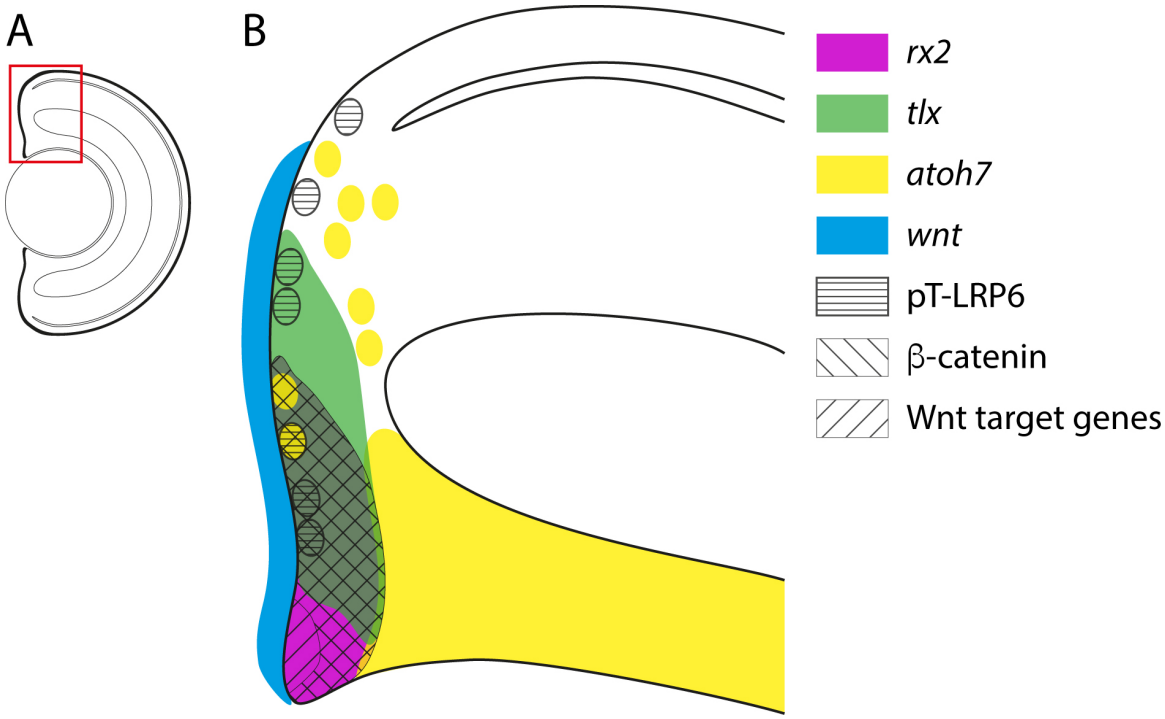

Figure 17. Major Wnt/β-catenin signalling components localise to the CMZ. (A) Scheme of the eye highlighting the area (red) that is depicted in B. (B) Scheme of the peripheral retina in which the CMZ is located. The expression patterns of important markers within the CMZ are shown: *rx2* (magenta), *tlx* (green) and *atoh7* (yellow). Wnt ligands (blue) are expressed in cells of the RPE directly adjacent to the stem and progenitor cells of the CMZ. pT-LRP6 (horizontal lines) localises to few probably mitotic cells within the *rx2*, *tlx* and *atoh7* domains but also outside of all three domains towards the apical side of the retina. Active β-catenin (backward diagonal lines) is present in the *rx2* domain (except for few cells at the tip) where several Wnt target genes (forward diagonal lines) are also expressed.

3.2 Modulation of Wnt signalling in single cells and their progeny

3.2.1 Generation of medaka lines that allow modulation of Wnt signalling in single cells and their progeny

After the detailed description where Wnt signalling is active in the CMZ, our next step is to specifically study the role of Wnt signalling in the differentiating lineage of retinal progenitors. In order to manipulate Wnt activity at single cell level, we have developed

tools for clonal expression of Wnt signalling components in the context of the entire retina, from stem cells to terminally differentiated cell types. To this end, I modified the GaudiRSG construct: The fluorescent protein that is only expressed upon Cre-mediated recombination was replaced by dominant negative GSK3 (DN-GSK3) fused to eGFP (in the following the line is referred to as eGFP-DN-GSK3) (Figure 18 and Figure 19 A). Thus, I am able to induce a fluorescent colour switch combined with functional modification of the canonical Wnt pathway in single cells (gainbow). I took advantage of the tight spatiotemporal organization of the fish retina to follow the complete lineage of a cell featuring modified Wnt signalling during the postembryonic life. This enables me to pinpoint the exact function Wnt fulfils in the retinal stem cell niche. The expression of DN-GSK3 results in the upregulation of Wnt/β-catenin signalling because β-catenin is no longer phosphorylated and thereby targeted for degradation (Pierce and Kimelman, 1995; Taelman et al., 2010; Yost et al., 1996). Although GSK3 is shared with other signalling pathways, it is a well-established component to test Wnt function (Jope and Johnson, 2004; Tejeda-Munoz and Robles-Flores, 2015).

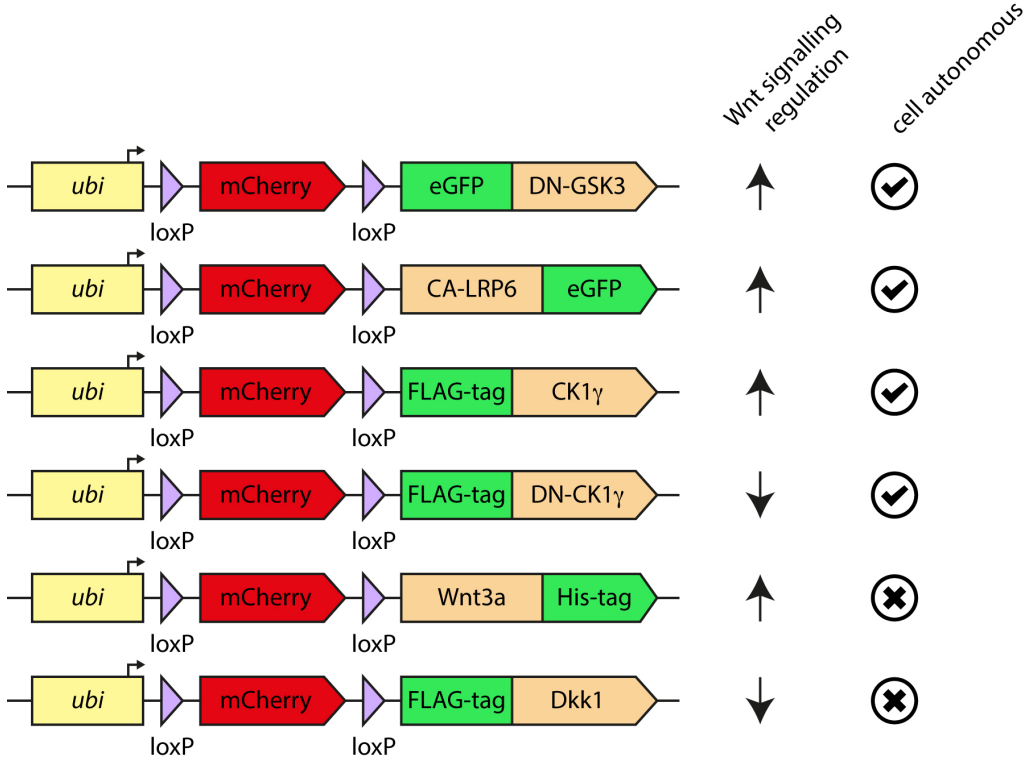

Figure 18. Transgenic lines that allow lineage tracing in combination with Wnt signalling modification created within this thesis. These lines allow Wnt signalling up- as well as downregulation either in a cell autonomous or non-autonomous manner. The FLAG-Dkk1 line was established by Daigo Inoue.

Beside the eGFP-DN-GSK3 line, we cloned constructs and created stable lines for several other Wnt signalling modifying components (Figure 18). All lines contain fusions between the Wnt signalling component and either fluorescent proteins or protein tags to allow for lineage tracing. With these lines, both Wnt signalling up- and downregulation can be addressed either in a cell autonomous or non-autonomous manner. This provides a comprehensive toolkit to study the Wnt pathway at various levels of the signalling cascade within the lineage of stem and progenitor cells.

Although we created several lines, this thesis focuses on the detailed analysis of eGFP-DN-GSK3 in different cell populations in the CMZ and their lineage.

To this end the eGFP-DN-GSK3 line was crossed to several different Cre expressing transgenic lines, namely: *hsp70*::Cre (Heat shock inducible ubiquitous Cre expression), *rx2*::CreERT2, *tlx*::CreERT2 and *atoh7*::CreERT2 (expression of Cre under the respective promoter plus tamoxifen-dependent nuclear localization of Cre) (Figure 19 A/B). The recombination construct consists of an ubiquitin promoter followed by a loxP-flanked mCherry in front of the fusion of eGFP and DN-GSK3. mCherry is expressed by default in all cells. Upon induction of Cre expression/translocation to the nucleus the mCherry is excised in a stochastic fashion and the recombined cells express eGFP-DN-GSK3. This fluorescent colour switch combined with DN-GSK3 expression is inherited by all daughter cells. Thus, I am able to address the specific effect DN-GSK3 expression has on *rx2*, *tlx* and *atoh7* positive cells and their lineages.

Figure 19 C illustrates a typical timeline of the lineage tracing experiments. Stochastic recombination is induced between stage 34 (heat shock) and hatch (tamoxifen incubation), then fish are allowed to grow for 2.5 weeks to 2.5 month and finally fixed and stained.

All lines mentioned are stable transgenic lines created using DNA microinjection combined with the meganuclease I-SceI (Thermes et al., 2002).

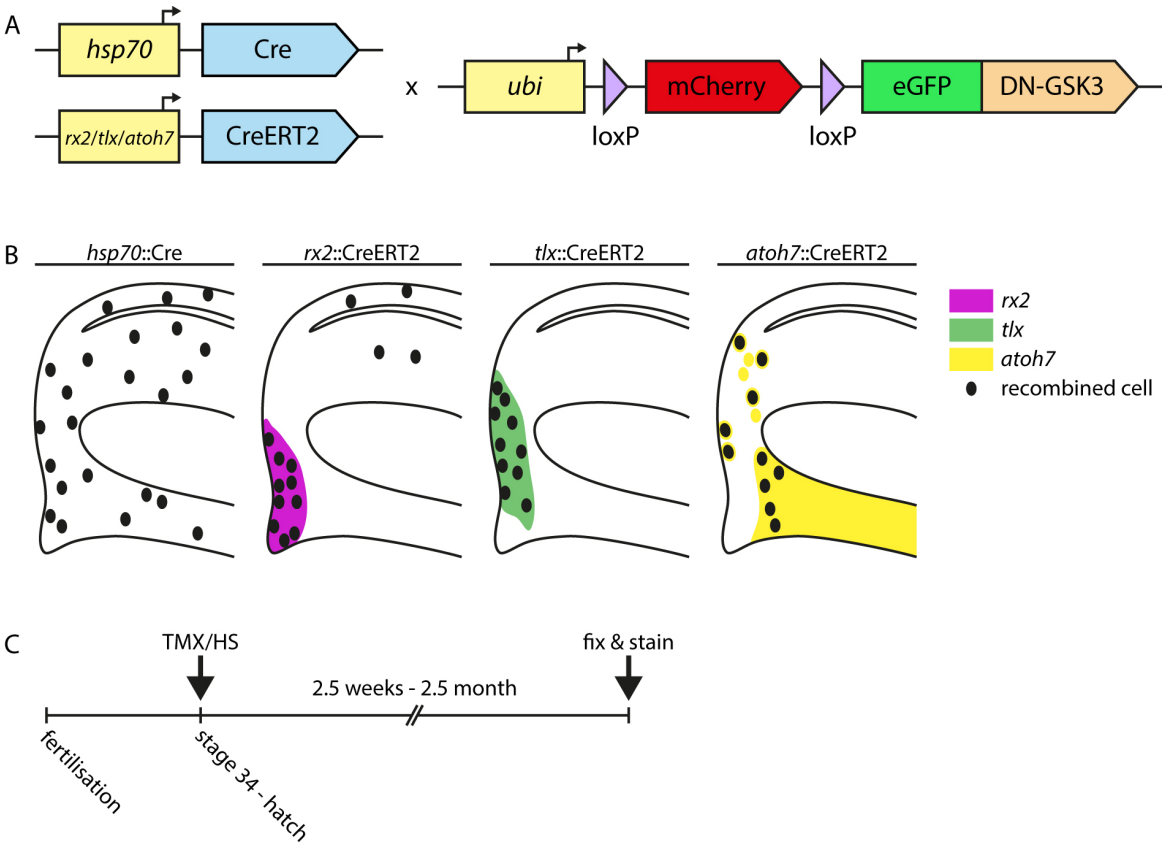

Figure 19. Experimental setup to study the impact of DN-GSK3 on different cell populations and their progeny. (A) Scheme of the transgenes used to induce stochastic Cre/loxP mediated recombination. Medaka lines carrying different transgenes for Cre expression were crossed to lines harbouring the recombination construct. The constructs for Cre expression are: *hsp70*::Cre (Heat shock inducible ubiquitous Cre expression), *rx2*::CreERT2, *tlx*::CreERT2 and *atoh7*::CreERT2 (expression of Cre under the respective promoter plus tamoxifen-dependent nuclear localization of Cre). The recombination construct consists of an ubiquitin promoter followed by a loxP-flanked mCherry in front of the fusion of eGFP and DN-GSK3. mCherry is expressed by default in all cells. Upon induction of Cre expression/translocation to the nucleus mCherry is excised in a stochastic fashion and the recombined cells express eGFP-DN-GSK3. This fluorescent colour switch combined with DN-GSK3 expression is inherited by all daughter cells. (B) Schemes of the peripheral retina illustrating the expression domains of the different Cre transgenes (*hsp70* ubiquitous, *rx2* magenta, *tlx* green & *atoh7* yellow) to show the areas in which stochastic recombination is induced (black oval cells). (C) Timeline of a standard recombination experiment: Cre mediated recombination is induced via heat shock or tamoxifen incubation between stage 34 and hatch followed by a growth period of 2.5 weeks up to 2.5 month. Finally the fish are fixed and stained.

3.2.2 Validation of Wnt modulation and expression pattern

Prior to analysing the impact of eGFP-DN-GSK3 on different cell types and their lineages, we validated two different aspects of the transgenic line: the functionality of eGFP-DN-GSK3 in medaka and the expression pattern of the ubiquitin promoter.

The eGFP-DN-GSK3 fusion was a gift from Edward De Robertis and published to function in *Xenopus* (Taelman et al., 2010). To confirm that it also upregulates Wnt/β-catenin signalling in medaka I injected eGFP-DN-GSK3, eGFP (negative control) or Wnt3a (positive control) mRNA into zygotes. At stage 17, I screened the embryos

injected with eGFP-DN-GSK3 or eGFP mRNA for green fluorescence, pooled the embryos for each construct into three groups (26-35 embryos/group), extracted the RNA and performed RT-qPCR for the Wnt/β-catenin target gene *axin2* (Figure 20 A). Transcription levels were normalised to the levels of the *GAPDH* housekeeping gene. *axin2* transcription increased more than 2-fold with Wnt3a mRNA compared to eGFP mRNA. The same effect could be observed with eGFP-DN-GSK3 injection and thus confirms that expression of this construct leads to Wnt/β-catenin upregulation in medaka. RT-qPCRs for *Wnt3a* and *GSK3* were performed as injection control and show that the mRNAs were injected successfully.

Next, I tested whether the Wnt/β-catenin upregulation could also be confirmed in the stable transgenic line. To this end I injected Cre mRNA into zygotes of three different lines: GaudiRSG (negative control), eGFP-DN-GSK3 and a line carrying a similar construct just with Wnt3a instead of eGFP-DN-GSK3 (see Figure 18, positive control). I discarded the injected embryos without transgenes (no red and/or green fluorescence) and screened the remaining embryos for phenotypes between 6 dpf and 8 dpf. I observed anterior truncations in the eGFP-DN-GSK3 as well as the Wnt3a line (Figure 20 B), which is a well known phenotype caused by Wnt upregulation (Bajoghli et al., 2009; Christian and Moon, 1993; Hoppler et al., 1996; Kelly et al., 1995; Kim et al., 2000) (see section 1.4.2) and which I also observed in the previous experiment. I categorised the severity of the phenotypes into “none”, “minor”, “medium” and “strong” and quantified them (Figure 20 B and C). All GaudiRSG embryos had wt phenotypes, meaning that the Cre mRNA does not cause any visible developmental defects. On the other hand, almost all of the Wnt3a embryos had strong anterior truncations. More than 60% of the eGFP-DN-GSK3 embryos also had anterior phenotypes although they were mostly not as severe as the Wnt3a ones.

Hence, injection of eGFP-DN-GSK3 mRNA and well as recombination in the stable eGFP-DN-GSK3 line leads to upregulation of Wnt/β-catenin signalling.

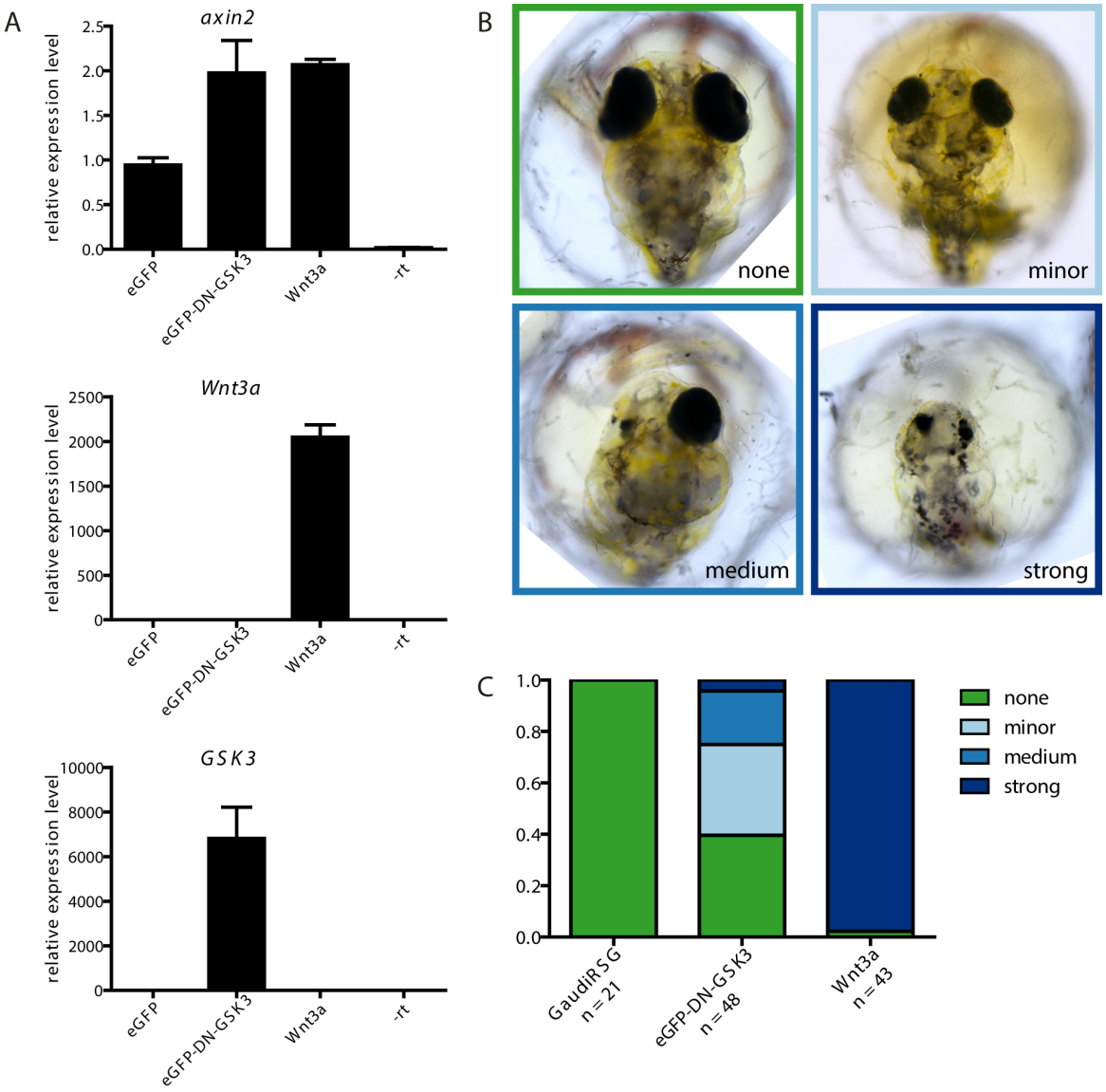

Figure 20. DN-GSK3 upregulates Wnt/β-catenin signalling in medaka. (A) Upper panel: Expression levels of the Wnt/β-catenin target gene *axin2* in stage 17 embryos injected with eGFP, eGFP-DN-GSK3 or Wnt3a mRNA into zygotes (concentrations: eGFP & eGFP-DN-GSK3 130 nM and Wnt3a 45 nM). *Axin2* levels are increased by 2-fold for Wnt3a and eGFP-DN-GSK3 compared to the control injections with eGFP. Middle and lower panel: RT-qPCRs for *Wnt3a* and *GSK3* on the same samples to verify successful mRNA injection. RT-qPCR was designed and analysed together with Sergio P. Acebron. (B & C) Validation of eGFP-DN-GSK3 in the stable transgenic medaka line. Embryos of the three stable transgenic recombination lines, GaudiRSG, eGFP-DN-GSK3 and Wnt3a (see **Figure 18**), were injected with Cre mRNA (20 ng/µl) into zygotes, non-transgenic animals were discarded and the remaining ones were screened for phenotypes at 6 – 8 dpf. Phenotypes were anterior truncations of varying severity, which I categorized into "none", "minor", "medium" and "strong". All GaudiRSG embryos had wt phenotypes and most Wnt3a embryos harboured strong anterior truncations. More than 60% of the eGFP-DN-GSK3 embryos also had phenotypes ranging from minor to strong.

With the following experiments I wanted to verify that the ubiquitin promoter of the eGFP-DN-GSK3 line actually allowed ubiquitous expression in the retina. As staining for mCherry in the transgenic lines did not result in signal with a satisfying quality that enabled me to clearly distinguish labelled from non-labelled cells, I pursued a different

approach: I transplanted cells at blastula stage from either GaudiRSG or eGFP-DN-GSK3 embryos into wt blastulae, screened them at hatch for red fluorescence in the eye and let them grow for three weeks to yield mCherry transplantation ArCoSs. Then I fixed and stained the retinae against mCherry. Cross sections of representative retinae (Figure 21 A and B) reveal that ArCoSs of both lines show mCherry signal in all three retinal cell layers (ONL, INL & GCL) (A' and B') and presumably also in all cell types. Thus, the ubiquitin promoter is indeed ubiquitous in the retinae of both lines.

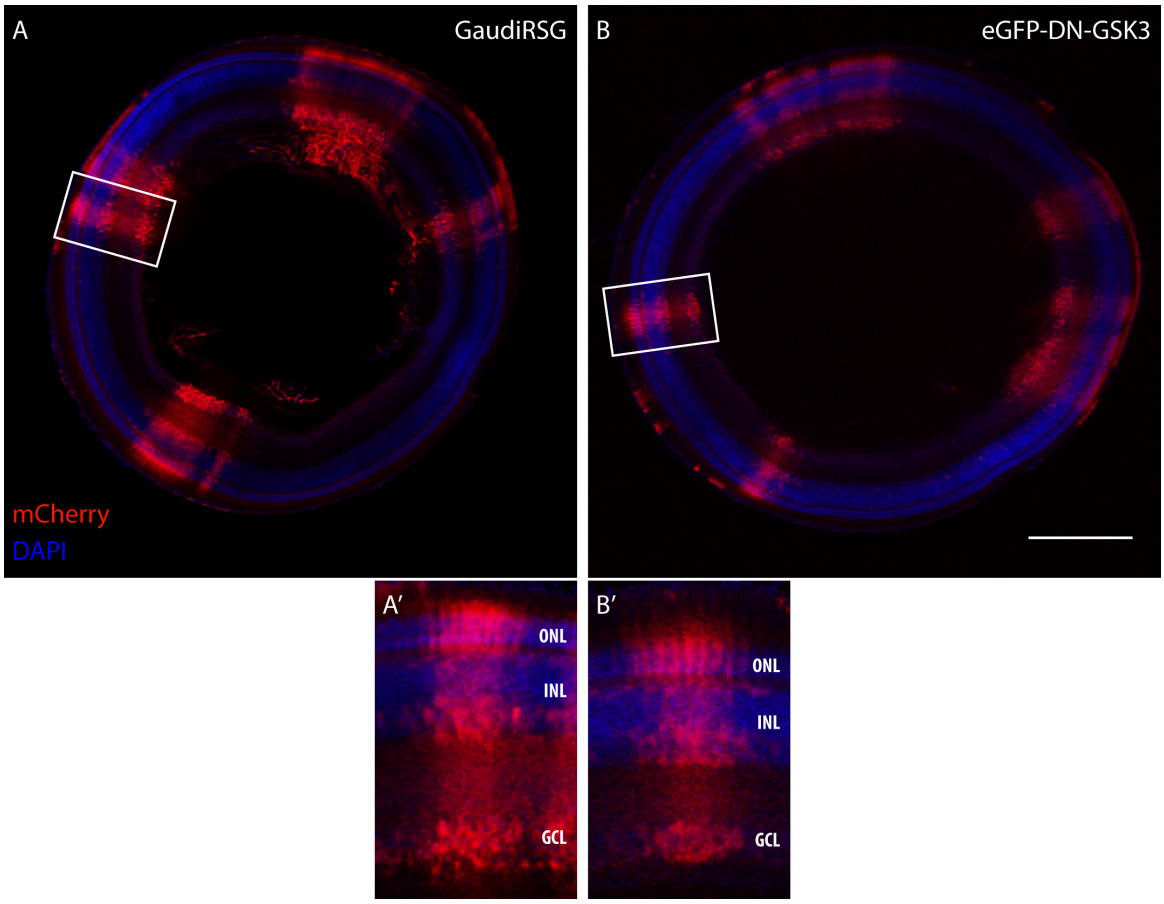

Figure 21. The ubiquitin promoter in the eGFP-DN-GSK3 transgenic line allows expression in all retinal cell types. Cells from the blastula stage embryos of GaudiRSG or eGFP-DN-GSK3 transgenic embryos were transplanted into wt blastulae. Embryos were screened for red fluorescence in the eye at hatch, allowed to grow for 3 weeks, fixed and stained against mCherry. A and B show confocal cross sections of the whole retina (front view) and A' and B' show close ups of one representative ArCoS each. The ArCoSs of both lines harbour cells in all retinal layers and presumably all retinal cell types. GaudiRSG n = 9 retinae; eGFP-DN-GSK3 n = 13 retinae. ONL – outer nuclear layer, INL – inner nuclear layer, GCL – ganglion cell layer. Scale bar 200 µm.

3.3 Analysis of Wnt activation in single cells of different populations

In the following paragraphs, I describe the detailed analysis of the impact of eGFP-DN-GSK3 on single cells of different potency and proliferation capacity and their progeny.

3.3.1 Activation of Wnt signalling in single *rx2* positive cells prevents the formation of ArCoSs

If Wnt signalling is required for stem cell maintenance and proliferation, I expected that hyperstimulation (via eGFP-DN-GSK3) in *rx2* positive stem cells would result in overproliferation and thus formation of overly thick ArCoSs.

To test this hypothesis, I crossed the eGFP-DN-GSK3 line to the *rx2*::CreERT2 line, recombined the offspring with tamoxifen as described in section 3.2.1 and let them grow for 2.5 to 4 weeks prior to fixation, staining and imaging. Recombination was successful, as plenty of presumably differentiated cells within the pre-induction circle are GFP positive (Figure 22 A, inner dashed ellipse). However, in contrast to the GaudiRSG controls (white arrowheads, 40 ArCoSs in 21 retinae) no ArCoSs were formed in the eGFP-DN-GSK3 fish (0 ArCoSs in 38 retinae) (Figure 22 A and B). Figure 22 C shows a schematic representation of these findings: recombined cells within the pre-induction zone, but no ArCoS. Thus, unexpectedly the *rx2* positive stem cells in the CMZ lose the ability to form ArCoS upon expression of eGFP-DN-GSK3.

As a next step I wanted to clarify why the *rx2* positive cells do not form ArCoS upon eGFP-DN-GSK3 expression. There are three likely answers: They stop proliferation and enter a quiescent state, they perform apoptosis or they change their mode of division from mainly asymmetric to symmetric. I addressed the proliferation status and apoptosis in the following experiments.

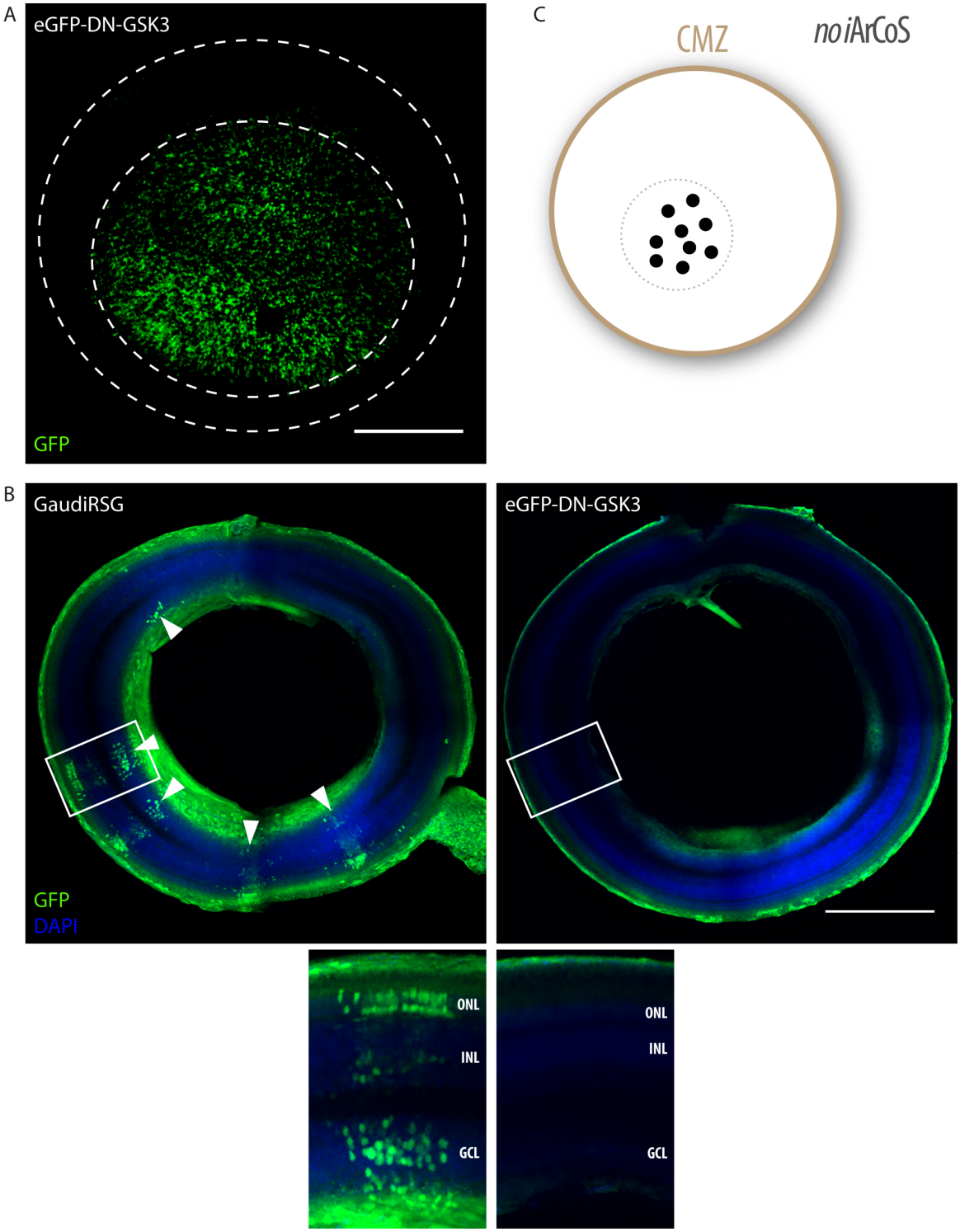

Figure 22. *rx2* positive cells lose the capacity to from ArCoS upon eGPF-DN-GSK3 expression. eGFP-DN-GSK3 fish were crossed to *rx2*::CreERT2 fish. The offspring was recombined, allowed to grow for 2.5 – 4 weeks, fixed and stained. (A) Back view of a whole eGFP-DN-GSK3 retina (confocal stack). (B) Front view of GaudiRSG and eGFP-DN-GSK3 retinae including close-ups (confocal stacks). Recombination was successful in the eGFP-DN-GSK3 line, because there are green fluorescent differentiated cells within the pre-induction circle (inner dashed ellipse in A). However, no ArCoSs were formed in the eGFP-DN-GSK3 line (0 ArCoS in 38 retinae) in contrast to the GaudiRSG controls (40 ArCoSs in 21 retinae) (white arrowheads). (C) Schematic back view of the retina illustrating that *rx2* positive cells do not form ArCoS upon eGFP-DN-GSK3 expression. ONL – outer nuclear layer, INL – inner nuclear layer, GCL – ganglion cell layer. Scale bar 200 µm. Scheme adapted from (Centanin et al., 2014).

To elucidate the proliferation behaviour, I crossed the GaudiRSG or eGFP-DN-GSK3 line to *hsp70*::Cre fish, recombined the offspring and incubated them in EdU for 2.5 days prior to fixation, serial sectioning, staining and imaging (Figure 23). I detected both EdU positive and negative recombined cells within the Rx2 domain for GaudiRSG (A and A') and eGFP-DN-GSK3 (B, B', C and C') fish. For each line examples are shown highlighting the recombined, GFP positive cells within the Rx2 domain with dashed lines. The number 1 marks examples for EdU negative cells and the EdU positive cells are marked with 2. I went on to quantify the recombined cells in the Rx2 domain and calculated the ratio of EdU positive over EdU negative cells (Figure 23 D). The ratios are 0,04 for GaudiRSG and 0,18 for eGFP-DN-GSK3. As the values are smaller than one, there are more EdU negative cells in both lines. Nevertheless, the ratio is considerably higher for eGFP-DN-GSK3, meaning that the proportion of proliferating cells is bigger, compared to the GaudiRSG line.

In contrast to the hypothesis that an increase in Wnt signalling induces dormancy in Rx2 positive stem cells, this data suggests that it induces proliferation instead. However, this does not explain the lack of ArCoS in those cells.

In order to assess whether Rx2 positive cells perform more or less apoptosis when Wnt signalling is increased, I crossed the GaudiRSG or eGFP-DN-GSK3 line to *hsp70*::Cre fish, recombined the offspring, and let them grow for 3 days followed by fixation, serial sectioning, TUNEL staining and microscopy (Figure 24). For GaudiRSG (A) as well as eGFP-DN-GSK3 (B) TUNEL positive cells (filled arrowheads) could be detected in the retina. Also the recombination was successful as there are GFP positive cells in the differentiated retina as well as in the Rx2 domain (empty arrowheads). Nonetheless, I did not detect a single recombined Rx2 positive cell that was undergoing apoptosis (eGFP-DN-GSK3 n = 3 fish; GaudiRSG n = 8 fish). Hence, neither in the GaudiRSG nor the eGFP-DN-GSK3 line apoptosis seems to occur in Rx2 positive stem cells.

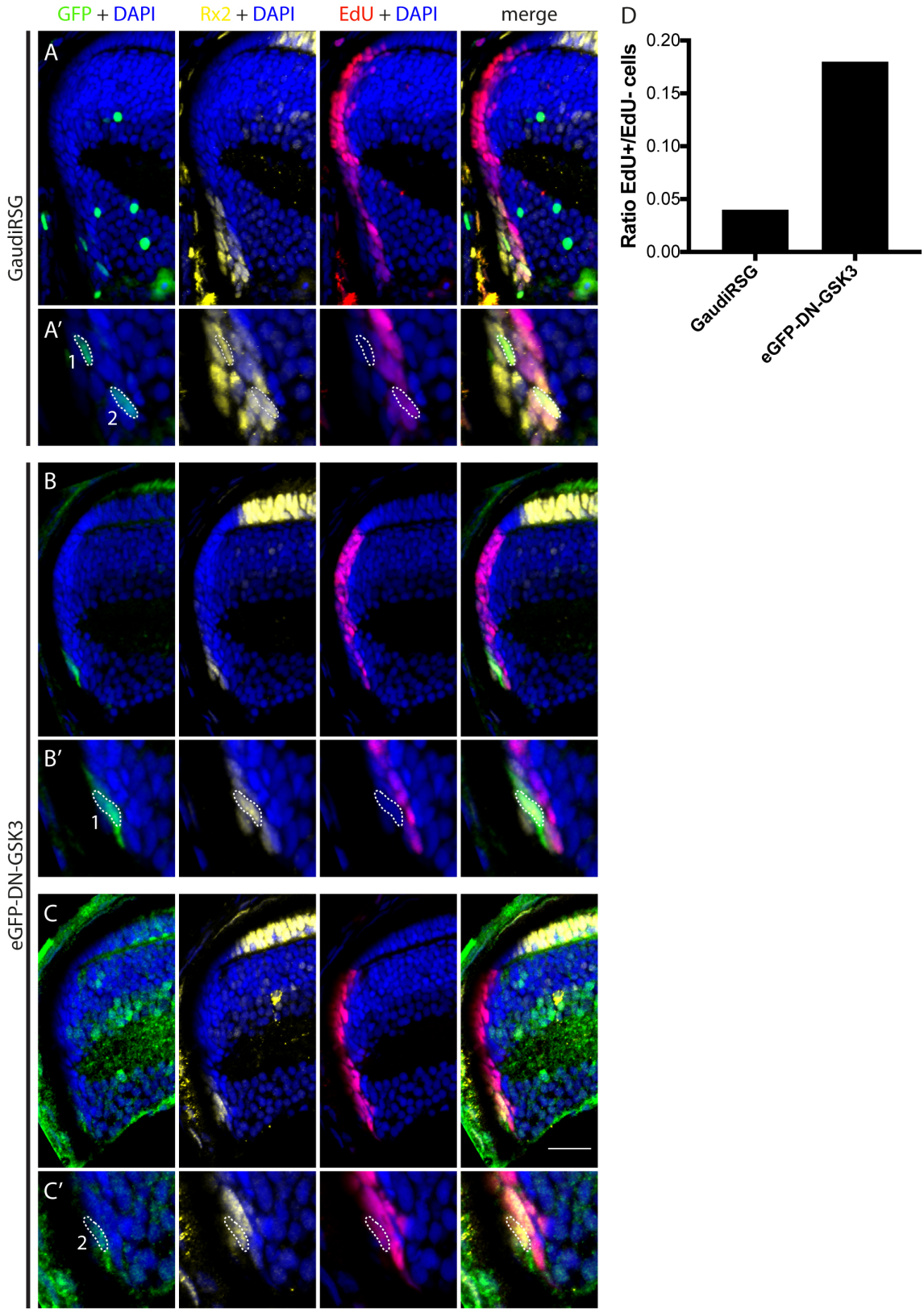

Figure 23. The proportion of proliferating recombined Rx2 positive cells is higher in the eGFP-DN-GSK3 than in the GaudiRSG line. eGFP-DN-GSK3 or GaudiRSG fish were crossed with *hsp70*::Cre, recombined and incubated in EdU for 2.5 days prior to fixation, sectioning and staining. Confocal stacks of the peripheral retina of GaudiRSG (A) and eGFP-DN-GSK3 (B and C) fish stained for GFP (green), Rx2 (yellow), EdU (red) and DAPI (blue). A' to C' show close ups of recombined cells within the Rx2 domain. Cell number one is EdU negative whereas cell number two is stained positive for EdU in both lines. D shows the ratio of EdU positive cells within the recombined cells of the Rx2 domain. With 0,18 the ratio is larger in the eGFP-DN-GSK3 line than in the GaudiRSG line (0,04). GaudiRSG n = 123 cells from 2 fish; eGFP-DN-GSK3 n = 71 cells from 8 fish. Scale bar 20 µm.

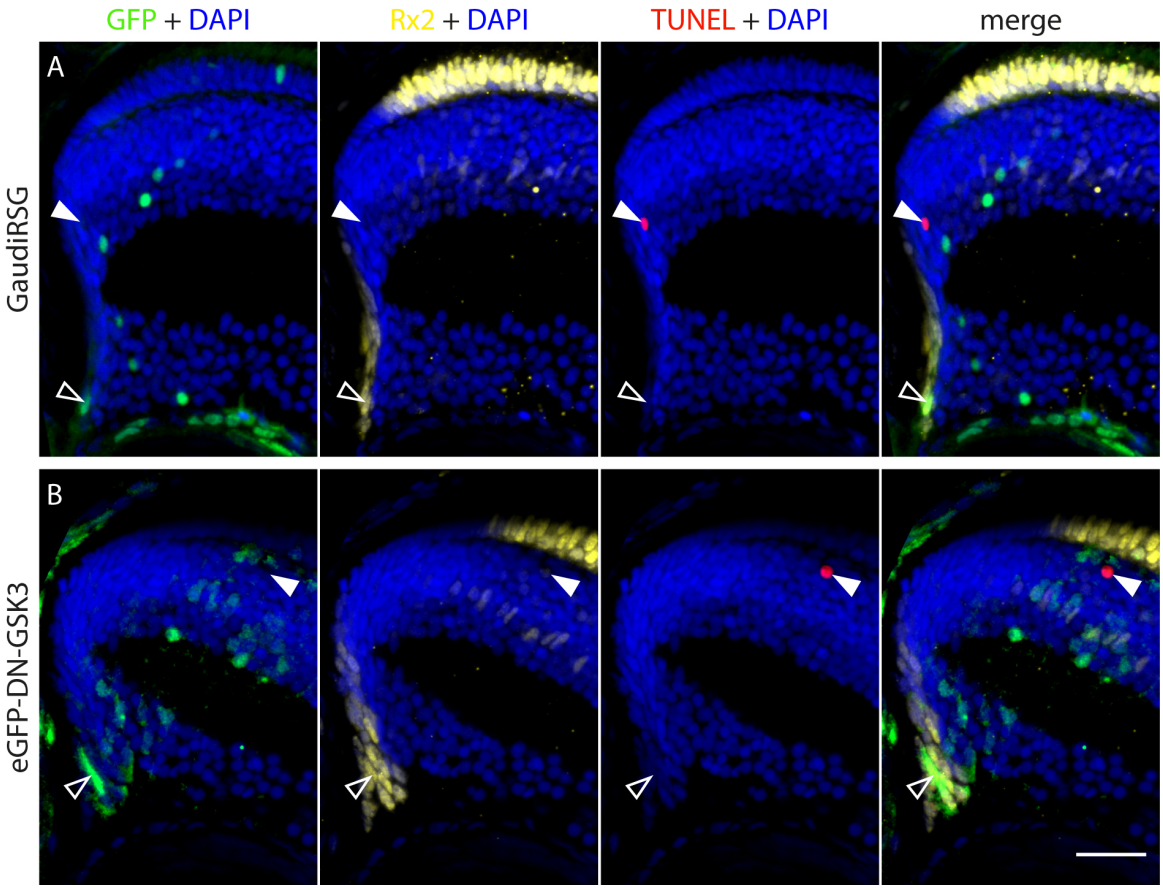

Figure 24. No apoptosis was observed in recombined Rx2 positive cells of neither the GaudiRSG nor the eGFP-DN-GSK3 line. Fish of the eGFP-DN-GSK3 or the GaudiRSG lines were crossed to *hsp70*::Cre fish. The offspring was recombined, allowed to grow for 3 days and then fixed, sectioned and stained. Typical results are shown in A for GaudiRSG and in B for eGFP-DN-GSK3. There are few cells in the retinae of both lines that undergo apoptosis and therefore stain positive for TUNEL (filled arrowheads). Recombination in the Rx2 domain was also successful (empty arrowheads). However, none of the recombined cells within the Rx2 domain showed positive TUNEL staining (GaudiRSG n = 3 fish; eGFP-DN-GSK3 n = 8 fish). Scale bar 20 µm.

As I had technical difficulties with the *rx2*::CreERT2 driver line, I had to use the *hsp70*::Cre line and just analysed Rx2 positive cells. However, this leaves the risk that recombined progenitor cells migrate back into the *rx2* domain and reacquire *rx2* expression. Although this has not been reported before, the analysis should be repeated with the *rx2*::CreERT2 line to exclude analysing progenitor cells by mistake.

3.3.2 There are cells in the CMZ that form ArCoSs upon Wnt activation

Since *rx2* positive cells do not have the capacity to form ArCoS when expressing eGFP-DN-GSK3, I asked next whether any (other) cells in the retina form ArCoSs in this context. To this end, I crossed fish of the GaudiLxBBW or eGFP-DN-GSK3 line to

hsp70::Cre fish and recombined their offspring. After 1.5 – 2.5 month of growth the fish were fixed and stained. Confocal stacks of retinal back views were imaged for both lines (Figure 25 A). Both exhibit recombined cells within the induction circle (inner dashed ellipse) and, surprisingly, several ArCoSs (area between the dashed ellipses). Although it seems that the eGFP-DN-GSK3 line has more ArCoSs, this is hard to compare as the GaudiLxBBW line has multiple recombination outcomes and the anti GFP antibody only detects GFP and YFP. Thus, in contrast to the stem cell specific recombination, ubiquitous stochastic recombination resulted in the formation of ArCoSs (summarised in the scheme in Figure 25 B). Meaning that there is a population in the neural retina that forms ArCoSs upon DN-GSK3 expression.

I then examined the cell fates within each ArCoS more closely. Therefore, I removed the peripheral-most part of the retinae including the CMZ using a vibratome to reveal the layering of the differentiated retina. The remaining part of the retinae was imaged as front view (Figure 25 C). Gaudi ArCoSs are exclusively multipotent, meaning they give rise to the complete spectrum of cell types in the neural retina (Centanin et al., 2014). eGFP-DN-GSK3 ArCoSs on the other hand are very diverse. Some comprise all (or almost all) cell types (11%), other ArCoSs feature only cells of the ONL and INL (photoreceptors and amacrine cells; 51%) and a proportion of ArCoSs solely consists of photoreceptors (38%). Consequently, ArCoSs formed by cells featuring upregulated Wnt signalling exhibit various degrees of fate restrictions

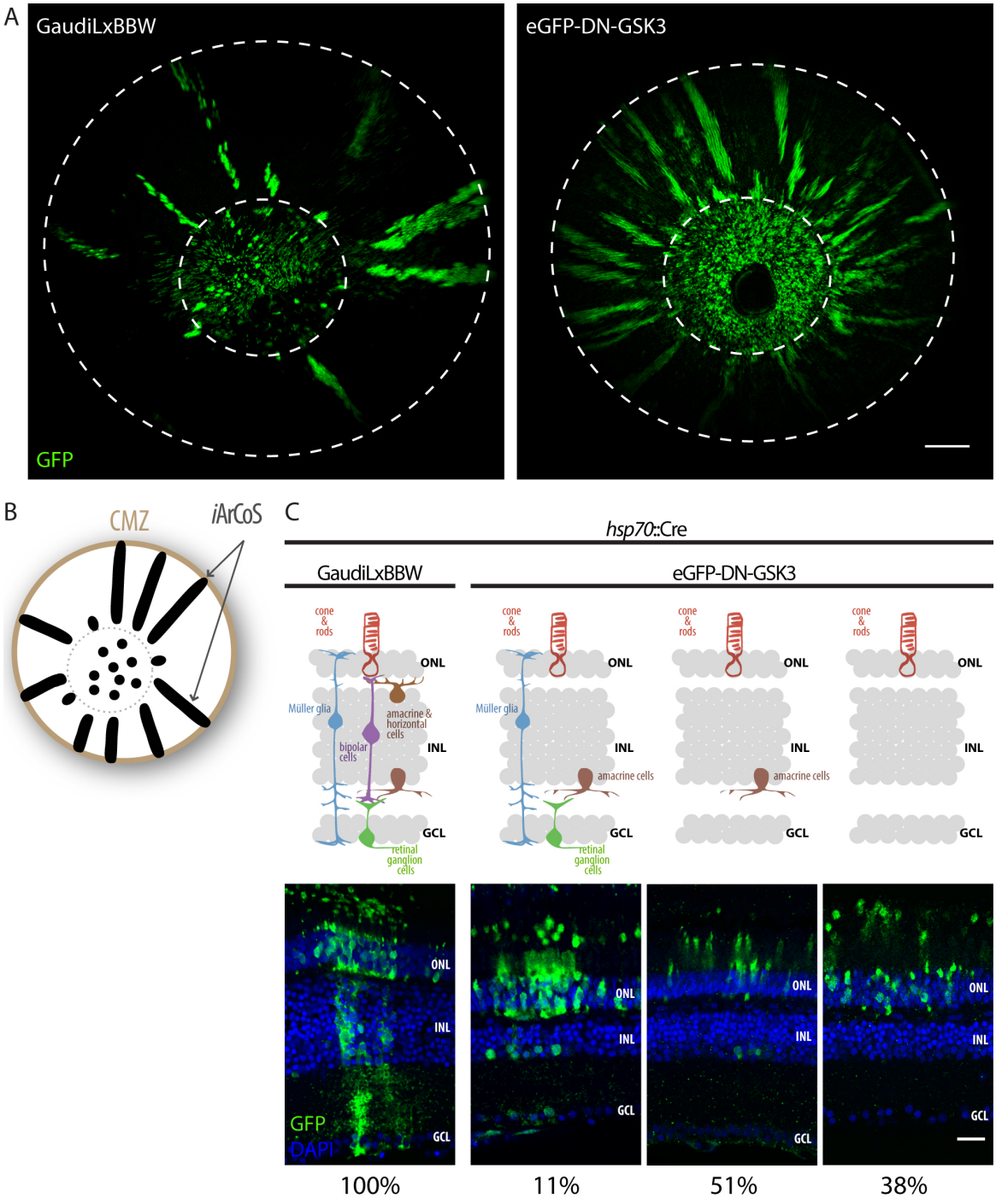

Figure 25. Induction of recombination with *hsp70*::Cre results in ArCoSs with varying fate restrictions upon eGFP-DN-GSK3 expression. GaudiLxBBW or eGFP-DN-GSK3 fish were crossed to *hsp70*::Cre fish. The offspring was induced, allowed to grow for 1.5 – 2.5 month prior to fixation and staining. (A) Depicted are confocal stacks of whole retinae as back views. Both lines show formation of ArCoSs. GaudiLxBBW n = 7 retinae; eGFP-DN-GSK3 n = 17 retinae. Scale bar 200 µm. (B) Schematic summary of A. (C) CMZ was cut off in doughnut sections using a vibratome to reveal the layers of the retina. Remaining part of the retinae was imaged as front view. Gaudi ArCoSs (n = 7) are always multipotent, meaning they consist of all retinal cell types. By contrast ArCoSs resulting from eGFP-DN-GSK3 ArCoSs (n = 37) are heterogeneous. 11% are multipotent, 51% are restricted to cells of the ONL and INL and 38% only consist of photoreceptors. Scale bar 20 µm. ONL – outer nuclear layer, INL – inner nuclear layer, GCL – ganglion cell layer. Schemes adapted from (Centanin et al., 2014).

3.3.3 *tlx* positive cells form few, but multipotent ArCoSs upon expression of eGFP-DN-GSK3

Next, I wanted to test whether *tlx* positive cells are able to form ArCoSs upon eGFP-DN-GSK3 expression. The *tlx* expression is located more apically than the *rx2* domain, but they partially overlap (Figure 17 and Figure 19). As explained in section 1.3.1 previous ArCoS experiments revealed that *tlx* marks stem and progenitor cells. The localisation of *tlx* within the CMZ additionally suggests that the progenitor cells, which are located directly adjacent to the *rx2* positive stem cells, arose from asymmetric stem cell divisions and are non-committed "early" progenitors. As in all other ArCoS experiments, I crossed GaudiRSG or eGFP-DN-GSK3 fish to the *tlx*::CreERT2 line. I recombined the offspring and allowed them to grow for 1.5 to 2 month, followed by fixation, staining and microscopy of the retinae as back views (Figure 26 A). The GaudiRSG controls show plenty ArCoSs in each retina (total of 38 ArCoSs in 5 retinae). The eGFP-DN-GSK3 line also features ArCoSs, however they are way less abundant (total of 8 ArCoSs in 6 retinae). This result is illustrated in Figure 26B. To examine the cell type composition of the ArCoSs, I cut off the peripheral retina with the vibratome to reveal the retinal layering and imaged the remaining parts of the retinae in a front view (Figure 26 C). Notably, all of the eGFP-DN-GSK3 ArCoSs do not feature varying cell fates (as achieved with *hsp70*::Cre) but are entirely multipotent as are their GaudiRSG controls. As *rx2* positive stem cells are not able to form ArCoS upon Wnt upregulation, the eGFP-DN-GSK3 ArCoSs formed by *tlx* positive cells probably did not originate from the *tlx* domain that overlaps with *rx2*. Hence, those multipotent ArCoSs may be formed by the "early" non-committed progenitors marked by *tlx*.

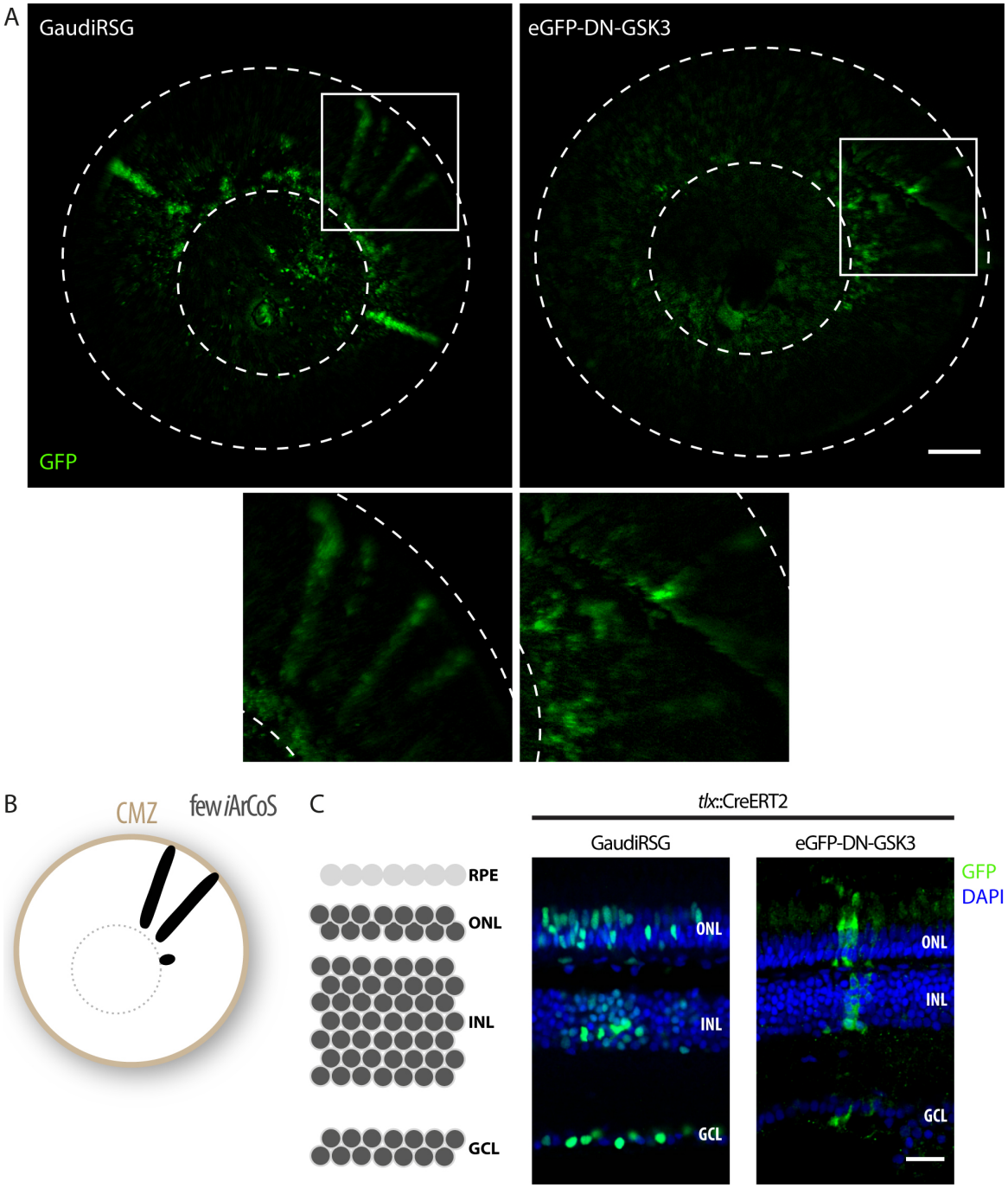

Figure 26. *tlx* positive cells form few, but multipotent ArCoSs upon expression of eGFP-DN-GSK3. GaudiRSG or eGFP-DN-GSK3 fish were crossed to *tlx*::CreERT2 fish. The offspring was induced, allowed to grow for 1.5 – 2 month prior to fixation and staining. (A) Depicted are confocal stacks of whole retinae as back views. Although both lines show formation of ArCoSs, they are much less abundant in the eGFP-DN-GSK3 line (total of 8 ArCoSs in 6 retinae) than in GaudiRSG fish (total of 38 ArCoSs in 5 retinae). Scale bar 200 µm. (B) Schematic summary of A. (C) CMZ was cut off in doughnut sections using a vibratome to reveal the layers of the retina. Remaining part of the retinae was imaged as front view. Here, GaudiRSG as well as eGFP-DN-GSK3 ArCoSs are exclusively multipotent, meaning they consist of all retinal cell types. Scale bar 20 µm. ONL – outer nuclear layer, INL – inner nuclear layer, GCL – ganglion cell layer. Schemes adapted from (Centanin et al., 2014).

3.3.4 eGFP-DN-GSK3 impacts cell fates of footprints formed by *atoh7* positive cells

The last cell population I addressed with my analysis were *atoh7* positive cells. *atoh7* was reported to label proliferating progenitors in the CMZ (Lust et al., 2016). For the *atoh7*::CreERT2 line (construct cloned by Beate Wittbrodt and Tinatini Tavelidse; transgenic line established by Katharina Lust) no ArCoS experiments had been done before. Thus, I firstly characterised the line by crossing it to GaudiRSG fish and recombining their offspring. The fish were allowed to grow for 3 weeks before they were fixed, stained and the whole retinae were analysed as back and front view (Figure 27 A and B). The GFP positive cells form a ring of footprints around the induction circle but no ArCoS (schematised in Figure 27 C). Hence, *atoh7* positive cells have limited proliferation capacity in contrast to stem cells that form ArCoSs. In order to reveal the cell fates of the footprints, I cut the retinae into sections (Figure 27 B). *atoh7* footprints consist of retinal ganglion cells, photoreceptors, amacrine and horizontal cells. Figure 27 D shows a scheme of those four cell types and their position within the retinal layers. Consequently, *atoh7* marks proliferation-restricted, committed progenitors.

Having uncovered that *atoh7* positive cells form footprints with specific cell fates, I wanted to know whether expression of eGFP-DN-GSK3 has an impact on those cells. Hence, I also crossed the eGFP-DN-GSK3 line to *atoh7*::CreERT2 fish and recombined their offspring. I let the fish grow for 3 weeks before fixation and staining. *atoh7* positive cells also form footprints upon expression of eGFP-DN-GSK3, although there are noticeably less footprints (Figure 28 A and B). To analyse the cell type composition of the footprints, I performed cross sections of the retinae and quantified the cell types (Figure 28 C and D). GaudiRSG footprints consist mainly of retinal ganglion cells (86%) and of roughly equal amounts of amacrine plus horizontal cells (6%) and photoreceptors (8%). In contrast, eGFP-DN-GSK3 footprints comprised almost only photoreceptors (98%) and very few amacrine and horizontal cells (2%). Additionally, there are considerably less GFP positive cells in the eGFP-DN-GSK3 than in the GaudiRSG retinae. In the GaudiRSG retinae a central section contained 99 cells on average (section 45 µm, whole retina ~1mm, roughly estimated total GFP+ cell number 3500) whereas the eGFP-DN-GSK3 retinae contained on average 17 cells in total. Although it is not possible to dissect the size of each clone in the GaudiRSG line, it is save to assume that the wt clones are much bigger than the ones expressing eGFP-DN-GSK3 (mostly 1-3

cells/clone). Hence, these results suggest that an increase of Wnt signalling in *atoh7* positive committed progenitors leads to a cell fate shift and inhibits proliferation.

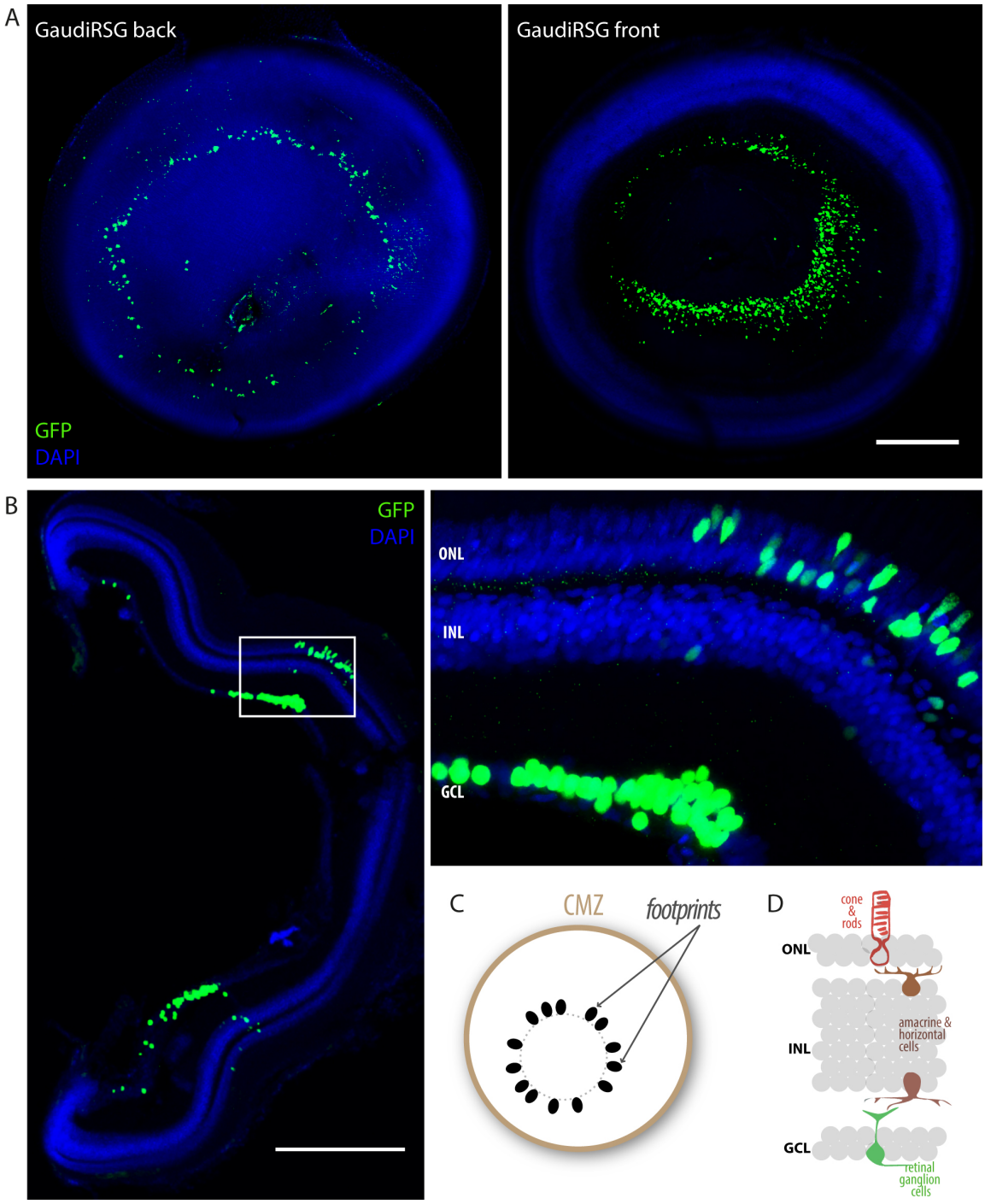

Figure 27. *atoh7* positive cells from footprints comprised of retinal ganglion cells, photoreceptors, amacrine and horizontal cells. GaudiRSG fish were crossed to *atoh7*::CreERT2 fish. The offspring was induced, allowed to grow for 3 weeks, fixed and stained. (A) Confocal stacks of the back and front views of a representative retina. Footprints are formed as a ring around the induction circle. (B) Cross sections were performed using a vibratome and reveal the layering of the retina. Footprints are made up of retinal ganglion cells, photoreceptors, amacrine and horizontal cells. (C) Schematic illustration of a retina with footprints. (D) Scheme of the cell type composition of *atoh7* footprints. Scale bar 200 µm. ONL – outer nuclear layer, INL – inner nuclear layer, GCL – ganglion cell layer. Schemes adapted from (Centanin et al., 2014).

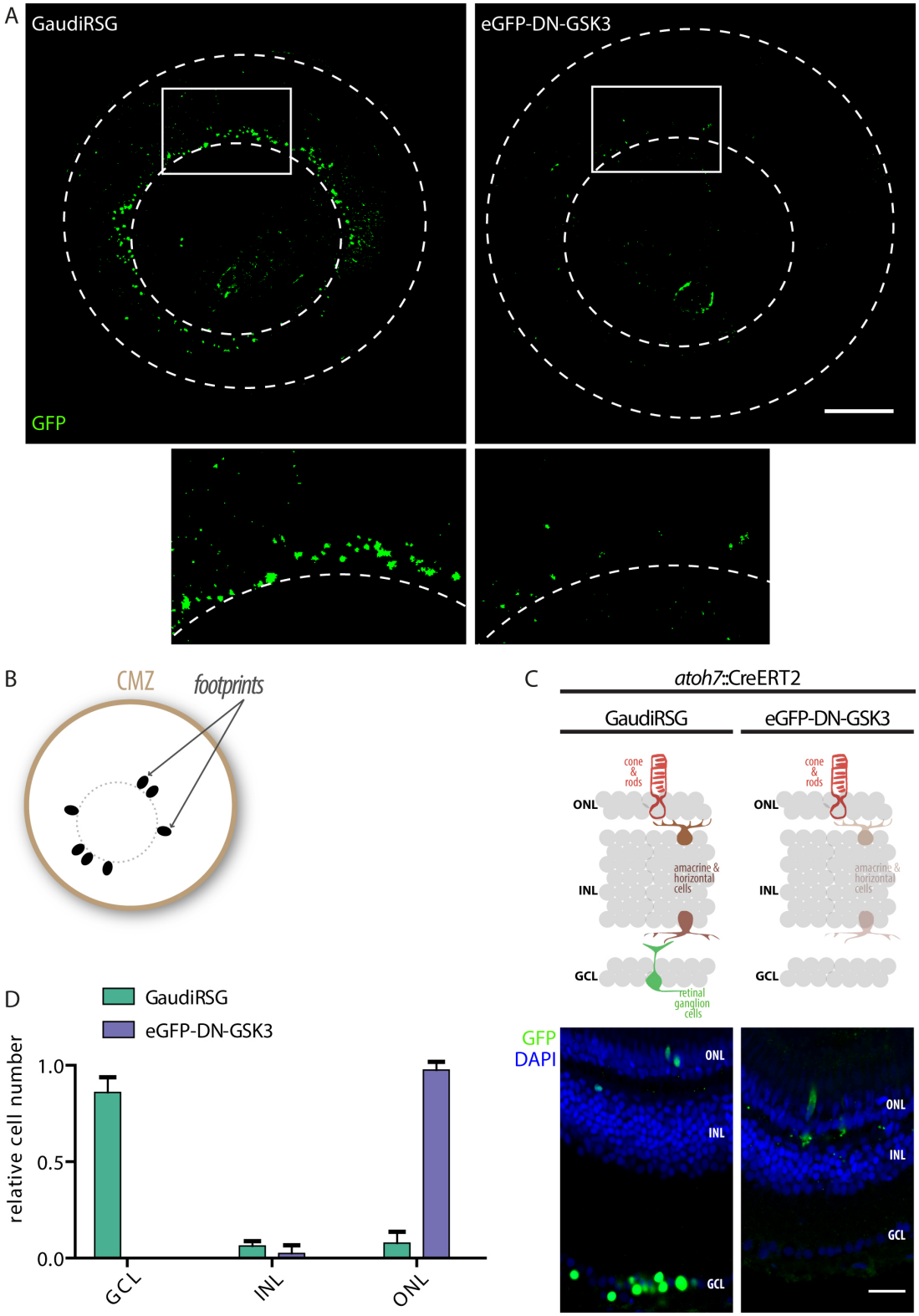

Figure 28. *atoh7* positive cells form few, small footprints mainly comprised of photoreceptors upon expression of eGFP-DN-GSK3. GaudiRSG or eGFP-DN-GSK3 fish were crossed to *atoh7*::CreERT2 fish. The offspring was recombined and allowed to grow for 3 weeks prior to fixation and staining. (A) Confocal stacks of retinal back views. In both lines footprints are visible although there are fewer in the eGFP-DN-GSK3 line. GaudiRSG: 6 out of 6 retinae have footprints; eGFP-DN-GSK3: 3 out of 6 retinae have footprints. Scale bar 200 µm. (B) Schematic illustration of the result. (C) Cross sections of the retinae reveals the cell type composition of the footprints. Scale bar 20 µm. (D) Quantification of cell types within the footprints of both lines. GaudiRSG footprints (n = 1578 cells from 4 retinae) mainly consist of retinal ganglion cells whereas eGFP-DN-GSK3 footprints (n = 51 cells from 3 retinae) are mostly comprised of Photoreceptors. ONL – outer nuclear layer, INL – inner nuclear layer, GCL – ganglion cell layer. Schemes adapted from (Centanin et al., 2014).

3.3.5 Summary: Impact of Wnt signalling activation on cells with different identities

In this thesis I have tested the impact of DN-GSK3 on cells with different identities and their progeny. Figure 29 summarises the results of all functional lineage-tracing experiments.

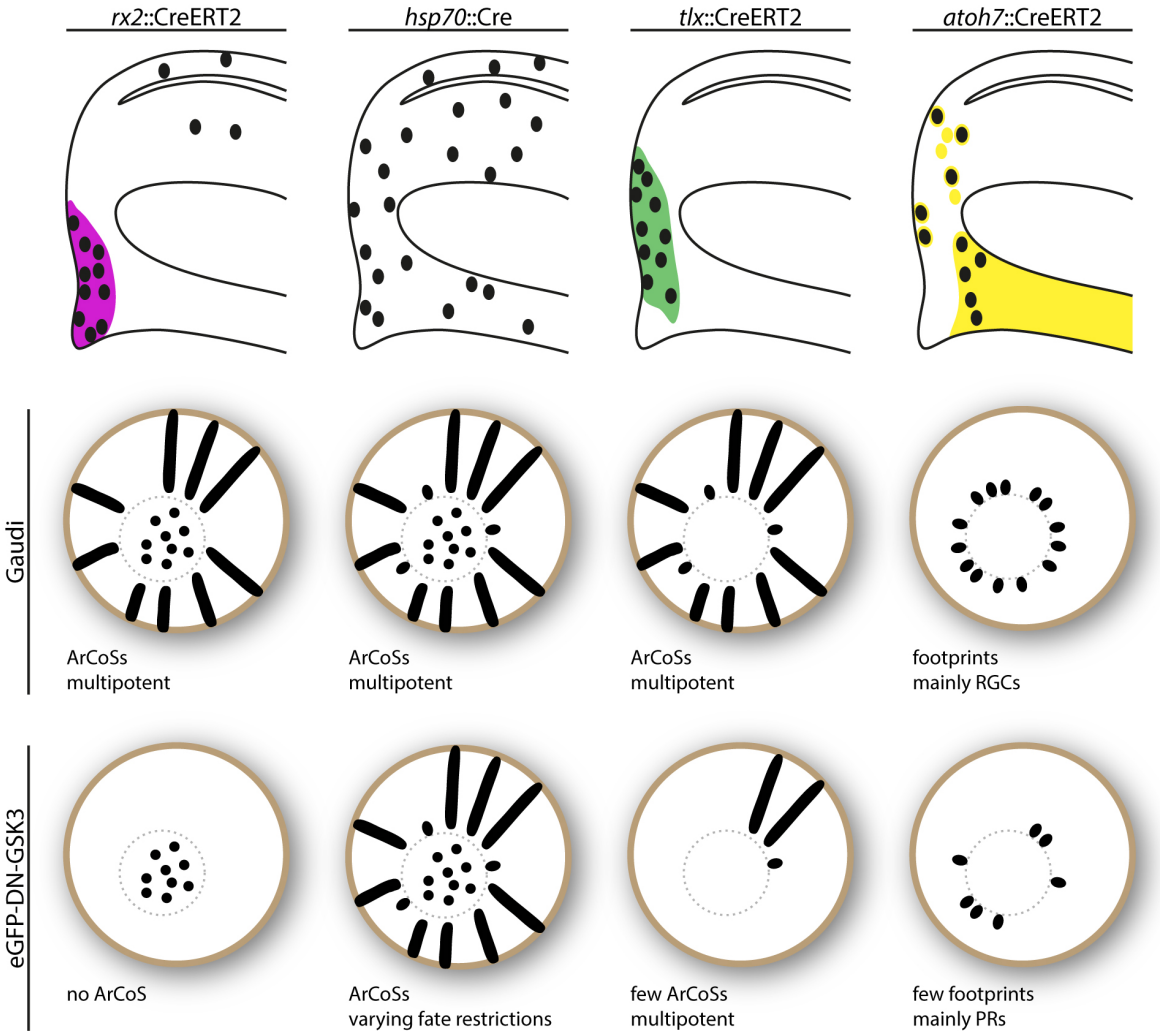

Figure 29. Summary: How DN-GSK3 impacts on cells with different identities. Lineage tracing outcomes in the retina of either Gaudi or eGFP-DN-GSK3 lines recombined with different Cre driver lines. Gaudi lines form multipotent ArCoSs with *rx2*::CreERT2, *hsp70*::Cre and *tlx*::CreERT2 and footprints consisting mainly of retinal ganglion cells with *atoh7*::CreERT2. The eGFP-DN-GSK3 line forms no ArCoS when recombined with *rx2*::CreERT2. It forms ArCoSs featuring varying fate restrictions with *hsp70*::Cre and few multipotent ArCoSs with *tlx*::CreERT2. Recombination of the eGFP-DN-GSK3 line with *atoh7*::CreERT2 leads to the formation of few footprints that mainly consist of photoreceptors. RGCs – retinal ganglion cells, PRs – photoreceptors. ArCoS schemes adapted from (Centanin et al., 2014).

The first row illustrates in which domains stochastic recombination occurs for each Cre driver line. The behaviour of wt cells was examined using Gaudi lines. Those lines form ArCoSs when induced with *rx2*::CreERT2, *hsp70*::Cre and *tlx*::CreERT2. In the eGFP-DN-GSK3 line all recombined cells express eGFP-DN-GSK3 and thus upregulate Wnt signalling. Here *rx2* positive stem cells are not able to form ArCoS. However, those cells show a higher proliferation ratio compared to GaudiRSG and no apoptosis could be detected. Surprisingly, ubiquitous stochastic recombination with *hsp*70::Cre did result in ArCoSs, which possess different levels of fate restrictions ranging from multipotent to only photoreceptors suggesting that they were initiated by progenitors featuring varying competencies. Lineage tracing of *tlx* (which partially overlaps with *rx2*) positive cells featuring eGFP-DN-GSK3 expression led to formation of few but multipotent ArCoSs probably formed by "early" non-committed progenitors. In the Gaudi lines *atoh7* positive cells have a restricted proliferation capacity and form footprints consisting mainly of retinal ganglion cells, but also of amacrine, horizontal cells and photoreceptors, hence they are committed progenitors. In contrast, *atoh7* positive cells expressing eGFP-DN-GSK3 form small footprints almost only comprised of photoreceptors suggesting a role for Wnt in the fate and/or proliferation of committed progenitors.

In, summary Wnt signalling has very diverging effects on stem cells, non-committed and committed progenitor cells.

4 Discussion

This work presents a detailed analysis of Wnt signalling localisation and function within different cell types and their lineages in the post-embryonic CMZ of medaka.

Wnt ligands are expressed by cells of the RPE located directly adjacent to the CMZ. Wnt/β-catenin signalling is restricted to *rx2* positive stem cells, whereas β-catenin independent Wnt/LRP6 signalling extends to dividing progenitor cells. This indicates that Wnt signalling has different functions in stem and progenitor cells.

To analyse the roles Wnt might play in individual cells of the CMZ, I employed an enhancement on lineage tracing. Clonal analysis enables us to follow lineages of cells. Thereby, it is possible to unambiguously distinguish stem from progenitor cells by the characteristics of stemness: self-renewal & multipotency. Wnt upregulation via DN-GSK3 has very different effects on the different cell types of the CMZ. *rx2* positive stem cells lose their capacity to form ArCoSs and therefore lose stem cell characteristics. However, other cells in the retina are able to form ArCoSs while expressing DN-GSK3, most probably progenitor cells that normally only form footprints. Hence, Wnt upregulation may impose self-renewal onto those cells. These ArCoSs feature varying fate restrictions. Therefore, it is tempting to speculate that they originate from progenitors at different stages with different fate restrictions. Following this argument Wnt imposes self-renewal, but does not reverse fate restrictions and thus has no influence on potency. On *atoh7* positive committed progenitors, however, it has a different effect: cells divide only few times and produce predominantly photoreceptors instead of mainly retinal ganglion cells suggesting a role for Wnt in the fate determination and/or proliferation of committed progenitors. Consequently, also the functional lineage tracing experiments show that Wnt has different effects on stem and progenitor cells.

In summary, my results suggest that Wnt signalling functionally divides the CMZ into *rx2*+ stem cells, *rx2*-/*tlx*+ non-committed progenitors and *atoh7*+ committed progenitors. The implications of these results shall be discussed in the following.

4.1 Wnt/β-catenin signalling is active in stem cells and β-catenin independent Wnt/LRP6 signalling is active in progenitors

We performed a thorough analysis of the localisation of Wnt/β-catenin signalling components in the CMZ. In the subsequent section the localisation of each investigated component shall be discussed and at the end integrated within the signalling pathway.

In situ hybridisation revealed that Wnt ligands are expressed in the RPE surrounding the CMZ. This is consistent with previous experiments in *Xenopus* and zebrafish (Borday et al., 2012; Thisse and Thisse, 2004). Moreover, in *Xenopus* and also chicken Wnt expression was additionally detected in few cells at the peripheral-most tip of the neural retina (Kubo, 2003). As the signal was quite weak in medaka it cannot be excluded that signal in tip cells of the CMZ was missed. Moreover, in *Xenopus* different Wnts showed slightly varying expression patterns. As we only assessed the expression patterns of 4 out of approximately 28 Wnts in teleost fish (Mwafi et al., 2014), it would be beneficial to perform *in situ* hybridisations for more Wnts to clarify the exact localisation of Wnt expression.

Phosphorylated and thus active LPR6 was detected in mitotic cells within the *rx2* positive stem cell compartment but also in progenitor cells (*tlx* positive, *atoh7* positive or *tlx*/*atoh7* negative). As this phosphorylation site (T1479) is strictly Wnt dependant (Davidson et al., 2005; Niehrs and Shen, 2010; Zeng et al., 2005), it is an excellent read out for all Wnt/LRP6 signalling pathways. This is a novel finding in the retina, as most other studies focus only on either Wnt ligand or Wnt/β-catenin target gene expression. However, pT-LRP6 was not detected in all retinal stem and progenitor cells, but only in few cells within those domains that undergo mitosis (detected by the condensed nuclei). It was shown in cell culture that Wnt/LRP6 signalling peaks in mitosis (Acebron et al., 2014; Davidson et al., 2009). This was explained by LRP6 PPPSP motifs being phosphorylated by CDK/CyclinY, which is a cell cycle complex active at G2/M (Nakayama and Nakayama, 2006). This phosphorylation primes LRP6 to be further phosphorylated (amongst others at T1479) and thus cells are more sensitive for Wnt ligands at G2/M (Davidson et al., 2009). Hence, it is not surprising that mitotic cells in the CMZ show clear pT-LRP6 staining. In non-mitotic cells the signal might be too weak to clearly distinguish it from background.

Non-phosphorylated β-catenin, which is not targeted for degradation and therefore called active β-catenin (ABC) localises to almost all Rx2 positive cells. This is consistent with ABC stainings in zebrafish, although these do not provide a detailed view on the CMZ (Meyers et al., 2012). Interestingly, in few cells at the peripheral-most tip of the Rx2 domain ABC levels are clearly lower than in all other Rx2 positive cells. This is also the location where normally the slow cycling stem cells reside (Xue and Harris, 2012). On one hand this is consistent with the studies showing that Wnt signalling is necessary for proliferation (Denayer et al., 2008; Kubo, 2003; Kubo and Nakagawa, 2009; Kubo et al., 2005; Meyers et al., 2012). On the other hand, Wnt was also shown to be essential to preserve quiescence in hematopoietic stem cells (Fleming et al., 2008). So its function in proliferation is apparently not mutually exclusive with functions in quiescence. It is also possible that Wnt function is dependent on the levels of activation. Hence, it is difficult to draw any comprehensible conclusions at this stage.

We assessed the localisation of 9 typical Wnt/β-catenin target genes in the retina and found that their expression is always confined to the CMZ, which was also reported in zebrafish, *Xenopus*, chicken and mouse (Borday et al., 2012; Denayer et al., 2008; Dorsky et al., 2002; Kubo, 2003; Liu et al., 2007). Using double fluorescent *in situ* hybridisation we could show that most of the tested genes co-localise to cells expressing *rx2*, meaning that most target genes are restricted to the stem cell compartment. However, there are three genes with slightly divergent expression patterns: *sox2*, *axin2.2* and *myc*. The expression of *sox2* extends a bit more towards the apical CMZ and, thus, towards progenitor cells. This observation is consistent with a recently published results in medaka (Reinhardt et al., 2015). In the developing *Xenopus* retina Wnt/β-catenin signalling is necessary for *sox2* expression. Sox2 in turn inhibits Wnt signalling probably through direct inhibition of β-catenin. Moreover, Sox2 is essential for the expression of proneural genes and thereby the transition from progenitors to differentiated neurons (Agathocleous et al., 2009; Van Raay et al., 2005). From these and other observations Agathocleous *et al.* concluded that feedback inhibition of Wnt signalling by Sox2 and inhibition of *sox2* by proneural genes provides a directional network in which each element activates the next and inhibits the previous element to govern the transition from progenitors to differentiated cells. As described above it was proposed that the temporal progression of events in the developing retina is recapitulated by the spatially encoded events in the CMZ of the adult retina (Perron and Harris, 2000). Hence, the feedback

inhibition of Sox2 on β-catenin could explain why expression of *sox2* extends towards the progenitors, where pT-LRP6 is still present but not β-catenin or other Wnt/β-catenin target genes. In contrast to *sox2*, the expression of *axin2.2* and *myc* is restricted to a subset of *rx2* positive cells. However, their paralogs *axin2.1* and *myca* overlap perfectly with *rx2*. Beside Wnt signalling also several growth factor signalling pathways are known to regulate members of the Myc family (Meyer and Penn, 2008; Misawa et al., 2000; Watt et al., 2008). In the zebrafish retina, different members of the Myc protein family were even shown to be differentially regulated by those pathways (Xue and Harris, 2012). Hence, it is possible that the restriction of *myc* and also *axin2.2* expression is due to additional regulation by other pathways. Nonetheless, the expression patterns of most Wnt target genes match *rx2* expression and also ABC immunohistochemistry. However, the reduction or absence of Wnt/β-catenin signalling in few cells at the peripheral tip of the CMZ as seen in the ABC staining was not observed in the *in situ* hybridisations for Wnt/β-catenin target genes. A possible explanation is that immunohistochemistry and *in situ* hybridisation are not entirely comparable or the cells might feature different levels of regulation in ABC and Wnt target genes.

Taken together, expression of Wnt ligands by cells of the RPE leads to activation of Wnt/LRP6 signalling throughout the CMZ. The β-catenin mediated activation of Wnt target genes however is restricted to *rx2* positive stem cells and does not happen in progenitor cells (Figure 30). Although Wnt/β-catenin signalling activity in the CMZ has been described before, this is the first detailed analysis of several readouts for active Wnt signalling. The activity of β-catenin independent Wnt/LRP6 signalling in progenitor cells gives hints that these pathways are not only relevant in transcriptionally silent cells (e.g. mature oocytes or spermatozoa (Huang et al., 2015; Koch et al., 2015)) but may also be of importance in adult stem cell niches.

The lack of active β-catenin and Wnt target genes in progenitors could be explained in two ways: First, Wnt/β-catenin signalling components downstream of LRP6 phosphorylation and upstream of β-catenin stabilisation may not be expressed in those cells. Second, those components could be inhibited by other factors. The latter could be

achieved by Sox2 inhibiting β-catenin as explained above. As this happens during retinal development it is likely that it also plays a role in the adult retina.

With this, the question arises which function Wnt/β-catenin or Wnt/LRP6 signalling has in stem and progenitor cells. It stands to reason that Wnt/β-catenin in stem cells may be responsible for maintenance of the stem cell identity and self-renewal by asymmetric cell divisions. The role β-catenin independent Wnt/LRP6 signalling may play in progenitor cells are less obvious since those pathways have only been discovered recently. Until now, they were associated with cell growth, cell cycle progression and coordination of mitosis (Acebron and Niehrs, 2016). As those processes play an important role in rapidly dividing progenitor cells it makes sense that progenitor cells feature active Wnt/LRP6 signalling.

The exact role Wnt pathways play in retinal stem and progenitor cells shall be discussed with the functional lineage tracing experiments.

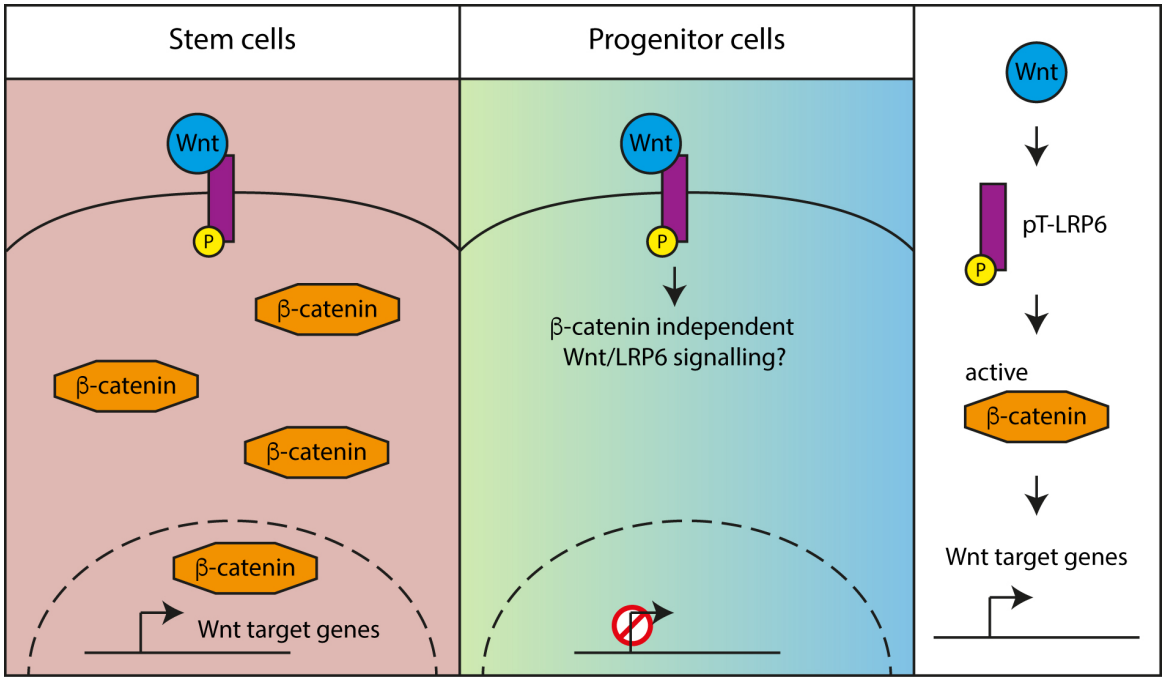

Figure 30. Wnt/β-catenin signalling is active in stem cells and β-catenin independent Wnt/LRP6 signalling is active in progenitors. In *rx2* positive stem cells pT-LRP6, active β-catenin and expression of Wnt/β-catenin target genes were detected. In progenitors only pT-LRP6 was detected suggesting that β-catenin independent Wnt/LRP6 signalling plays a role in those cells.

4.2 eGFP-DN-GSK3 causes upregulation of Wnt/β-catenin signalling

In order to manipulate Wnt signalling clonally in retinal cell lineages, we chose dominant negative GSK3 fused to eGFP, as a (fluorescent) marker is essential for lineage tracing. This fusion was already published to function in *Xenopus* (Taelman et al., 2010), however we validated its functionality in medaka. mRNA injections of eGFP-DN-GSK3 and Wnt3a resulted in equal elevation of Wnt/β-catenin target gene *axin2* levels by roughly 2-fold. However, in the stable functional lineage tracing lines anterior truncations were more severe with Wnt3a than with eGFP-DN-GSK3 injected with Cre mRNA. This is not surprising as Wnt is upstream of GSK3 and as it is secreted, it has cell non-autonomous effects. Also in mouse it could be observed, that elevation of Wnt/β-catenin signalling through a mutation in LRP6 yielded less severe phenotypes than a mutation in DKK1 (Arkell et al., 2013; Fossat et al., 2011). Hence, recombination in the eGFP-DN-GSK3 functional lineage tracing line results in increased Wnt/β-catenin signalling. Nevertheless, GSK3 has β-catenin independent functions and for this reason it cannot be excluded that those are also modified by eGFP-DN-GSK3. On one hand, β-catenin independent Wnt/LRP6 signalling may be activated (Acebron and Niehrs, 2016). On the other hand GSK3 is also part of other pathways, such as Hedgehog, Notch and Growth factor signalling (Tejeda-Munoz and Robles-Flores, 2015). Hence, those pathways may also be activated via eGFP-DN-GSK3.

4.3 Upregulation of Wnt signalling functionally divides the CMZ into stem cells, non-committed and committed progenitor cells

To elucidate functions of different pathways or single proteins in adult tissues, drug treatments or inducible gene expression systems have been usually employed to inhibit or activate the protein of interest. Those methods have one common drawback: The pathway/molecule of interest is always modified in either the whole organism, or in case of inducible expression systems, at least in a pool of cells expressing the same genetic marker. Therefore, neither systemic effects can be excluded nor changes in single cells can be followed. The effect on a given tissue or pool of cells can be analysed, which

provides valuable information on this entity of cells as a whole but does not allow dissecting the function of a protein in single cells with unmodified surroundings. Therefore, coupling clonal labelling strategies with functional modifications is a powerful tool to study the impact of functional modifications on single cells and their progeny in an otherwise intact organism. If the number of modified cells is small enough, systemic effects can be excluded and differences of single cells in a pool can be spotted. Hence, the functional lineage tracing lines created within this thesis present a valuable addition to the tools available to study Wnt signalling in the CMZ but also in all other stem cell niches.

The different transgenic Cre driver lines enabled testing Wnt function in several cell types and their progeny. In the following, the results of each Cre line shall be discussed.

rx2 positive stem cells form ArCoSs under wt conditions but cease to do so when expressing eGFP-DN-GSK3. There are three likely scenarios that cause stem cells not to form ArCoS any more: They might stop proliferating, undergo apoptosis or divide symmetrically (Figure 31). A symmetric division could be either caused by symmetric distribution of Wnt/β-catenin responsive genes (Habib et al., 2013) or β-catenin independently via orientation of division plane through Wnt/LRP6 signalling components (Acebron and Niehrs, 2016). Dormancy could be mediated by Wnt/β-catenin signalling. Although it is usually associated with promoting proliferation, in the hematopoietic system Wnt was shown to be necessary for maintenance of quiescent stem cells (Fleming et al., 2008). For apoptosis there are no records that show β-catenin causing cell death as Wnt/β-catenin signalling is usually linked to cell survival instead of apoptosis (Reya and Clevers, 2005). However, inhibition of GSK3 was shown to sensitize cancer cell lines to tumor necrosis factor-related apoptosis-inducing ligand (TRAIL) mediated apoptosis (Beurel et al., 2009; Mamaghani et al., 2012).

I performed experiments to evaluate proliferation status and apoptosis in *rx2* positive cells expressing eGFP-DN-GSK3. TUNEL stainings revealed apoptosis neither in wt nor in eGFP-DN-GSK3 expressing cells. It was also reported in *Xenopus* that elevated Wnt signalling does not cause cells of the CMZ to perform apoptosis (Denayer et al., 2008). However, both this work and the published results might not detect apoptotic cells if they are cleared away too quickly. In the zebrafish brain for instance, apoptotic cells are

removed by microglia in the timescale of minutes as the majority of apoptotic neurons are found already engulfed by microglia (Peri and Nüsslein-Volhard, 2008; Schlegelmilch et al., 2011). In order to exclude clearance of apoptotic cells, it would be beneficial to monitor activity of microglia in the retina. Hence, apoptosis of eGFP-DN-GSK3 expressing stem cells cannot be excluded although I was not able to detect it.

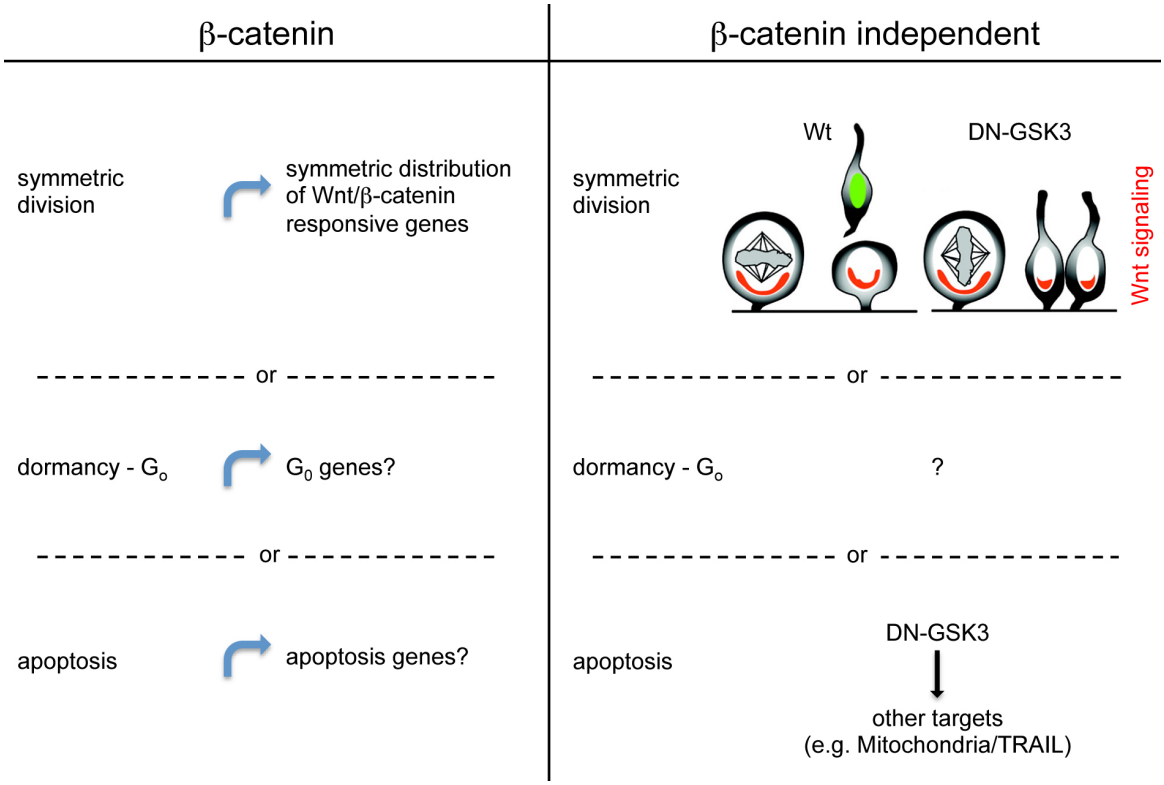

Figure 31. β-catenin dependent and independent possibilities of how eGFP-DN-GSK3 impacts on *rx2* positive cells. *rx2* positive cells most likely undergo symmetric divisions, dormancy or apoptosis upon eGFP-DN-GSK3 expression. Symmetric division could be mediated via symmetric distribution of Wnt/β-catenin responsive components or orientation of division plane through Wnt/LRP6 signalling components. Dormancy could potentially be mediated via Wnt/β-catenin responsive genes and apoptosis could be induced via other phosphorylation targets of GSK3 and the tumor necrosis factor-related apoptosis-inducing ligand (TRAIL). Illustration adapted from (Haydar et al., 2003).

Proliferation analysis showed that the percentage of proliferating *rx2* positive cells is higher in the eGFP-DN-GSK3 than in the GaudiRSG line. However, as I cannot exclude apoptosis it is possible that in the eGFP-DN-GSK3 line non-proliferating cells died prior to analysis leaving relatively more proliferating cells behind. Although in the hematopoietic system Wnt was reported to be necessary for maintenance of quiescent stem cells (Fleming et al., 2008), my results strongly indicate that expression of eGFP-DN-GSK3 does not cause quiescence in *rx2* positive cells. It rather causes either non-

proliferating cells to perform apoptosis or increases proliferation in *rx2* positive cells. The latter would be consistent with the literature for the CMZ across vertebrates (Denayer et al., 2008; Kubo, 2003; Kubo and Nakagawa, 2009; Kubo et al., 2005; Meyers et al., 2012) but also other mammalian organs (Reya and Clevers, 2005).

But if the cells expressing eGFP-DN-GSK3 proliferate equally or more than wt cells, why do they not form ArCoS? A possible explanation is that they need a Wnt gradient during cell division to divide asymmetrically, leaving one stem and one progenitor cell. In case they divide symmetrically and their division plane is not oriented in a way that always retains one cell in the niche and the other cell outside, the cells might get pushed out of the niche quickly by neighbouring cells dividing asymmetrically. This scenario is supported by studies in ESC culture, where a directed Wnt signal oriented the division plane as well as the cell fates of the resulting daughter cells (Habib et al., 2013).

In consequence, although I was not able to fully unravel the mechanisms underlying eGFP-DN-GSK3 expression in *rx2* positive cells, it is likely that they either undergo apoptosis or switch to a symmetric division mode.

Since *rx2* positive cells do not form ArCoS when they express eGFP-DN-GSK3, I tested whether any other cells in the retina change their behaviour in this context. Therefore, I used the *hsp70*::Cre driver line to induce recombination stochastically in all retinal cell types. To my surprise those experiments revealed that there are cells in the retina that form ArCoSs upon expression of eGFP-DN-GSK3. Those ArCoSs are not initiated by *rx2* positive stem cells as I could already show that those cells are not able to form ArCoS upon expression of eGFP-DN-GSK3. It is also very unlikely that terminally differentiated cells dedifferentiate, re-enter the cell cycle and regain stemness when they increase Wnt signalling. This is supported by experiments in zebrafish and *Xenopus* where upregulation of Wnt signalling did not affect already differentiated cells (Denayer et al., 2008; Meyers et al., 2012). Hence, it is most likely that expression of eGFP-DN-GSK3 causes progenitor cells to form ArCoSs. This means, that they reacquire the ability to self-renew, as they are able to continually contribute to the growth of the retina for months. As the hallmarks of stemness are self-renewal and multipotency, I analysed the cell type composition of the eGFP-DN-GSK3 ArCoSs. As explained above, wt ArCoSs are exclusively multipotent. In contrast, eGFP-DN-GSK3 ArCoSs have varying fate

restrictions, ranging from multipotent, via restricted to cells of the INL and ONL down to ArCoSs only consisting of photoreceptors. Thus, ectopic Wnt stimulation does not reset fate restrictions. The ArCoSs with varying fate restrictions were likely initiated by progenitors with different competencies. Accordingly, multipotent ArCoSs where initiated by "early" progenitors and fate restricted ArCoSs where initiated by already fate restricted progenitors. This explanation fits well with the competence model of successive fate restriction described in section 1.2.2 (Livesey and Cepko, 2001). It can also be excluded that the fate restricted ArCoSs are artefacts of the ubiquitin promoter, as the transplantation ArCoSs were always multipotent.

The formation of ArCoSs by progenitors with upregulated Wnt signalling also raises the question why their progeny is still able to differentiate, as those cells also harbour high Wnt signalling. Studies in mouse and chicken show that Wnt hyperstimulation leads to inhibition of differentiation (Kubo, 2003; Kubo et al., 2005; Liu et al., 2007). In *Xenopus*, however, it was shown that cells in the CMZ can still differentiate and are directed correctly to their retinal layers upon Wnt hyperstimulation (Denayer et al., 2008). The differentiation of cells with upregulated Wnt signalling could be achieved through another pathway that either inhibits Wnt signalling or makes the cells less susceptible or sensitive for it. A possible candidate pathway is Hedgehog since it was shown to antagonise Wnt signalling at the central boundary of the *Xenopus* CMZ (Borday et al., 2012), but also other proneural genes could be involved.

In order to define the identity of cells forming ArCoSs upon Wnt upregulation further, I performed ArCoS experiments with two more Cre driver lines: *tlx*::CreERT2 and *atoh7*::CreERT2. As *tlx* supposedly marks stem and "early" progenitor cells, I expected ArCoSs initiated by "early" progenitors. According to my hypothesis that Wnt upregulation causes formation of ArCoS in progenitors but does not reset already existing fate restrictions, the "early", non-committed progenitors marked by *tlx* should form multipotent ArCoS. And that was exactly the experimental outcome. eGFP-DN-GSK3 expression in *tlx* positive cells yielded few ArCoSs, which may be explained by *tlx* labelling stem cells, which do nor form ArCoS upon Wnt upregulation, and only a small part of the progenitors in the CMZ. But all ArCoSs that I detected were multipotent indicating that they were indeed initiated by "early", not fate restricted progenitors.

Atoh7 is essential for RGC lineage specification and differentiation (Mu and Klein, 2004), but it is already expressed in proliferating progenitors in the CMZ (Lust et al., 2016). Hence, I chose *atoh7*::CreERT2 to test Wnt upregulation in supposedly committed progenitors. With GaudiRSG I first confirmed that *atoh7* indeed labels proliferation-restricted progenitors, as they form footprints consisting mainly of RGCs but also of amacrine, horizontal cells and photoreceptors. *atoh7* positive cells expressing eGFP-DN-GSK3, in contrast, form only small footprints consisting of 1 - 3 cells per clone, which consist mainly of photoreceptors with very few amacrine and horizontal cells. Wnt signalling is required for expression of *atoh7* in *Xenopus* (Agathocleous et al., 2009). However, in the zebrafish *apc* mutant, which features constantly upregulated Wnt signalling, the *atoh7* expression domain in the CMZ is shifted toward the central retina (Stephens et al., 2010). This indicates that Wnt signalling also restricts *atoh7* expression. Consequently, if *atoh7* positive cells express eGFP-DN-GSK3 and thus upregulate Wnt signalling, *atoh7* expression might be initially inhibited and RGC differentiation suppressed. Another possibility is that expression of eGFP-DN-GSK3 alters the division plane and mode to symmetrically differentiating divisions, which may also explain the small clone size. However, it is not clear why Wnt signalling imposes stem cell features on some progenitor populations but restricts proliferation in another. This also hints at diverging functions of Wnt signalling in the CMZ.

Taken together, upregulation of Wnt signalling has very diverse effects on the cells of the CMZ (Figure 32). *rx2* positive stem cells lose their capacity to form ArCoS and therefore lose stem cell characteristics. They probably change their division mode or undergo apoptosis. Progenitors may reacquire the capacity to self-renew, but their pre-existing fate restrictions are irreversible. *atoh7* positive committed progenitors shift their fate and/or change their division mode and proliferation characteristics. Consequently, functional lineage tracing confirms that Wnt has different effects on stem and progenitor cells although the mechanistic details of those effects remain elusive. My results suggest that the CMZ can be functionally divided into *rx2*+ stem cells, *rx2*-/*tlx*+ non-committed progenitors and *atoh7*+ committed progenitors according to their characteristics in response to eGFP-DN-GSK3 expression.

Coming back to Waddington's landscape described at the beginning of this work. In this landscape of slopes and ridges, where a ball running down the slope represents a stem cell in its differentiation process, Wnt signalling may be capable to impose self-renewal onto this ball, but it may not be sufficient to push the ball back up the slopes. Hence, Wnt may be sufficient to direct self-renewal but not multipotency.

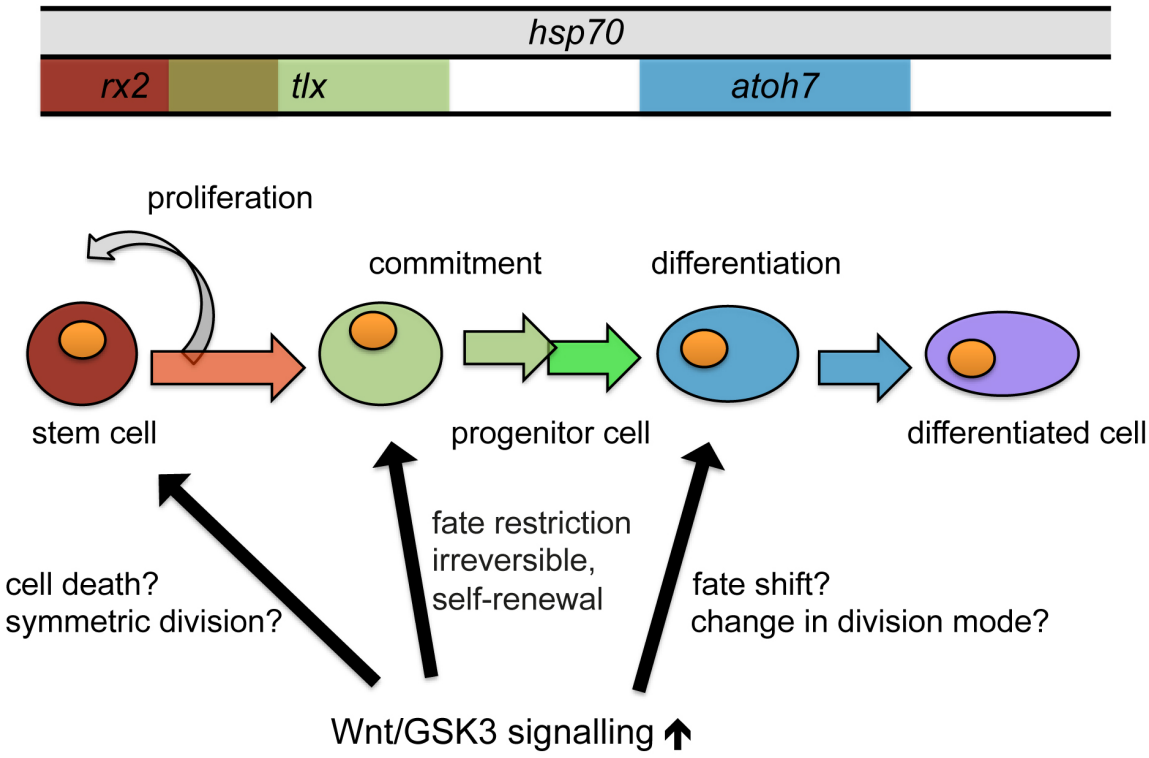

Figure 32. Wnt/GSK3 signalling has various effects on the different cell types within the CMZ. The bars on top indicate the different expression domains of all Cre drivers used: *rx2* (red), *tlx* (green), *atoh7* (blue) and *hsp70* (grey). Increased Wnt/GSK3 signalling possibly causes cell death or symmetric divisions in stem cells. On progenitor cells it imposes self-renewal, but may not reset already existing fate restrictions. In atoh7 positive progenitors it causes either a fate shift or a change in the division mode.

4.4 Integration of Wnt signalling localisation and function within the CMZ

Now that localisation and function of Wnt signalling in the CMZ are addressed, the next logical step is to discuss how those two sets of experiments fit together. As *rx2* positive stem cells feature Wnt/β-catenin signalling and progenitor cells β-catenin independent Wnt/LRP6 signalling it is not surprising that upregulation of Wnt signalling has different

effects on both cell types. *rx2* positive cells may require an asymmetric distribution of β-catenin and Wnt target genes to perform asymmetric cell division producing one stem and one progenitor cell. If Wnt signalling is upregulated during cell division this necessary gradient may be abolished leaving both daughter cells with high levels of β-catenin and Wnt target genes. However, this raises the question why progenitor cells are able to self-renew in this context. A possible explanation is that at this position within the niche invariant asymmetric division are not strictly necessary, but progenitors may self-renew through population asymmetry. Meaning that they divide symmetrically and to compensate, another cell gets pushed out of the niche and differentiates. However, the lineage tracing with *hsp70*::Cre or *tlx*::CreERT2 still revealed continuous stripes, which argues for invariant asymmetric divisions. Another possibility is that the position of progenitor cells within the niche, which is more apical than the stem cell position, received different other cues that allow for asymmetric divisions even if Wnt signalling is upregulated. This may be Hedgehog signalling for instance as described above.

On the other hand it seems logical that progenitors regain some aspects of stem cells if they reacquire Wnt/β-catenin signalling, which is associated with stemness (Reya and Clevers, 2005) and which they normally would not possess. Progenitors are very likely to be receptive for β-catenin mediated activation of Wnt target genes, as the Wnt reporter domain extends towards progenitors in the *Xenopus* CMZ when Wnt is hyperstimulated (Borday et al., 2012). Nevertheless, Wnt/β-catenin signalling is not sufficient to restore multipotency, which may be explained by other proneural genes being active in the progenitor area of the CMZ.

However, the localisation of Wnt signalling components did not give any hints as to why Wnt upregulation has such different effects on *atoh7* positive cells. Here, a possible explanation is that eGFP-DN-GSK3 also upregulates other pathways beside Wnt, such as Hedgehog, Notch and Growth factor signalling (Tejeda-Munoz and Robles-Flores, 2015). Especially Hedgehog seems to be a likely candidate, as components of the pathway are expressed at the central edge of the CMZ (Borday et al., 2012). Hence, studying other pathways in the CMZ may provide a deeper mechanistic insight into the characteristics of *atoh7* positive cells in response to eGFP-DN-GSK3 expression.

4.5 Relevance for other stem cell niches

The work presented here is highly relevant to other stem cell niches and stem cell research in general. As Wnt signalling is important across species and also across organs, findings within this thesis may have implications for a lot of other stem cell systems. The localisation of Wnt signalling components give the first hints that β-catenin independent Wnt/LRP6 signalling plays a role in progenitor cell divisions of adult stem cell niches. Although I was not able to shed light onto the mechanistic details of Wnt upregulation in retinal stem and progenitor cells, it is apparent that it has very different effects on those cell types. As Wnt hyperstimulation is normally associated with over-proliferation and cancer (Clevers and Nusse, 2012; Reya and Clevers, 2005), it is surprising that Wnt upregulation in *rx2* positive cells does not lead to the formation of overly thick ArCoSs or cell aggregations. Hence, this may be part of the tight regulation of retinal growth and a powerful mechanism to prevent abnormal proliferation. Moreover, my results indicate that progenitor cells are able to regain certain stem cell characteristics upon Wnt upregulation. It is also known for the intestinal crypt that progenitors can regain stem cell potential upon injury to repopulate a destroyed niche. This process is also thought to require Wnt signalling (Beumer and Clevers, 2016). However, Wnt signalling is not sufficient to restore multipotency to progenitors of the CMZ, indicating that other niche cell factors are required for this process.

4.6 Outlook

In this work, I established transgenic medaka lines that allow the combination of lineage tracing and functional modifications of cells *in vivo*. Those tools in combination with *in vivo* imaging and possibly other genetic markers will enable to elucidate how exactly Wnt signalling impacts on single stem and progenitor cells in an intact organism. *In vivo* imaging bears the advantage that the behaviour of cells with increased Wnt signalling could be followed over time. This provides more precise information about division plane, proliferation and apoptosis, than “snapshots” of fixed samples generate. Additionally, mathematical modelling would help to unravel division modes of progenitors and how those are influenced by Wnt signalling.

Furthermore, I created but was not able to analyse transgenic lines that allow clonal inhibition of Wnt signalling. In addition to upregulation, inhibition of Wnt signalling will provide valuable information about the functions of the pathway in stem and progenitor cells of the retina.

Finally, those tools are ideal to study Wnt signalling in other organs beside the retina. In addition to addressing Wnt signalling in healthy organ growth or homeostasis, the involvement of GSK3 in pathologies like Alzheimer's, diabetes or cancer (Tejeda-Munoz and Robles-Flores, 2015) could be exploited to study those diseases.

Hence, my tools provide the basis for multiple complementary and novel scientific questions.

5 References

Acebron, S. P. and Niehrs, C. (2016). b-Catenin-Independent Roles of Wnt/LRP6 Signaling. *Trends Cell Biol.* **26**, 956–967.

Acebron, S. P., Karaulanov, E., Berger, B. S., Huang, Y.-L. and Niehrs, C. (2014). Mitotic Wnt Signaling Promotes Protein Stabilization and Regulates Cell Size. *Mol. Cell* 1–12.

Agathocleous, M., Iordanova, I., Willardsen, M. I., Xue, X. Y., Vetter, M. L., Harris, W. a and Moore, K. B. (2009). A directional Wnt/beta-catenin-Sox2-proneural pathway regulates the transition from proliferation to differentiation in the Xenopus retina. *Development* **136**, 3289–99.

Amato, M. A., Arnault, E. and Perron, M. (2004). Retinal stem cells in vertebrates: parallels and divergences. *Int. J. Dev. Biol.* **48**, 993–1001.

Arkell, R. M., Fossat, N. and Tam, P. P. L. (2013). Wnt signalling in mouse gastrulation and anterior development: New players in the pathway and signal output. *Curr. Opin. Genet. Dev.* **23**, 454–460.

Bajoghli, B., Aghaallaei, N., Jung, G. and Czerny, T. (2009). Induction of otic structures by canonical Wnt signalling in medaka. *Dev. Genes Evol.* **219**, 391–8.

Barker, N., van Es, J. H., Kuipers, J., Kujala, P., van den Born, M., Cozijnsen, M., Haegebarth, A., Korving, J., Begthel, H., Peters, P. J., et al. (2007). Identification of stem cells in small intestine and colon by marker gene Lgr5. *Nature* **449**, 1003–7.

Barker, N., Bartfeld, S. and Clevers, H. (2010). Tissue-resident adult stem cell populations of rapidly self-renewing organs. *Cell Stem Cell* **7**, 656–670.

Barkho, B. Z., Song, H., Aimone, J. B., Smrt, R. D., Kuwabara, T., Nakashima, K., Gage, F. H. and Zhao, X. (2006). Identification of astrocyte-expressed factors that modulate neural stem/progenitor cell differentiation. *Stem Cells Dev.* **15**, 407–21.

Beumer, J. and Clevers, H. (2016). Regulation and plasticity of intestinal stem cells during homeostasis and regeneration. *Development* **143**, 3639–3649.

Beurel, E., Blivet-Van Eggelpoël, M.-J., Kornprobst, M., Moritz, S., Delelo, R., Paye,

F., Housset, C. and Desbois-Mouthon, C. (2009). Glycogen synthase kinase-3 inhibitors augment TRAIL-induced apoptotic death in human hepatoma cells. *Biochem. Pharmacol.* **77**, 54–65.

Blanpain, C. and Simons, B. D. (2013). Unravelling stem cell dynamics by lineage tracing. *Nat. Rev. Mol. Cell Biol.* **14**, 489–502.

Bonaguidi, M. A., Wheeler, M. A., Shapiro, J. S., Stadel, R. P., Sun, G. J., Ming, G. L. and Song, H. (2011). In vivo clonal analysis reveals self-renewing and multipotent adult neural stem cell characteristics. *Cell* **145**, 1142–1155.

Borday, C., Cabochette, P., Parain, K., Mazurier, N., Janssens, S., Tran, H. T., Sekkali, B., Bronchain, O., Vleminckx, K., Locker, M., et al. (2012). Antagonistic cross-regulation between Wnt and Hedgehog signalling pathways controls post-embryonic retinal proliferation. *Development* **139**, 3499–509.

Centanin, L. and Wittbrodt, J. (2014). Retinal neurogenesis. *Development* **141**, 241–4.

Centanin, L., Hoeckendorf, B. and Wittbrodt, J. (2011). Fate restriction and multipotency in retinal stem cells. *Cell Stem Cell* **9**, 553–62.

Centanin, L., Ander, J.-J., Hoeckendorf, B., Lust, K., Kellner, T., Kraemer, I., Urbany, C., Hasel, E., Harris, W. a, Simons, B. D., et al. (2014). Exclusive multipotency and preferential asymmetric divisions in post-embryonic neural stem cells of the fish retina. *Development* 3472–3482.

Christian, J. L. and Moon, R. T. (1993). Interactions between Xwnt-8 and Spemann organizer signaling pathways generate dorsoventral pattern in the embryonic mesoderm of Xenopus. *Genes Dev.* **7**, 13–28.

Clayton, E., Doupé, D. P., Klein, A. M., Winton, D. J., Simons, B. D. and Jones, P. H. (2007). A single type of progenitor cell maintains normal epidermis. *Nature* **446**, 185–9.

Clevers, H. (2016). Modeling Development and Disease with Organoids. *Cell* **165**, 1586–1597.

Clevers, H. and Nusse, R. (2012). Wnt/β-catenin signaling and disease. *Cell* **149**, 1192–205.

Clevers, H., Loh, K. M. and Nusse, R. (2014). An integral program for tissue renewal and regeneration: Wnt signaling and stem cell control. *Science (80-.).* **346**, 1248012–1248012.

Cotsarelis, G., Cheng, S. Z., Dong, G., Sun, T. T. and Lavker, R. M. (1989). Existence of slow-cycling limbal epithelial basal cells that can be preferentially stimulated to proliferate: Implications on epithelial stem cells. *Cell* **57**, 201–209.

Cotsarelis, G., Sun, T. T. and Lavker, R. M. (1990). Label-retaining cells reside in the bulge area of pilosebaceous unit: Implications for follicular stem cells, hair cycle, and skin carcinogenesis. *Cell* **61**, 1329–1337.

Darken, R. S. and Wilson, P. A. (2001). Axis induction by wnt signaling: Target promoter responsiveness regulates competence. *Dev. Biol.* **234**, 42–54.

Das, A. V, Zhao, X., James, J., Kim, M., Cowan, K. H. and Ahmad, I. (2006). Neural stem cells in the adult ciliary epithelium express GFAP and are regulated by Wnt signaling. *Biochem. Biophys. Res. Commun.* **339**, 708–716.

Davidson, G., Wu, W., Shen, J., Bilic, J., Fenger, U., Stannek, P., Glinka, A. and Niehrs, C. (2005). Casein kinase 1 gamma couples Wnt receptor activation to cytoplasmic signal transduction. *Nature* **438**, 867–872.

Davidson, G., Shen, J., Huang, Y.-L., Su, Y., Karaulanov, E., Bartscherer, K., Hassler, C., Stannek, P., Boutros, M. and Niehrs, C. (2009). Cell cycle control of wnt receptor activation. *Dev. Cell* **17**, 788–799.

Denayer, T., Locker, M., Borday, C., Deroo, T., Janssens, S., Hecht, A., van Roy, F., Perron, M. and Vleminckx, K. (2008). Canonical Wnt signaling controls proliferation of retinal stem/progenitor cells in postembryonic Xenopus eyes. *Stem Cells* **26**, 2063–74.

Doe, C. Q. and Bowerman, B. (2001). Asymmetric cell division: Fly neuroblast meets worm zygote. *Curr. Opin. Cell Biol.* **13**, 68–75.

Dorsky, R. I., Sheldahl, L. C. and Moon, R. T. (2002). A transgenic Lef1/beta-catenin-dependent reporter is expressed in spatially restricted domains throughout zebrafish development. *Dev. Biol.* **241**, 229–37.

Doupé, D. P., Klein, A. M., Simons, B. D. and Jones, P. H. (2010). The Ordered Architecture of Murine Ear Epidermis Is Maintained by Progenitor Cells with Random Fate. *Dev. Cell* **18**, 317–323.

Dowling, J. E. (2012). *The retina: an approachable part of the brain*. Revised Ed. Cambridge, MA: Belknap Press of Harvard University Press.

Egger, B., Chell, J. M. and Brand, A. H. (2008). Insights into neural stem cell biology from flies. *Philos Trans R Soc L. B Biol Sci* **363**, 39–56.

Eiraku, M., Takata, N., Ishibashi, H., Kawada, M., Sakakura, E., Okuda, S., Sekiguchi, K., Adachi, T. and Sasai, Y. (2011). Self-organizing optic-cup morphogenesis in three-dimensional culture. *Nature* **472**, 51–56.

Erter, C. E., Wilm, T. P., Basler, N., Wright, C. V and Solnica-Krezel, L. (2001). Wnt8 is required in lateral mesendodermal precursors for neural posteriorization in vivo. *Development* **128**, 3571–3583.

Farin, H. F., Jordens, I., Mosa, M. H., Basak, O., Korving, J., Tauriello, D. V. F., Punder, K. De, Angers, S., Peters, P. J., Maurice, M. M., et al. (2016). intestinal stem-cell niche. *Nature* **530**, 340–343.

Filali, M., Cheng, N., Abbott, D., Leontiev, V. and Engelhardt, J. F. (2002). Wnt-3A/β-catenin signaling induces transcription from the LEF-1 promoter. *J. Biol. Chem.* **277**, 33398–33410.

Fischer, A. J., Bosse, J. L. and El-Hodiri, H. M. (2013). The ciliary marginal zone (CMZ) in development and regeneration of the vertebrate eye. *Exp. Eye Res.* 8–13.

Fleming, H. E., Janzen, V., Lo Celso, C., Guo, J., Leahy, K. M., Kronenberg, H. M. and Scadden, D. T. (2008). Wnt Signaling in the Niche Enforces Hematopoietic Stem Cell Quiescence and Is Necessary to Preserve Self-Renewal In Vivo. *Cell Stem Cell* **2**, 274–283.

Fossat, N., Jones, V., Khoo, P.-L., Bogani, D., Hardy, A., Steiner, K., Mukhopadhyay, M., Westphal, H., Nolan, P. M., Arkell, R., et al. (2011). Stringent requirement of a proper level of canonical WNT signalling activity for head formation in mouse embryo. *Development* **138**, 667–76.

Fuchs, E. and Horsley, V. (2011). Ferreting out stem cells from their niches. *Nat. Cell Biol.* **13**, 513–518.

Fujimura, N., Vacik, T., Machon, O., Vlcek, C., Scalabrin, S., Speth, M., Diep, D., Krauss, S. and Kozmik, Z. (2007). Wnt-mediated down-regulation of Sp1 target genes by a transcriptional repressor Sp5. *J. Biol. Chem.* **282**, 1225–1237.

Fujimura, N., Taketo, M. M., Mori, M., Korinek, V. and Kozmik, Z. (2009). Spatial and temporal regulation of Wnt/??-catenin signaling is essential for development of the retinal pigment epithelium. *Dev. Biol.* **334**, 31–45.

Fuller, M. T. and Spradling, A. C. (2007). Male and female Drosophila germline stem cells: two versions of immortality. *Science* **316**, 402–4.

Gage, F. H. (2012). Mammalian Neural Stem Cells. *Science (80-.).* **287**, 1433–1438.

Ghaffarizadeh, A., Podgorski, G. J. and Flann, N. S. (2014). Modeling and visualizing cell type switching. *Comput. Math. Methods Med.* **2014**,.

Glinka, A., Wu, W., Onichtchouk, D., Blumenstock, C. and Niehrs, C. (1997). Head induction by simultaneous repression of Bmp and Wnt signalling in Xenopus. *Nature* **389**, 517–519.

Glinka, A., Wu, W., Delius, H., Monaghan, A. P., Blumenstock, C. and Niehrs, C. (1998). Dickkopf-1 is a member of a new family of secreted proteins and functions in head induction. *Nature* **391**, 357–362.

Habib, S. J., Chen, B.-C., Tsai, F.-C., Anastassiadis, K., Meyer, T., Betzig, E. and Nusse, R. (2013). A Localized Wnt Signal Orients Asymmetric Stem Cell Division in Vitro. *Science (80-.).* **339**, 1445–1448.

Hägglund, A. C., Berghard, A. and Carlsson, L. (2013). Canonical Wnt/β-catenin signalling is essential for optic cup formation. *PLoS One* **8**, e81158.

Hamilton, F. S., Wheeler, G. N. and Hoppler, S. (2001). Difference in XTcf-3 dependency accounts for change in response to beta-catenin-mediated Wnt signalling in Xenopus blastula. *Development* **128**, 2063–73.

Han, Y.-G., Spassky, N., Romaguera-Ros, M., Garcia-Verdugo, J.-M., Aguilar, A.,

Schneider-Maunoury, S. and Alvarez-Buylla, A. (2008). Hedgehog signaling and primary cilia are required for the formation of adult neural stem cells. *Nat. Neurosci.* **11**, 277–84.

Hashimoto, H., Itoh, M., Yamanaka, Y., Yamashita, S., Shimizu, T., Solnica-Krezel, L., Hibi, M. and Hirano, T. (2000). Zebrafish Dkk1 functions in forebrain specification and axial mesendoderm formation. *Dev. Biol.* **217**, 138–152.

Haydar, T. F., Ang, E. and Rakic, P. (2003). Mitotic spindle rotation and mode of cell division in the developing telencephalon. *Proc. Natl. Acad. Sci. U. S. A.* **100**, 2890–5.

He, T. C., Sparks, A. B., Rago, C., Hermeking, H., Zawel, L., da Costa, L. T., Morin, P. J., Vogelstein, B., Kinzler, K. W., Groden, J., et al. (1998). Identification of c-MYC as a target of the APC pathway. *Science* **281**, 1509–12.

He, J., Zhang, G., Almeida, A. D., Cayouette, M., Simons, B. D. and Harris, W. A. (2012). How Variable Clones Build an Invariant Retina. *Neuron* **75**, 786–798.

Heisenberg, C. P., Houart, C., Take-Uchi, M., Rauch, G. J., Young, N., Coutinho, P., Masai, I., Caneparo, L., Concha, M. L., Geisler, R., et al. (2001). A mutation in the Gsk3-binding domain of zebrafish masterblind/Axin1 leads to a fate transformation of telencephalon and eyes to diencephalon. *Genes Dev.* **15**, 1427–1434.

Ho, R. K. and Kane, D. A. (1990). Cell-autonomous action of zebrafish spt-1 mutation in specific mesodermal precursors. *Nature* **348**, 728–730.

Hoppler, S., Brown, J. D. and Moon, R. T. (1996). Expression of a dominant-negative wnt blocks induction of MyoD in Xenopus embryos. *Genes Dev.* **10**, 2805–2817.

Hovanes, K., Li, T. W. H., Munguia, J. E., Truong, T., Milovanovic, T., Lawrence Marsh, J., Holcombe, R. F. and Waterman, M. L. (2001). Beta-catenin-sensitive isoforms of lymphoid enhancer factor-1 are selectively expressed in colon cancer. *Nat. Genet.* **28**, 53–57.

Huang, Y.-L., Anvarian, Z., Döderlein, G., Acebron, S. P. and Niehrs, C. (2015). Maternal Wnt/STOP signaling promotes cell division during early Xenopus

embryogenesis. *Proc. Natl. Acad. Sci.* **112**, 201423533.

Inoue, T., Kagawa, T., Fukushima, M., Shimizu, T., Yoshinaga, Y., Takada, S., Tanihara, H. and Taga, T. (2006). Activation of canonical Wnt pathway promotes proliferation of retinal stem cells derived from adult mouse ciliary margin. *Stem Cells* **24**, 95–104.

Jaenisch, R. and Young, R. (2008). Stem Cells, the Molecular Circuitry of Pluripotency and Nuclear Reprogramming. *Cell* **132**, 567–582.

Jho, E., Zhang, T., Domon, C., Joo, C.-K., Freund, J.-N. and Costantini, F. (2002). Wnt/beta-catenin/Tcf signaling induces the transcription of Axin2, a negative regulator of the signaling pathway. *Mol. Cell. Biol.* **22**, 1172–83.

Johns, P. R. (1977). Growth of the adult goldfish eye. III. Source of the new retinal cells. *J. Comp. Neurol.* **176**, 343–57.

Jope, R. S. and Johnson, G. V. W. (2004). The glamour and gloom of glycogen synthase kinase-3. *Trends Biochem. Sci.* **29**, 95–102.

Kazanskaya, O., Glinka, A. and Niehrs, C. (2000). The role of Xenopus dickkopf1 in prechordal plate specification and neural patterning. *Development* **127**, 4981–92.

Kelly, G. M., Greenstein, P., Eerzyilmaz, D. F. and Moon, R. T. (1995). Zebrafish Wnt8 and Wnt8B Share a Common Activity But Are Involved in Distinct Developmental Pathways. *Development* **121**, 1787–1799.

Kiecker, C. and Niehrs, C. (2001). A morphogen gradient of Wnt/beta-catenin signalling regulates anteroposterior neural patterning in Xenopus. *Development* **128**, 4189–4201.

Kiel, M. J., He, S., Ashkenazi, R., Gentry, S. N., Teta, M., Kushner, J. A., Jackson, T. L. and Morrison, S. J. (2007). Haematopoietic stem cells do not asymmetrically segregate chromosomes or retain BrdU. *Nature* **449**, 238–42.

Kim, C. H., Oda, T., Itoh, M., Jiang, D., Artinger, K. B., Chandrasekharappa, S. C., Driever, W. and Chitnis, A. B. (2000). Repressor activity of Headless/Tcf3 is essential for vertebrate head formation. *Nature* **407**, 913–6.

Klein, A. M., Nakagawa, T., Ichikawa, R., Yoshida, S. and Simons, B. D. (2010). Mouse germ line stem cells undergo rapid and stochastic turnover. *Cell Stem Cell* **7**, 214–24.

Koch, S., Acebron, S. P., Herbst, J., Hatiboglu, G. and Niehrs, C. (2015). Post-transcriptional Wnt Signaling Governs Epididymal Sperm Maturation. *Cell* **163**, 1225–1236.

Koster, R., Stick, R., Loosli, F. and Wittbrodt, J. (1997). Medaka spalt acts as a target gene of hedgehog signaling. *Development* **124**, 3147–3156.

Kubo, F. (2003). Wnt2b controls retinal cell differentiation at the ciliary marginal zone. *Development* **130**, 587–598.

Kubo, F. and Nakagawa, S. (2009). Hairy1 acts as a node downstream of Wnt signaling to maintain retinal stem cell-like progenitor cells in the chick ciliary marginal zone. *Development* **136**, 1823–33.

Kubo, F., Takeichi, M. and Nakagawa, S. (2005). Wnt2b inhibits differentiation of retinal progenitor cells in the absence of Notch activity by downregulating the expression of proneural genes. *Development* **132**, 2759–70.

Lancaster, M. A. and Knoblich, J. A. (2014). Organogenesis in a dish: modeling development and disease using organoid technologies. *Science* **345**, 1247125.

Lawson, D. A., Xin, L., Lukacs, R. U., Cheng, D. and Witte, O. N. (2007). Isolation and functional characterization of murine prostate stem cells. *Proc. Natl. Acad. Sci. U. S. A.* **104**, 181–186.

Lekven, A. C., Thorpe, C. J., Waxman, J. S. and Moon, R. T. (2001). Zebrafish wnt8 Encodes Two Wnt8 Proteins on a Bicistronic Transcript and Is Required for Mesoderm and Neurectoderm Patterning. *Dev. Cell* **1**, 103–114.

Lie, D. C., Colamarino, S. A., Song, H. J., Désiré, L., Mira, H., Consiglio, A., Lein, E. S., Jessberger, S., Lansford, H., Dearie, A. R., et al. (2005). Wnt signalling regulates adult hippocampal neurogenesis. *Nature* **437**, 1370–1375.

Lim, D. A., Tramontin, A. D., Trevejo, J. M., Herrera, D. G., García-Verdugo, J. M. and Alvarez-Buylla, A. (2000). Noggin antagonizes BMP signaling to create a

niche for adult neurogenesis. *Neuron* **28**, 713–726.

Liu, H., Xu, S., Wang, Y., Mazerolle, C., Thurig, S., Coles, B. L. K., Ren, J. C., Taketo, M. M., van der Kooy, D. and Wallace, V. A. (2007). Ciliary margin transdifferentiation from neural retina is controlled by canonical Wnt signaling. *Dev. Biol.* **308**, 54–67.

Liu, H. K., Belz, T., Bock, D., Takacs, A., Wu, H., Lichter, P., Chai, M. and Schütz, G. (2008). The nuclear receptor tailless is required for neurogenesis in the adult subventricular zone. *Genes Dev.* **22**, 2473–2478.

Livesey, F. J. and Cepko, C. L. (2001). Vertebrate neural cell-fate determination: lessons from the retina. *Nat. Rev. Neurosci.* **2**, 109–18.

Livet, J., Weissman, T. a, Kang, H., Draft, R. W., Lu, J., Bennis, R. a, Sanes, J. R. and Lichtman, J. W. (2007). Transgenic strategies for combinatorial expression of fluorescent proteins in the nervous system. *Nature* **450**, 56–62.

Logan, C. Y. and Nusse, R. (2004). The Wnt signaling pathway in development and disease. *Annu. Rev. Cell Dev. Biol.* **20**, 781–810.

Loosli, F., Köster, R. W., Carl, M., Krone, A. and Wittbrodt, J. (1998). Six3, a medaka homologue of the Drosophila homeobox gene sine oculis is expressed in the anterior embryonic shield and the developing eye. *Mech. Dev.* **74**, 159–164.

Lopez-Garcia, C., Klein, A. M., Simons, B. D. and Winton, D. J. (2010). Intestinal stem cell replacement follows a pattern of neutral drift. *Science (80-.).* **330**, 822–825.

Luisier, F., Vonesch, C., Blu, T. and Unser, M. (2010). Fast interscale wavelet denoising of Poisson-corrupted images. *Signal Processing* **90**, 415–427.

Lust, K., Sinn, R., Saturnino, A. P., Centanin, L. and Wittbrodt, J. (2016). De novo neurogenesis by targeted expression of Atoh7 to Müller glia cells. *Development* 1874–1883.

Lustig, B., Jerchow, B., Sachs, M., Weiler, S., Pietsch, T., Karsten, U., van de Wetering, M., Clevers, H., Schlag, P. M., Birchmeier, W., et al. (2002). Negative feedback loop of Wnt signaling through upregulation of conductin/axin2 in

colorectal and liver tumors. *Mol. Cell. Biol.* **22**, 1184–93.

Ma, D. K., Ming, G. L. and Song, H. (2005). Glial influences on neural stem cell development: Cellular niches for adult neurogenesis. *Curr. Opin. Neurobiol.* **15**, 514–520.

MacDonald, B. T., Tamai, K. and He, X. (2009). Wnt/beta-catenin signaling: components, mechanisms, and diseases. *Dev. Cell* **17**, 9–26.

Mamaghani, S., Simpson, C. D., Cao, P. M., Cheung, M., Chow, S., Bandarchi, B., Schimmer, A. D. and Hedley, D. W. (2012). Glycogen synthase kinase-3 inhibition sensitizes pancreatic cancer cells to TRAIL-induced apoptosis. *PLoS One* **7**, e41102.

Margolis, J. and Spradling, A. (1995). Identification and behavior of epithelial stem cells in the Drosophila ovary. *Development* **121**, 3797–807.

Marshman, E., Booth, C. and Potten, C. S. (2002). The intestinal epithelial stem cell. *BioEssays* **24**, 91–98.

Masatake Osawa, K. H. H. N. (1996). Long-Term Lymphohematopoietic Reconstitution by a Single CD34-Low/Negative Hematopoietic Stem Cell. *Science (80-.).* **273**, 242–245.

McGrew, L. L., Lai, C. J. and Moon, R. T. (1995). Specification of the anteroposterior neural axis through synergistic interaction of the Wnt signaling cascade with noggin and follistatin. *Dev. Biol.* **172**, 337–342.

McGrew, L. L., Hoppler, S. and Moon, R. T. (1997). Wnt and FGF pathways cooperatively pattern anteroposterior neural ectoderm in Xenopus. *Mech. Dev.* **69**, 105–114.

Mello, C. C., Draper, B. W., Krause, M., Weintraub, H. and Priess, J. R. (1992). The pie-1 and mex-1 genes and maternal control of blastomere identity in early C. elegans embryos. *Cell* **70**, 163–176.

Mello, C. C., Schubert, C., Draper, B., Zhang, W., Lobel, R. and Priess, J. R. (1996). The PIE-1 protein and germline specification in C. elegans embryos. *Nature* **382**, 710–712.

Meyer, N. and Penn, L. Z. (2008). Reflecting on 25 years with MYC. *Nat. Rev. Cancer* **8**, 976–90.

Meyers, J. R., Hu, L., Moses, A., Kaboli, K., Papandrea, A. and Raymond, P. a (2012). β-catenin/Wnt signaling controls progenitor fate in the developing and regenerating zebrafish retina. *Neural Dev.* **7**, 30.

Ming, G. li and Song, H. (2011). Adult Neurogenesis in the Mammalian Brain: Significant Answers and Significant Questions. *Neuron* **70**, 687–702.

Misawa, A., Hosoi, H., Arimoto, A., Shikata, T., Akioka, S., Matsumura, T., Houghton, P. J. and Sawada, T. (2000). N-Myc induction stimulated by insulin-like growth factor I through mitogen-activated protein kinase signaling pathway in human neuroblastoma cells. *Cancer Res.* **60**, 64–69.

Morris, R. J., Liu, Y., Marles, L., Yang, Z., Trempus, C., Li, S., Lin, J. S., Sawicki, J. A. and Cotsarelis, G. (2004). Capturing and profiling adult hair follicle stem cells. *Nat Biotechnol* **22**, 411–417.

Morrison, S. J. and Kimble, J. (2006). Asymmetric and symmetric stem-cell divisions in development and cancer. *Nature* **441**, 1068–1074.

Moshiri, A. and Reh, T. A. (2004). Persistent progenitors at the retinal margin of ptc+/- mice. *J. Neurosci.* **24**, 229–237.

Moshiri, A., McGuire, C. R. and Reh, T. A. (2005). Sonic hedgehog regulates proliferation of the retinal ciliary marginal zone in posthatch chicks. *Dev. Dyn.* **233**, 66–75.

Mu, X. and Klein, W. H. (2004). A gene regulatory hierarchy for retinal ganglion cell specification and differentiation. *Semin. Cell Dev. Biol.* **15**, 115–123.

Mukhopadhyay, M., Shtrom, S., Rodriguez-Esteban, C., Chen, L., Tsukui, T., Gomer, L., Dorward, D. W., Glinka, A., Grinberg, A., Huang, S. P., et al. (2001). Dickkopf1 Is Required for Embryonic Head Induction and Limb Morphogenesis in the Mouse. *Dev. Cell* **1**, 423–434.

Mwafi, N., Beretta, C. A., Paolini, A. and Carl, M. (2014). Divergent Wnt8a gene expression in teleosts. *PLoS One* **9**, e85303.

Nadauld, L. D., Chidester, S., Shelton, D. N., Rai, K., Broadbent, T., Sandoval, I. T., Peterson, P. W., Manos, E. J., Ireland, C. M., Yost, H. J., et al. (2006). Dual roles for adenomatous polyposis coli in regulating retinoic acid biosynthesis and Wnt during ocular development. *Proc. Natl. Acad. Sci. U. S. A.* **103**, 13409–14.

Nakayama, K. I. and Nakayama, K. (2006). Ubiquitin ligases: cell-cycle control and cancer. *Nat. Rev. Cancer* **6**, 369–81.

Niehrs, C. and Acebron, S. P. (2012). Mitotic and mitogenic Wnt signalling. *EMBO J.* **31**, 2705–13.

Niehrs, C. and Shen, J. (2010). Regulation of Lrp6 phosphorylation. *Cell. Mol. Life Sci.* **67**, 2551–62.

Nusse, R. (2008). Wnt signaling and stem cell control. *Cell Res.* **18**, 523–7.

Nusse, R. (2017). The Wnt homepage - http://web.stanford.edu/group/nusselab/cgi-bin/wnt/target_genes. *accessed 27.01.2017*.

Ohnuma, S., Hopper, S., Wang, K. C., Philpott, A. and Harris, W. a (2002). Co-ordinating retinal histogenesis: early cell cycle exit enhances early cell fate determination in the Xenopus retina. *Development* **129**, 2435–46.

Orford, K. W. and Scadden, D. T. (2008). Deconstructing stem cell self-renewal: genetic insights into cell-cycle regulation. *Nat Rev Genet* **9**, 115–128.

Palmer, T. D., Willhoite, A. R. and Gage, F. H. (2000). Vascular niche for adult hippocampal neurogenesis. *J. Comp. Neurol.* **425**, 479–494.

Peri, F. and Nüsslein-Volhard, C. (2008). Live Imaging of Neuronal Degradation by Microglia Reveals a Role for v0-ATPase a1 in Phagosomal Fusion In Vivo. *Cell* **133**, 916–927.

Perron, M. and Harris, W. a (2000). Retinal stem cells in vertebrates. *Bioessays* **22**, 685–8.

Perron, M., Kanekar, S., Vetter, M. L. and Harris, W. a (1998). The genetic sequence of retinal development in the ciliary margin of the Xenopus eye. *Dev. Biol.* **199**, 185–200.

Pierce, S. E. and Kimelman, D. (1995). Regulation of Spemann organiser formation by the intracellular Xgsk-3. *Development* **121**, 755–765.

Pierfelice, T., Alberi, L. and Gaiano, N. (2011). Notch in the Vertebrate Nervous System: An Old Dog with New Tricks. *Neuron* **69**, 840–855.

Qu, Q., Sun, G., Li, W., Yang, S., Ye, P., Zhao, C., Yu, R. T., Gage, F. H., Evans, R. M. and Shi, Y. (2010). Orphan nuclear receptor TLX activates Wnt/beta-catenin signalling to stimulate neural stem cell proliferation and self-renewal. *Nat. Cell Biol.* **12**, 31-40–9.

Raymond, P. A., Barthel, L. K., Bernardos, R. L. and Perkowski, J. J. (2006). Molecular characterization of retinal stem cells and their niches in adult zebrafish. *BMC Dev. Biol.* **6**, 36.

Reese, K. J., Dunn, M. A., Waddle, J. A. and Seydoux, G. (2000). Asymmetric segregation of PIE-1 in C. elegans is mediated by two complementary mechanisms that act through separate PIE-1 protein domains. *Mol. Cell* **6**, 445–455.

Reh, T. A. and Levine, E. M. (1998). Multipotential stem cells and progenitors in the vertebrate retina. *J. Neurobiol.* **36**, 206–220.

Reinhardt, R., Centanin, L., Tavhelidse, T., Inoue, D., Wittbrodt, B., Concordet, J.-P., Martinez-Morales, J. R. and Wittbrodt, J. (2015). Sox2, Tlx, Gli3, and Her9 converge on Rx2 to define retinal stem cells in vivo. *EMBO J.* **34**, 1572–1588.

Rembold, M., Lahiri, K., Foulkes, N. S. and Wittbrodt, J. (2006a). Transgenesis in fish: efficient selection of transgenic fish by co-injection with a fluorescent reporter construct. *Nat. Protoc.* **1**, 1133–9.

Rembold, M., Loosli, F., Adams, R. J. and Wittbrodt, J. (2006b). Individual cell migration serves as the driving force for optic vesicle evagination. *Science* **313**, 1130–4.

Renault, V. M., Rafalski, V. A., Morgan, A. A., Salih, D. A. M., Brett, J. O., Webb, A. E., Villeda, S. A., Thekkat, P. U., Guillerey, C., Denko, N. C., et al. (2009). FoxO3 Regulates Neural Stem Cell Homeostasis. *Cell Stem Cell* **5**, 527–539.

Reya, T. and Clevers, H. (2005). Wnt signalling in stem cells and cancer. *Nature* **434**,

843–50.

Reynolds, B. A. and Weiss, S. (1992). Generation of neurons and astrocytes from isolated cells of the adult mammalian central nervous system. *Science* **255**, 1707–10.

Rock, J. R., Onaitis, M. W., Rawlins, E. L., Lu, Y., Clark, C. P., Xue, Y., Randell, S. H. and Hogan, B. L. M. (2009). Basal cells as stem cells of the mouse trachea and human airway epithelium. *Proc. Natl. Acad. Sci. U. S. A.* **106**, 12771–5.

Rumman, M., Dhawan, J. and Kassem, M. (2015). Concise Review: Quiescence in Adult Stem Cells: Biological Significance and Relevance to Tissue Regeneration. *Stem Cells* **33**, 2903–2912.

Sato, T., van Es, J. H., Snippert, H. J., Stange, D. E., Vries, R. G., van den Born, M., Barker, N., Shroyer, N. F., van de Wetering, M. and Clevers, H. (2011). Paneth cells constitute the niche for Lgr5 stem cells in intestinal crypts. *Nature* **469**, 415–418.

Schlegelmilch, T., Henke, K. and Peri, F. (2011). Microglia in the developing brain: From immunity to behaviour. *Curr. Opin. Neurobiol.* **21**, 5–10.

Schofield, R. (1978). The relationship between the spleen colony-forming cell and the haemopoietic stem cell. *Blood Cells* **4**, 7–25.

Shackleton, M., Vaillant, F., Simpson, K. J., Stingl, J., Smyth, G. K., Asselin-Labat, M. L., Wu, L., Lindeman, G. J. and Visvader, J. E. (2006). Generation of a functional mammary gland from a single stem cell. *Nature* **439**, 84–88.

Shinin, V., Gayraud-Morel, B., Gomès, D. and Tajbakhsh, S. (2006). Asymmetric division and cosegregation of template DNA strands in adult muscle satellite cells. *Nat. Cell Biol.* **8**, 677–687.

Sierra, A., Encinas, J. M., Deudero, J. J. P., Chancey, J. H., Enikolopov, G., Overstreet-Wadiche, L. S., Tsirka, S. E. and Maletic-Savatic, M. (2010). Microglia shape adult hippocampal neurogenesis through apoptosis-coupled phagocytosis. *Cell Stem Cell* **7**, 483–495.

Simons, B. D. and Clevers, H. (2011). Strategies for homeostatic stem cell self-renewal in adult tissues. *Cell* **145**, 851–62.

Snippert, H. J. and Clevers, H. (2011). Tracking adult stem cells. *EMBO Rep.* **12**, 113–22.

Snippert, H. J., van der Flier, L. G., Sato, T., van Es, J. H., van den Born, M., Kroon-Veenboer, C., Barker, N., Klein, A. M., van Rheenen, J., Simons, B. D., et al. (2010). Intestinal crypt homeostasis results from neutral competition between symmetrically dividing Lgr5 stem cells. *Cell* **143**, 134–44.

Song, H., Stevens, C. F. and Gage, F. H. (2002). Astroglia induce neurogenesis from adult neural stem cells. *Nature* **417**, 39–44.

Souren, M., Martinez-Morales, J. R., Makri, P., Wittbrodt, B. and Wittbrodt, J. (2009). A global survey identifies novel upstream components of the Ath5 neurogenic network. *Genome Biol.* **10**, R92.

Spradling (2009). Lineage analysis of stem cells. *StemBook* 1–18.

Stephens, W. Z., Senecal, M., Nguyen, M. and Piotrowski, T. (2010). Loss of adenomatous polyposis coli (apc) results in an expanded ciliary marginal zone in the zebrafish eye. *Dev. Dyn.* **239**, 2066–77.

Straznicky, K. and Gaze, R. M. (1971). The growth of the retina in Xenopus laevis: an autoradiographic study. *J. Embryol. Exp. Morphol.* **26**, 67–79.

Strome, S. and Wood, W. B. (1983). Generation of asymmetry and segregation of germ-line granules in early C. elegans embryos. *Cell* **35**, 15–25.

Taelman, V. F., Dobrowolski, R., Plouhinec, J.-L., Fuentealba, L. C., Vorwald, P. P., Gumper, I., Sabatini, D. D. and De Robertis, E. M. (2010). Wnt signaling requires sequestration of glycogen synthase kinase 3 inside multivesicular endosomes. *Cell* **143**, 1136–48.

Tejeda-Munoz, N. and Robles-Flores, M. (2015). Glycogen synthase kinase 3 in Wnt signaling pathway and cancer. *IUBMB Life* **67**, 914–922.

Thermes, V., Grabher, C., Ristoratore, F., Bourrat, F., Choulika, A., Wittbrodt, J. and Joly, J.-S. (2002). I-SceI meganuclease mediates highly efficient transgenesis in fish. *Mech. Dev.* **118**, 91–8.

Thisse, B. and Thisse, C. (2004). Fast Release Clones: A High Throughput Expression Analysis. ZFIN Direct Data Submission (http://zfin.org).

Ueki, T., Tanaka, M., Yamashita, K., Mikawa, S., Qiu, Z., Maragakis, N. J., Hevner, R. F., Miura, N., Sugimura, H. and Sato, K. (2003). A novel secretory factor, Neurogenesin-1, provides neurogenic environmental cues for neural stem cells in the adult hippocampus. *J. Neurosci.* **23**, 11732–40.

van de Water, S., van de Wetering, M., Joore, J., Esseling, J., Bink, R., Clevers, H. and Zivkovic, D. (2001). Ectopic Wnt signal determines the eyeless phenotype of zebrafish masterblind mutant. *Development* **128**, 3877–3888.

Van Keymeulen, A. and Blanpain, C. (2012). Tracing epithelial stem cells during development, homeostasis, and repair. *J. Cell Biol.* **197**, 575–584.

Van Raay, T. J., Moore, K. B., Iordanova, I., Steele, M., Jamrich, M., Harris, W. A. and Vetter, M. L. (2005). Frizzled 5 signaling governs the neural potential of progenitors in the developing Xenopus retina. *Neuron* **46**, 23–36.

Voog, J. and Jones, D. L. (2010). Stem Cells and the Niche: A Dynamic Duo. *Cell Stem Cell* **6**, 103–115.

Waddington, C. H. (1957). *The Strategy of Genes*. London: George Unwin & Unwin.

Wan, Y., Almeida, A. D., Rulands, S., Chalour, N., Muresan, L., Wu, Y., Simons, B. D., He, J. and Harris, W. (2016). The ciliary marginal zone of the zebrafish retina: clonal and time-lapse analysis of a continuously growing tissue. *Development* 1099–1107.

Watt, F. M. and Hogan, B. L. (2000). Out of Eden: stem cells and their niches. *Science* **287**, 1427–1430.

Watt, F. M., Frye, M. and Benitah, S. A. (2008). MYC in mammalian epidermis: how can an oncogene stimulate differentiation? *Nat. Rev. Cancer* **8**, 234–42.

Wehman, A. M., Staub, W., Meyers, J. R., Raymond, P. A. and Baier, H. (2005). Genetic dissection of the zebrafish retinal stem-cell compartment. *Dev. Biol.* **281**, 53–65.

Weidinger, G., Thorpe, C. J., Wuennenberg-Stapleton, K., Ngai, J. and Moon, R. T. (2005). The Sp1-related transcription factors sp5 and sp5-like act downstream of Wnt/??-catenin signaling in mesoderm and neuroectoderm patterning. *Curr. Biol.* **15**, 489–500.

Weissman, I. L. (2000). Stem cells: units of development, units of regeneration, and units in evolution. *Cell* **100**, 157–168.

Wend, P., Holland, J. D., Ziebold, U. and Birchmeier, W. (2010). Wnt signaling in stem and cancer stem cells. *Semin. Cell Dev. Biol.* **21**, 855–63.

Westenskow, P., Piccolo, S. and Fuhrmann, S. (2009). Beta-catenin controls differentiation of the retinal pigment epithelium in the mouse optic cup by regulating Mitf and Otx2 expression. *Development* **136**, 2505–10.

Wexler, E. M., Paucer, A., Kornblum, H. I., Plamer, T. D. and Geschwind, D. H. (2009). Endogenous Wnt signaling maintains neural progenitor cell potency. *Stem Cells* **27**, 1130–1141.

Wittbrodt, J., Shima, A. and Schartl, M. (2002). Medaka — a Model Organism From the Far East. *Nat. Rev. Genet.* **3**, 53–64.

Xue, X. Y. and Harris, W. a (2012). Using myc genes to search for stem cells in the ciliary margin of the Xenopus retina. *Dev. Neurobiol.* **72**, 475–90.

Yamaguchi, M., Tonou-Fujimori, N., Komori, A., Maeda, R., Nojima, Y., Li, H., Okamoto, H. and Masai, I. (2005). Histone deacetylase 1 regulates retinal neurogenesis in zebrafish by suppressing Wnt and Notch signaling pathways. *Development* **132**, 3027–43.

Yan, D., Wiesmann, M., Rohan, M., Chan, V., Jefferson, A. B., Guo, L., Sakamoto, D., Caothien, R. H., Fuller, J. H., Reinhard, C., et al. (2001). Elevated expression of axin2 and hnkd mRNA provides evidence that Wnt/beta -catenin signaling is activated in human colon tumors. *Proc. Natl. Acad. Sci. U. S. A.* **98**, 14973–8.

Yost, C., Torres, M., Miller, J. R., Huang, E., Kimelman, D. and Moon, R. T. (1996). The axis-inducing activity, stability, and subcellular distribution of beta-catenin is regulated in Xenopus embryos by glycogen synthase kinase 3. *Genes Dev.* **10**, 1443–

1454.

Zeng, X., Tamai, K., Doble, B., Li, S., Huang, H., Habas, R., Okamura, H., Woodgett, J. and He, X. (2005). A dual-kinase mechanism for Wnt co-receptor phosphorylation and activation. *Nature* **438**, 873–7.

Zhang, Y. V., Cheong, J., Ciapurin, N., McDermitt, D. J. and Tumbar, T. (2009). Distinct Self-Renewal and Differentiation Phases in the Niche of Infrequently Dividing Hair Follicle Stem Cells. *Cell Stem Cell* **5**, 267–278.

Zygar, C. A., Colbert, S., Yang, D. and Fernald, R. D. (2005). IGF-1 produced by cone photoreceptors regulates rod progenitor proliferation in the teleost retina. *Dev. Brain Res.* **154**, 91–100.

7 Abbreviations

%	percent
°C	degrees Celsius
ABC	active β-catenin
AP	alkaline phosphatase
APC	adenomatous polyposis coli
ArCoS	arched continuous stripe
atoh7	*atonal bHLH transcription factor 7*
AZ	azakenpaullone
BBW	brainbow
BCIP	5-bromo-4-chloro-3-indolyl phosphate
bp	basepair
BrdU	bromodeoxyuridine
BS	binding solution
BSA	bovine serum albumin
CBC	crypt-based columnar cell
CK1α	casein kinase 1 alpha
cmlc2	cardiac myosin light chain 2
CMZ	ciliary marginal zone
CNS	central Nervous system
DAPI	2-(4-amidinophenyl)-1H-indole-6-carboxamidine
dATP	deoxyadenosine triphosphate
ddH_2O	purified water
dig	digoxigenin
digUTP	digoxigenin deoxyuridine triphosphate
DKK	Dickkopf
DMSO	dimethyl sulfoxide
DN-GSK3	dominant negative GSK3
DNA	deoxyribonucleic acid
dNTP	deoxynucleoside triphosphate
DTT	dithiothreitol
E. coli	*Escherichia coli*
EB	Elution Buffer
EDTA	ethylenediaminetetraacetic acid
EdU	ethynyldeoxyuridine
eGFP	enhanced Green fluorescent protein
EGTA	Triethylene glycol diamine tetraacetic acid
ERM	embryo rearing medium
ERM	embryo rearing medium
ERT2	selectively tamoxifen-sensitive estrogen receptor
ESC	embryonic Stem cell
EtBr	ethidium bromide

g	gramme
GCL	ganglion cell layer
GSK3	glycogen synthase kinase 3
h	hour
H_2O	water
H_2O_2	hydrogen peroxide
HCl	hydrogen chloride
hpf	hours post fertilization
hsp70	70 kilodalton heat shock protein
Hyb	hybridisation
INL	inner nuclear layer
IPTG	isopropyl β-D-1-thiogalactopyranoside
kb	kilobases
KOH	potassium hydroxide
l	litre
LB	lysogeny broth
LRP6	low-density lipoprotein receptor-related protein 6
M	molar
m	milli-
m	metre
MeOH	Methanol
$MgCl_2$	magnesium chloride
min	Minute
mRNA	messenger ribonucleic acid
n	nano-
n	quantity
NaCl	sodium chloride
NBT	nitro blue tetrazolium chloride
NEB	New England Biolabs
NLS	nuclear localisation signal
NR	neural retina
NSC	neuronal stem cells
ONL	outer nuclear layer
PBS	phosphate buffered saline
PBST	phosphate buffered saline plus Triton X100
PCNA	proliferating cell nuclear antigen
PCR	polymerase chain reaction
PEG	polyethylene glycol
PFA	paraformaldehyde
PMT	photomultiplier tube
POD	horse-radishperoxidase
pT	phosphorylated threonine
PTW	phosphate buffered saline plus Tween 20

RFP	red fluorescent protein
RNA	ribonucleic acid
rNTP	ribonucleotide triphosphate
RPC	retinal progenitor cell
RPE	retinal pigment epithelium
rpm	rotations per minute
RSC	retinal stem cell
RT	reverse transcriptase
RT-qPCR	quantitative real-time PCR
rx2	*retina-specific homeobox gene-2*
s	second
SDS	sodium dodecyl sulfate
SGZ	subgranular zone
SSC	saline sodium citrate
SSCT	saline sodium citrate plus Tween 20
SVZ	subventricular zone
TA	transit amplifying
TAE	tris-acetate-EDTA
TB	terrific broth
TE	tris-EDTA
tlx	*orphan nuclear receptor*
TN	tris sodium buffer
TNB	tris sodium Tween 20 blocking buffer
TNT	tris sodium Tween 20 buffer
TRAIL	tumor necrosis factor-related apoptosis-inducing ligand
Tris	tris hydroxymethyl aminomethane
TUNEL	terminal deoxynucleotidyl transferase dUTP nick end labeling
U	unit
ubi	ubiquitin
UPL	universal probe library
UV	ultraviolet
V	volt
WM-dFISH	Whole mount double fluorescent *in situ* hybridisation
Wnt/STOP	Wnt-dependent stabilization of proteins
wt	wildtype
x	-fold
X-Gal	5-bromo-4-chloro-3-indolyl- beta-D-galactopyranoside
YFP	Yellow fluorescent protein
µ	micro-

8 Publications

Kirchmaier, S., Höckendorf, B., Möller, E. K., Bornhorst, D., Spitz, F. and Wittbrodt, J. (2013). Efficient site-specific transgenesis and enhancer activity tests in medaka using PhiC31 integrase. *Development* **140**, 4287–95.

Czech, D. P., Lee, J., Correia, J., Loke, H., Möller, E. K. and Harley, V. R. (2014). Transient neuroprotection by SRY upregulation in dopamine cells following injury in males. *Endocrinology* **155**, 2602–2612.

9 Acknowledgements

At first, I would like to thank my supervisor, Jochen Wittbrodt, for giving me the opportunity to work in his group and for providing me with an exiting project. You gave guidance when I needed it, but also gave me the freedom to develop and pursue own ideas. I am thankful for your contagious optimism and excitement about my work.

I am grateful to my thesis advisory committee, Lázaro Centanin, Christof Niehrs and Jan Lohmann, for their suggestions and helpful discussions during and outside of my TAC meetings.

I want to thank Daigo Inoue for sharing his extensive experimental expertise with me, especially during the initial period of my PhD and for providing me with valuable data for my project. I also thank Ann Kathrin Heilig for being the first Master thesis student I got to supervise. Thanks for being patient as I learned how to juggle finishing my own experiments and supervising yours. I enjoyed working with you on a common goal.

I am indebted to Sergio P. Acebron for your advise on everything about Wnt signalling, for great ideas for my project and for helping me to improve presentations and my thesis. Thank you for giving Anni and me the opportunity to perform experiments in your lab that would have taken much effort to establish on our own.

I would like to thank all other members of the Wittbrodt lab for being great colleagues and for creating a working environment I felt comfortable and stimulated in: Alicia Perez, Arturo Gutierrez-Triana, Beate Wittbrodt, Clara Buchta, Colin Schäfer, Erika Tsingos, Eva Hasel, Frederike Seibold, Jakob Gierten, Juan Mateo, Katharina Lust, Lea Schertel, Narges Aghaallaei, Tanja Kellner, Thomas Thumberger, Tinatini Tavhelidse und Ute Volbehr. I would like to thank you all for cheering me up after unsuccessful experiments and for all the laughs we shared. Special thanks go to Bay 3 for the nice bay environment, especially to Arturo for eye-opening comments on my thesis. Also special thanks to Colin, who now started working on Wnt signalling and to Katha and Eva who shared the experience of finishing our theses under time pressure with me. I am also grateful to the technicians, as they facilitated my work without expecting anything in return.

Finally, I want to thank my parents. With their upbringing they provided me with the opportunity and support to pursue my dreams. Of course, I thank Florian for his love,

patience and for always knowing how to make me laugh. I am very lucky to have you at my side.